Revised Version: 4 August 2011

SCIENTIFIC COMMITTEE
SEVENTH REGULAR SESSION

9-17 August 2011
Pohnpei, Federated States of Micronesia

SEAPODYM working progress and applications to Pacific skipjack tuna population and fisheries

---

WCPFC-SC7-2011/EB-WP 06 rev. 1

P. Lehodey[1], I. Senina[1], B. Calmettes[1]
John Hampton[2], Simon Nicol[2], Peter Williams[2], J. Jurado Molina[2]
M. Ogura[3], H. Kiyofuji[3], and S. Okamoto[3]

---

[1] Affiliation Marine Ecosystem Department, CLS, France
[2] Oceanic Fisheries Programme, SPC, New Caledonia
[3] National Research institute of Far Seas Fisheries, Japan

SEAPODYM working progress and applications to Pacific skipjack tuna population and fisheries

P. Lehodey, I. Senina, B. Calmettes
Marine Ecosystem Department, CLS, France

John Hampton, Simon Nicol, Peter Williams, J. Jurado Molina
Oceanic Fisheries Programme, SPC, New Caledonia

M. Ogura, H. Kiyofuji, and S. Okamoto
National Research institute of Far Seas Fisheries, Japan

1 Executive Summary

The development of SEAPODYM to Pacific tuna and billfish species has been included in the WCPFC SC's programme of work as an affiliated, independently funded project. Progress in the model development and its application to Pacific skipjack tuna are presented. Key new developments included the implementation of robustify-normal likelihood for the parameter optimization approach and code upgrade allowing optimization experiment at any temporal and spatial resolution. Research studies funded by the oceanic fisheries programme of SPC and the NRIFSF of the Fisheries Research Agency of Japan allowed to develop a new skipjack model configuration using realistic high resolution environmental forcing, increased resolution of fishing data, and robustify-normal likelihood approach. This led to improvements in the optimization of parameters for skipjack tuna with a better fit to fishing data and a lower total biomass estimate. It would be essential to investigate if such a tendency remains while continuing to run optimization experiments with increased resolution and corresponding resolution of fishing data sets (at least partially).

Skipjack adult biomass was predicted to be in its lower range in 2008 and 2009, but higher recruitment occurred in 2010 following the 2009-10 El Niño event. The powerful La Niña event developing in 2010-11 resulted in lower skipjack recruitment in the 1st quarter of 2011. Based on this relationship between skipjack recruitment and ENSO, it is possible to forecast the future trend of the stock. Since ENSO-neutral conditions have developed in the 2nd quarter of 2011 and are expected to continue until the end of the year, skipjack biomass would reach a low peak at the end of 2011. Unless an El Niño event develops in 2012, the skipjack biomass forecasted for 2012-13 should remain in the low range of its long term productivity.

After scaling the new parameterization to a pre-operational model at resolution 0.25°x week, analyses can be done to investigate fine scale changes in the skipjack population dynamics and fisheries. Examples are provided at regional level with the Japanese domestic fleets and at EEZ scale in Papua New Guinea. It becomes also possible to envisage near real time monitoring of the stock. The interest of such products for the monitoring of fisheries need to be discussed and evaluated.

The model is also used to investigate the impact of climate change under IPCC A2 scenario for the next Century. After correction of a temperature bias in the climate model outputs, a new projection of skipjack dynamics was achieved with parameter estimates close to the values obtained using more realistic reanalyses of the historical fishing period. Results showed a more clear extension of habitat towards higher latitude and stabilization of skipjack total biomass in the WCPO until 2060s (without considering fishing). The result is insensitive to a "no change" scenario for oxygen concentration.

2 Introduction

SEAPODYM is a model developed for investigating spatial tuna population dynamics, under the influence of both fishing and environmental effects. Details on the model development have been published in the peer-reviewed scientific literature, and results based on the development and applications of this model to Pacific tuna species have been regularly presented to the meetings of the Standing Committee on Tuna and Billfishes (SCTB) and then the Scientific Committee (SC) of the WCPFC (see section references). At the 5th SC, it was recommended that SEAPODYM be included as an affiliated, independently funded, project in the SC's programme of work. The last meeting (SC6) suggested that the application of fine-scale spatial models such as SEAPODYM to skipjack tuna could potentially provide a useful source of auxiliary information that could be included in MFCL-based assessments. The model is also used for other tuna and billfish species, and for various applications including the exploration of management scenarios or the climate change impact on tuna stocks.

3 Recent and ongoing code developments

Since the previous SC meeting, the code of SEAPODYM has been enhanced with the objective of facilitate its use by non-developers colleagues. More important changes have been conducted that can have direct effects on the skills of the model and its predictions:

1. Sea surface temperature is now used instead of average temperature of the surface layer to define the spawning index, allowing a direct comparison of optimized parameters with the available scientific literature.
2. Feeding habitat is now computed relatively to density of forage rather than integrated biomass in the layer. This change gives a better representation of the vertical dimension, since for a same biomass, the accessibility increases with the concentration related to the thickness of the layer.
3. The robustify-normal likelihood has been implemented and is now used instead of normal likelihood for the parameter optimization approach. Robustify-normal likelihood includes σ parameter that account for the size and the variance of the different samples (i.e., fisheries).
4. The code has been upgraded to allow running optimization simulations at any temporal and spatial resolution. The highest resolution being limited by those of the environmental forcing. The interest of running higher resolution optimization experiments is also limited by the resolution of fishing data available. Alternatively the fishing resolution can be degraded to lower resolution to account for a lack of good mesoscale representation or errors in the fishing data.
5. Options are now available to run various fishing effort scenarios based on spatial management measures. Using a mask file, EEZ or any area defined by a polygon can be closed to any fishery. The corresponding effort can be chosen to be lost; redistributed proportionally to CPUE outside the selected area, or transferred to another fishery (e.g. FAD to school sets). Example of application is provided in document SC7-MI-WP-5 exploring fishing area closure scenarios.
6. Routines (R scripts) for the analysis of outputs at EEZ scale have been updated and now account for the exact area of the EEZ in each cell (i.e., surface area of partial cells are computed).

These changes in the code still need to be detailed in a new version of the model documentation.

Finally, ongoing key developments are concerning two major objectives:

1. ***The optimization of the energy transfer coefficients for the Mid-Trophic Level component (tuna forage) of the model.*** These parameters are optimized to fit the relative ratios of micronekton biomass deduced from acoustical values (NASC) between layers changing during day and night periods. The code was validated by a derivative check (approximation between analytical gradient and finite difference stay very low for at least two consecutive step sizes for all parameter), and twin experiments. In a twin experiment, the initial parameterization of the model is considered as the truth. A set of pseudo-observations is extracted from these simulation outputs. Then values of parameters are changed and optimization experiments run to check that the model converges towards the 'true' (i.e., initial) parameter values. Optimization experiments using actual acoustic data are now starting and will benefit of collaborations with colleagues under several research projects, in particular the PFRP project "Assimilating *in situ* bioacoustic data in a mid-trophic level model", the European FP7 project EURO-BASIN (http://www.euro-basin.eu/), and a French ANR project focusing on myctophids distribution in the southern Indian Ocean.

2. ***The use of tagging data in the optimization approach of tuna population dynamic.*** A new PFRP project has been successfully proposed with the objective of "Integrating conventional and electronic tagging data into SEAPODYM". This project includes collaboration between CLS, SPC and the National Research Institute of Far Seas Fisheries. Both conventional and electronic tagging data will be integrated in the rigorous numerical methodology developed to optimize the model parameters. Different approaches to incorporate tagging data into a simplified one-cohort version of SEAPODYM have been tested already. But due to computing limitation, a new one is envisaged that consists in estimating from the tagging datasets a space/time vector field of movement and incorporating these intermediary results into SEAPODYM's likelihood formulation.

4 SEAPODYM Pacific skipjack assessment at high resolution

Thanks to research studies funded by the oceanic fisheries programme of SPC under SCICOFISH project and the National Research Institute of Far Seas Fisheries of the Fisheries Research Agency of Japan, a new model configuration of SEAPODYM has been developed for the Pacific skipjack population. In previous skipjack applications (Lehodey and Senina 2009; Lehodey et al. 2010), a series of simulations has been carried out for Pacific skipjack tuna with optimization at basin-scale using different low-resolution (2°xmonth) environmental forcing and fishing dataset (5°x5°x month), but over the whole historical industrial fishing period, i.e., back to the early 1960s. Here the first objective was to develop the highest possible resolution with a realistic mesoscale activity that could explain high and low peaks in the catch associated to local concentration of fish by fronts and eddies. A second objective was to investigate the reasons of a recent decrease in the CPUE of Japanese domestic fisheries (Uosaki et al 2010). Finally, this application could be used now with regular near real time (e.g., 2 months delay) update to investigate the environmental and fishing impact from basin to regional and EEZ levels.

4.1 Method

Running optimization experiments at high resolution is still challenging in term of computing requirement. Indeed the code of the model would need to be upgraded to allow for parallel computing to achieve this task. Here, the approach was to degrade the high resolution environmental forcing at 1°degree x month to run optimization and then to scale the parameters before running a new simulation at the original resolution. Updated fishing data sets with resolution at 1° degree were also used.

4.1.1 Oceanic data

Satellite derived primary production (Behrenfeld and Falkowsky, 1997) and two ocean reanalyses have been used to run simulations with the SEAPODYM model. Both ocean reanalyses (SODA: http://www.atmos.umd.edu/~ocean/ and GLORYS: http://www.mercator-ocean.fr/) use data assimilation techniques (with altimetry and SST in particular) to reproduce realistic spatial and temporal variability. Original resolution is ¼°x 1d for GLORYS (2002-2009) and ½°x 5d for SODA (1998-2008). GLORYS is an eddy permitting global ocean and thus predicts realistic mesoscale activity (Tranchant et al., 2008). The GLORYS reanalysis is updated for the recent period using the operational Mercator Ocean (http://www.mercator-ocean.fr/eng) global ocean model PSY3 (using the same grid and assimilation scheme than GLORYS). Because the ocean circulation model assimilates satellites (SST and altimetry) and in situ data, predicted fields of temperature and current are fully coherent with those of primary production derived from ocean color data.

4.1.2 Fishing data

The stratification of fisheries has been revised (Table 3.1) with the best available fishing data sets that have been provided by the Japan FRA, the WCPFC (through SPC), and the IATTC (public domain data) at a resolution of 1° x month or 5°x month. These data were used to run optimization experiments at Pacific basin-scale to estimate the status of the skipjack stock, and thus requiring taking into account the fishing mortality due to all fisheries. After optimization, Japanese fishing data (pole-and-line and purse-seine) at resolution ¼°x week were used in the analysis of changes at high resolution in the Kuroshio region. For EEZ scale analysis, a high resolution dataset (1/4° x week) of WCPO tropical purse seine fisheries has been provided by OFP covering the period 2002-2008.

Table 3.1 – Definition of fisheries and fishing data used in basin scale optimization experiments

Id	Gear	Region	Description	Nationality	Resolution catch data	Resolution Size data
SKIPJACK available data						
P1	PL	12N-35N; 120E-160E	PL small boats	Japan	1x1	1x1
P2	PL	35N-35S; 130E-150W	PL large boats	Japan	1x1	1x1
P3	PL	15S-0; 140E-160E	Pole and line	Papua New Guinea	1x1	5x5, 10x20
P3	PL	15S-0; 150E-165E	Pole and line	Solomon Islands	1x1	5x5
S4	PS	25N-35N; 140E-165E	PS subtropical fishery	Japan	1x1	5x5
S5	PS	20S-15N; 130E-150W	PS on LOG	All	1x1	5x5, 10x20
S6	PS	20S-15N; 130E-150W	PS on FAD	All	1x1	5x5, 10x20
S7	PS	20S-15N; 130E-150W	PS on free school	All	1x1	5x5, 10x20
L8	LL	20S-25N; 115E-150W	LL exploratory fishery	Japan	5x5	5x5
D9	DOM	15N-10S; 115E-130E	mixed set types	Philippines and Indonesia	5x5	-
S10	PS	EPO	PS on Dolphin schools	EPO (IATTC public data)	1x1	IATTC stratification areas
S11	PS	EPO	PS on Floating objects	EPO (IATTC public data)	1x1	IATTC stratification areas
S12	PS	EPO	PS on free school	EPO (IATTC public data)	1x1	IATTC stratification areas
P13	PL	15N-35N 120W-100W	Pole and Line	EPO (IATTC public data)	5x5	IATTC stratification areas

4.2 Results

4.2.1 SEAPODYM new experiments: SODA (1998-2008) and GLORYS (2002-2011)

A series of optimization experiments was conducted with the updated fishing datasets (catch and sizes) and the SODA configuration at 1°x month for the period 1998-2008.

The structure of the population is defined by age (cohorts) with variable time unit allowing to save computation time. There is 1- month cohort for larvae life stage, one 2-month cohort for juvenile stage, four 2-month cohorts for young fish (before age at maturity) and 12 cohorts for adult stages (one of 2 months, eight of 3 months, two of 4 months and one of 6 months). The last one is a "+ cohort" accumulating older fish.

All parameters cannot be optimized all together due to antagonistic and correlated mechanisms, e.g., mortality and recruitment. Thus, a series of simulations was carried out to achieve the optimal parameterization with this model configuration. Despite a relatively short time series (10 years), it was possible to achieve convergence thanks to the large fishing dataset at 1° resolution and the realistic environment provided by the SODA reanalysis and satellite derived primary production.

Optimal spawning temperature (SST) was estimated to 28.7 °C, and the optimal value for the oldest cohort to 20.6°C but with a large standard error that reached the maximum fixed boundary. The threshold value for the oxygen function was close to 2.5 ml/l (Table 2; Fig. 3.1). Estimates of movement parameters are not yet fully satisfactory since they reached also the fixed boundaries (Table 2). Nevertheless, reasonable estimates of catchability and selectivity coefficient were obtained (Fig. 3.2 and 3.3) when allowing a linear temporal increase.

Table 2: Estimates of habitats and movement parameters of previous simulations and the new one using SODA.

Parameters estimated by the model		Unit	ESSIC	ERA40	NCEP	SODA-1°
	Habitats					
T_s	Optimum of the spawning temperature function	^oC	30.5	27.8	29.8	28.68
σ_s	Std. Err. of the spawning temperature function	^oC	3.5*	2.5]	2.05	0.75*
α	Larvae food-predator trade-off coefficient	-	3.67	0.38	2]	1.03
T_a	Optimum of the adult temperature function at maximum age	^oC	26*	21.1	23.4	20.64
σ_a	Std. Err. of the adult temperature function at maximum age	^oC	1.62	1.14	3.5]	4.5]
$\hat{O}$	Oxygen value at Ψ_O =0.5	$ml \cdot l^{-1}$	3.86	0.93	1.5	2.47
γ	Curvature coefficient of the oxygen function	-	7.3e-5	0.001*	0.001*	0.001*
	Movements					
V_M	Maximum sustainable speed	$B.L. \cdot s^{-1}$	1.3	0.96	1.13	[1
C	coefficient of diffusion habitat dependence	-	0.4	0.3	0.3	6]**

*Fixed; [val = value close to mimimum boundary value; val] = value close to maximum boundary value

** The maximum value of the function has been changed

The overall fit to fishing data (Fig. 3.4) is high for total catch for all fisheries over the entire time series used in the optimization experiment (1998-2007). It is also very good for CPUE though there are relatively lower values of correlation in the western equatorial area which is a major fishing ground for tropical purse seiners (Fig. 3.4). All details of model fit to catch, CPUE and size frequency of catch are provided in appendix 1.

SEAPODYM predicted biomass is still higher than the biomass estimates from the last stock assessment study with the model MULTIFAN-CL used by the WCPFC (Hoyle et al 2010), roughly by a factor two for the WCPO (Fig. 3.5). Time series show a discrepancy in their fluctuations between the two estimates until 2004, but converge in the last recent years from 2005-2008 both for young and adult fish, and thus total biomass also (Fig. 3.5). Though still high compared to MULTIFAN-CL results, this new SEAPODYM biomass estimate has decreased substantially compared to previous lower resolution simulations, by roughly 20% and 30% for total and adult biomasses respectively. This decrease can be linked to the increase in resolution – from 2° to 1° for the environmental forcing and from 5° to 1° for several fishing data sets – with a more realistic environmental forcing due to data assimilation in the physical model. Thus, the model can reach convergence with less diffuse biomass and more patchy spatial density distribution, due to a better match between position of high/low catch and fish density (Fig. 3.6). This result suggests that further optimization experiments using higher resolution and more realistic forcing data sets could still decrease the biomass estimate. Given the importance of this estimate for assessing the fishing impact, it would be critical to identify at which level of resolution the biomass estimate tends to reach a steady minimum.

The optimization experiment achieved above was used to calibrate the simulation at high resolution ¼ °x week using GLORYS reanalysis (2002-2009). Taking advantage of the operational (i.e., real-time) production of ocean conditions at Mercator-Ocean (PSY3 model) and satellite-derived primary production at CLS, it was possible to extend the skipjack SEAPODYM-GLORYS application with regular update of the environmental forcing. Based on the optimization achieved in previous experiments, the simulation is updated every two-three months.

This high resolution simulation showed the same large basin-scale patterns than at lower resolution (Fig. 3.6 and 3.7). However, this first version of GLORYS reanalysis included strong anomalies in the western equatorial ocean circulation that can create strong discrepancies between observed and predicted catch (Fig. 3.7). A new version of the physical reanalysis will be produced to correct the anomaly due to wrong altimetry data assimilation in this key area for tuna fisheries. The situation seems to improve in this region with the forcing from the Mercator-Ocean (PSY3) operational model for the recent period 2009-11. In particular, both SEAPODYM and MULTIFAN-CL predicted low adult biomass in 2008 and 2009 (Fig. 3.5) but a high peak of recruitment occurred in 2010 coinciding with the El Niño event that developed in the Pacific during the second semester of 2009 until the 1st quarter of 2010.

These results confirm previous relationships established between skipjack recruitment and the El Niño Southern Oscillation (ENSO). The powerful La Niña event developing in 2010 resulted in lower skipjack recruitment (i.e., biomass of young fish) in the 1st quarter of 2011 (Fig 3.5). The impact of ENSO is particularly obvious in the central Pacific region R3 (Fig. 3.8), where both SEAPODYM and MULTIFAN-CL variability in young and adult biomass estimates converge particularly well after 2004 (Fig. 3.9), even if the biomass predicted by SEAPODYM remains higher by about 0.5-0.7 million tonnes for young and adult cohorts.

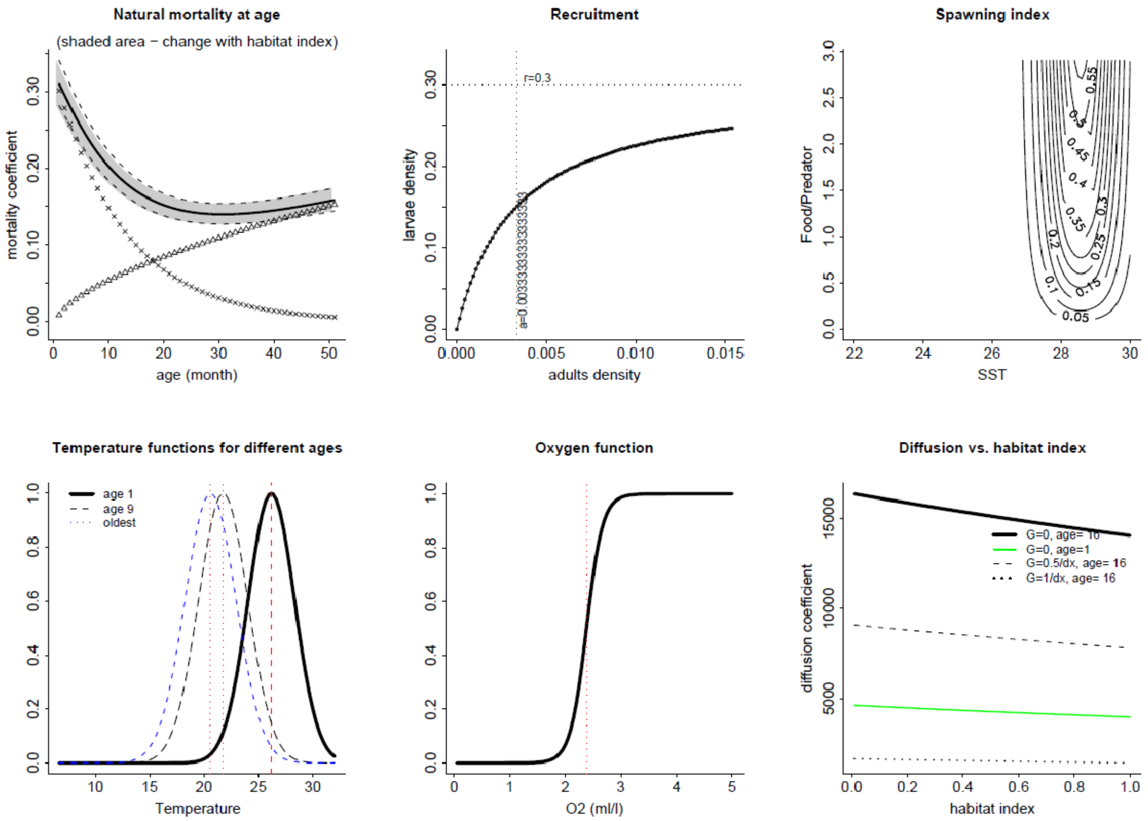

Figure 3.1: Main parameterization obtained from SEAPODYM-SODA.1° optimization experiments for natural mortality, stock-recruitment, spawning index, thermal habitat, oxygen habitat and habitat-size related diffusion movement.

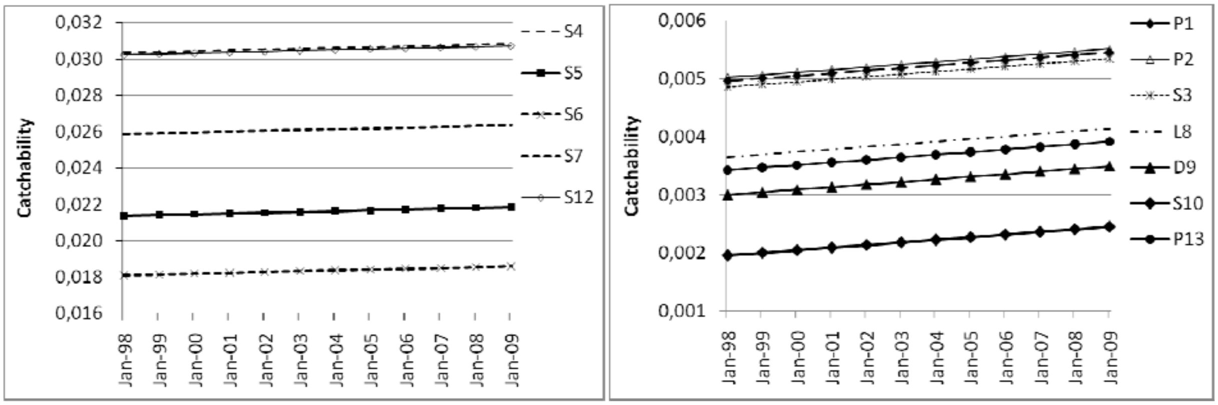

Figure 3.2. Change in catchability by fishery over the optimization period (1998-2008).

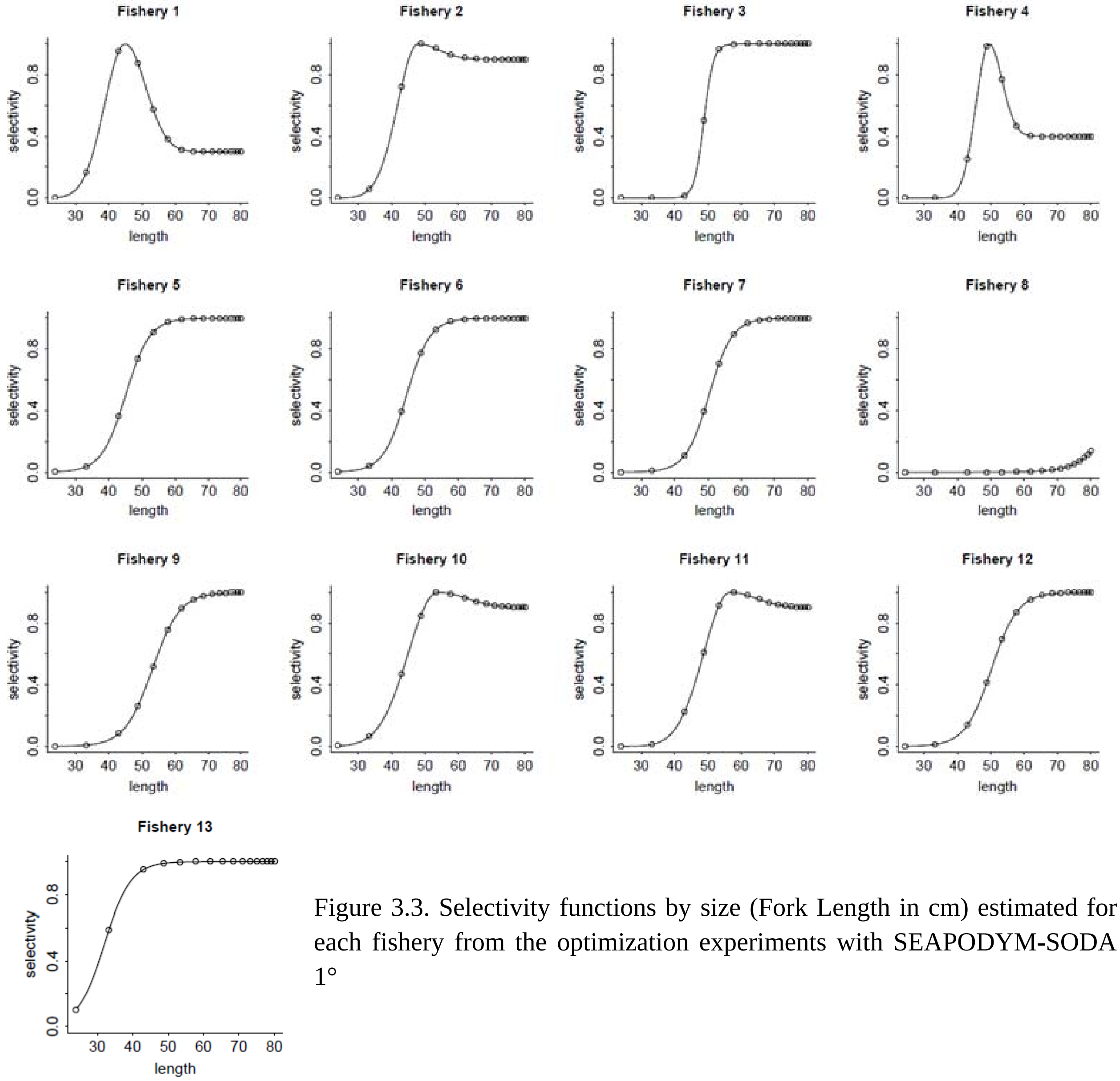

Figure 3.3. Selectivity functions by size (Fork Length in cm) estimated for each fishery from the optimization experiments with SEAPODYM-SODA 1°

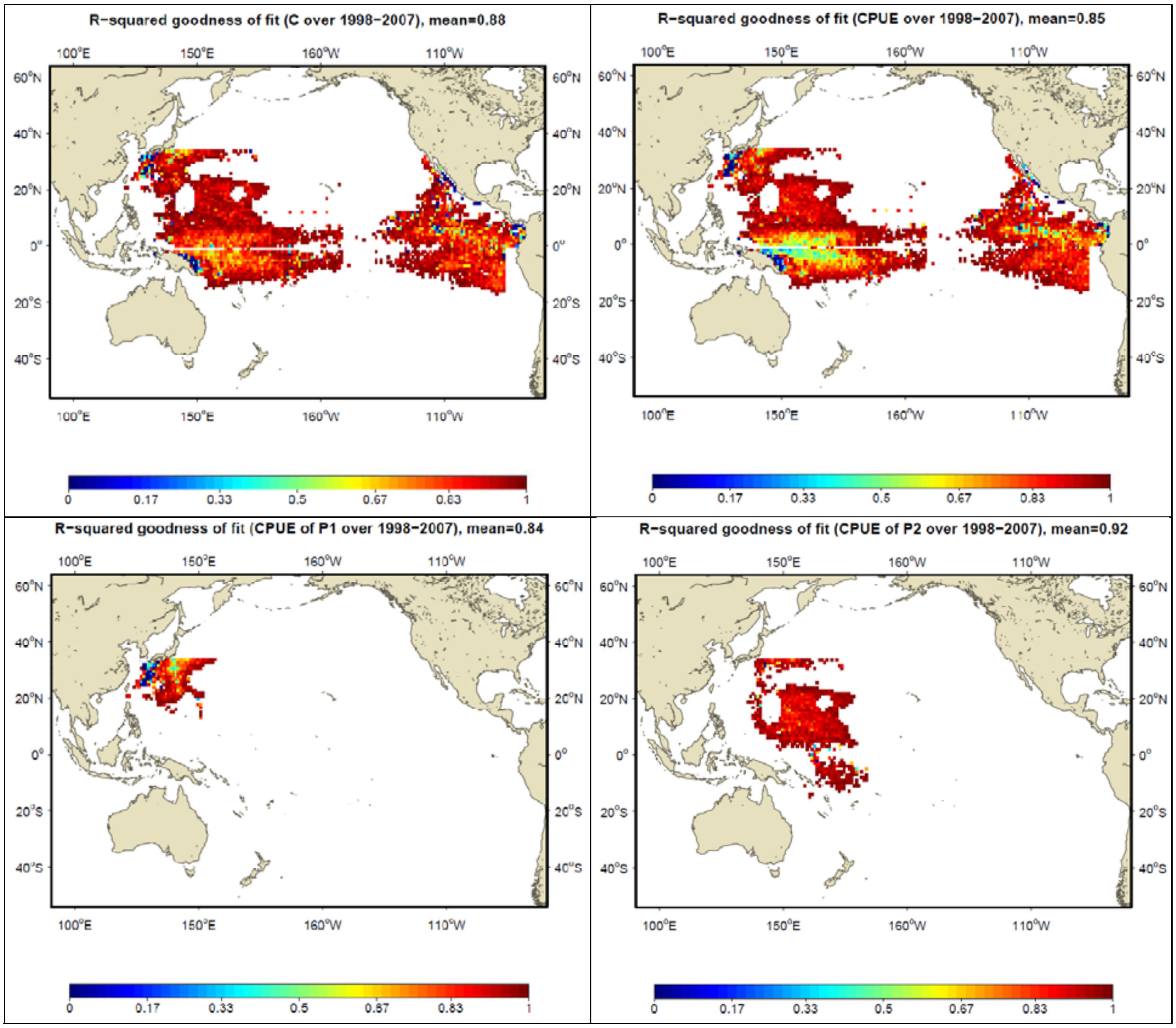

Figure 3.4. SEAPODYM-SODA.1° optimization experiments. Top: Spatial fit to observed catch (left) and cpue (right) of skipjack for all fisheries over the entire time series used for optimization. Bottom: Spatial fit to observed skipjack CPUE of offshore (left) and tropical (right) Japanese pole-and-line fleets.

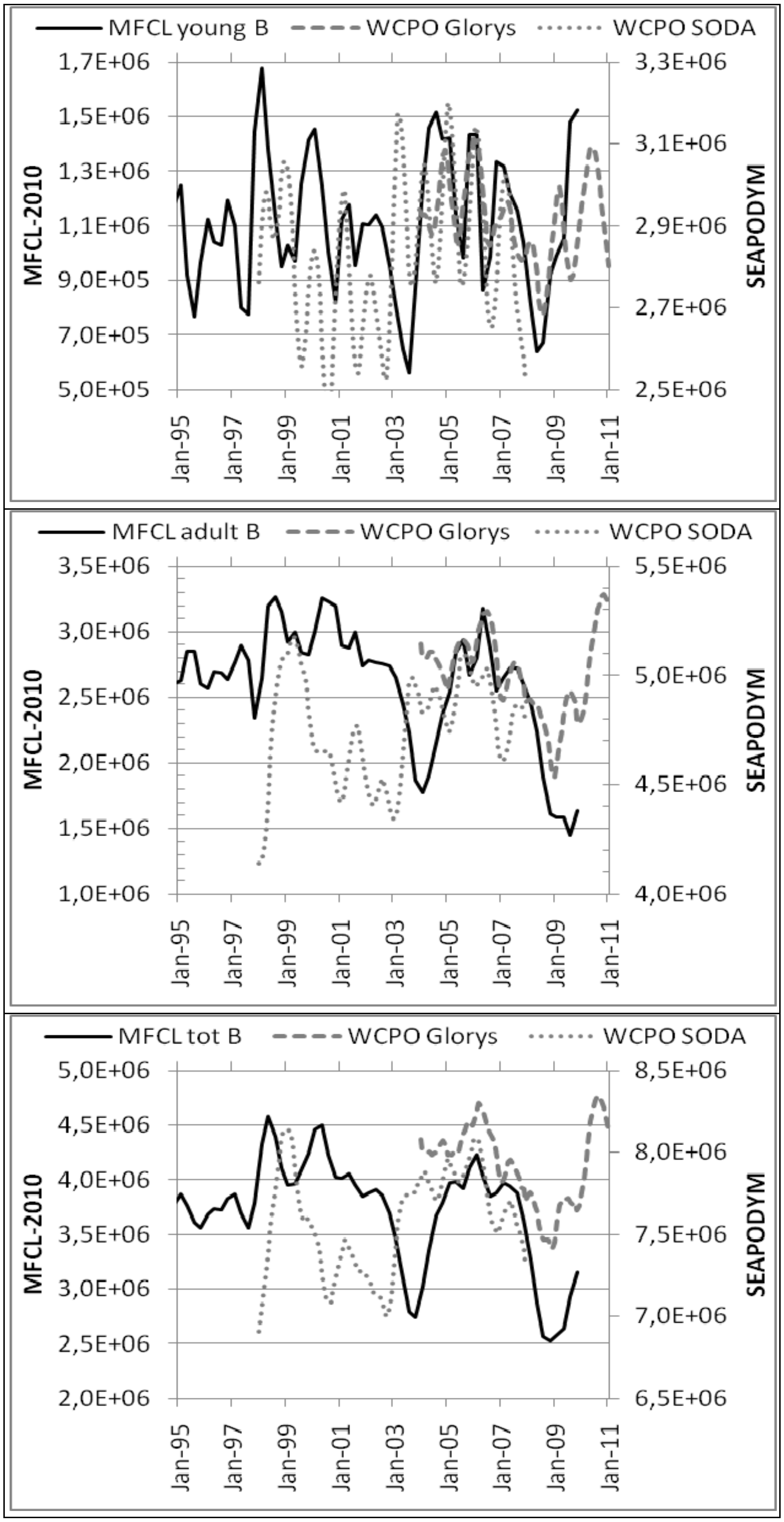

Figure 3.5. Comparison between the last biomass estimates from MULTIFAN-CL (continuous line) and SEAPODYM estimates of skipjack in WCPO using SODA and GLORYS-PSY3 simulations (dotted lines).

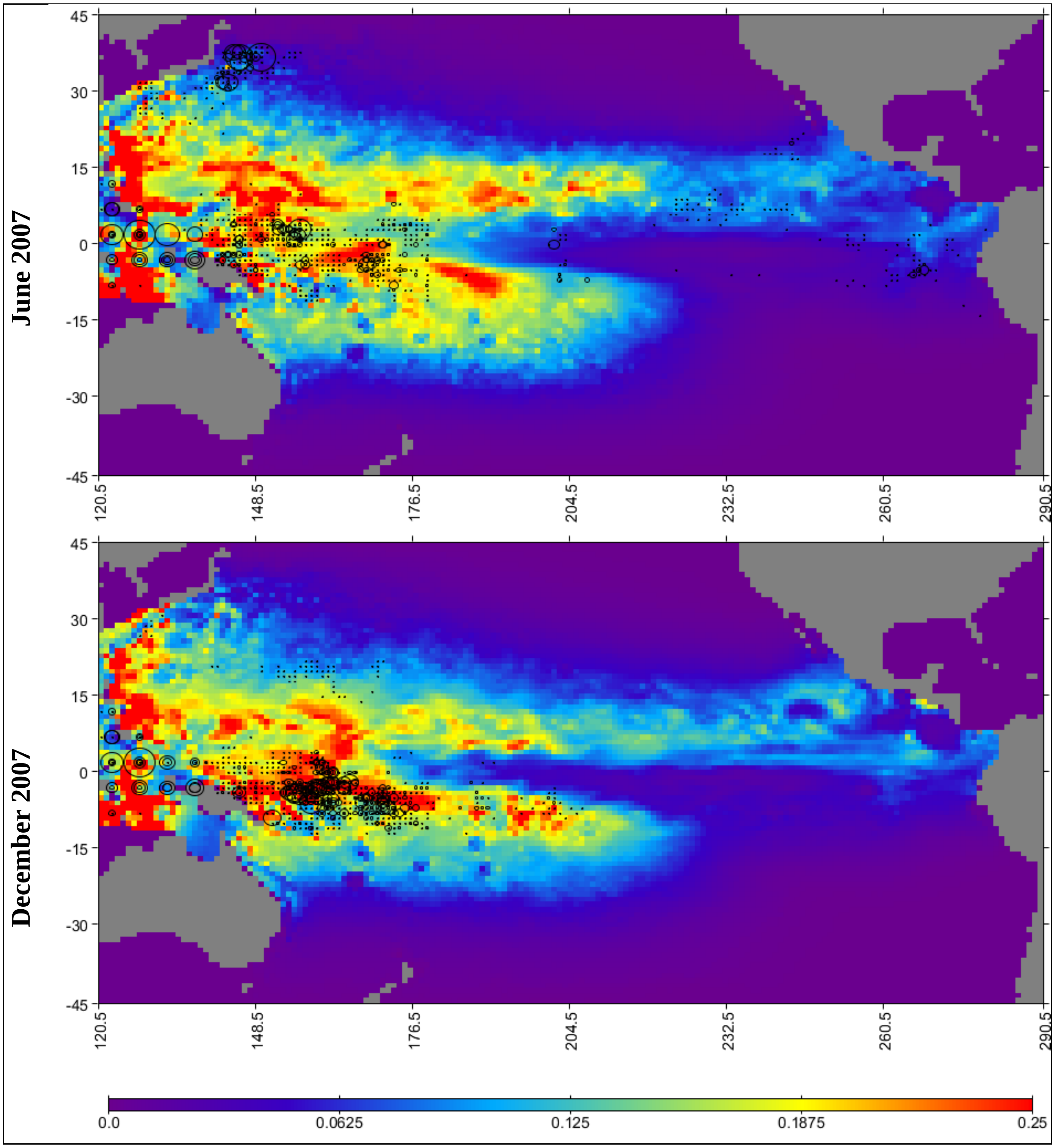

Figure 3.6. Predicted density of skipjack (sum of all cohorts) and total observed catch (proportional to circles) for the months of June and December 2007, with the SEAPODYM-SODA.1° optimized configuration

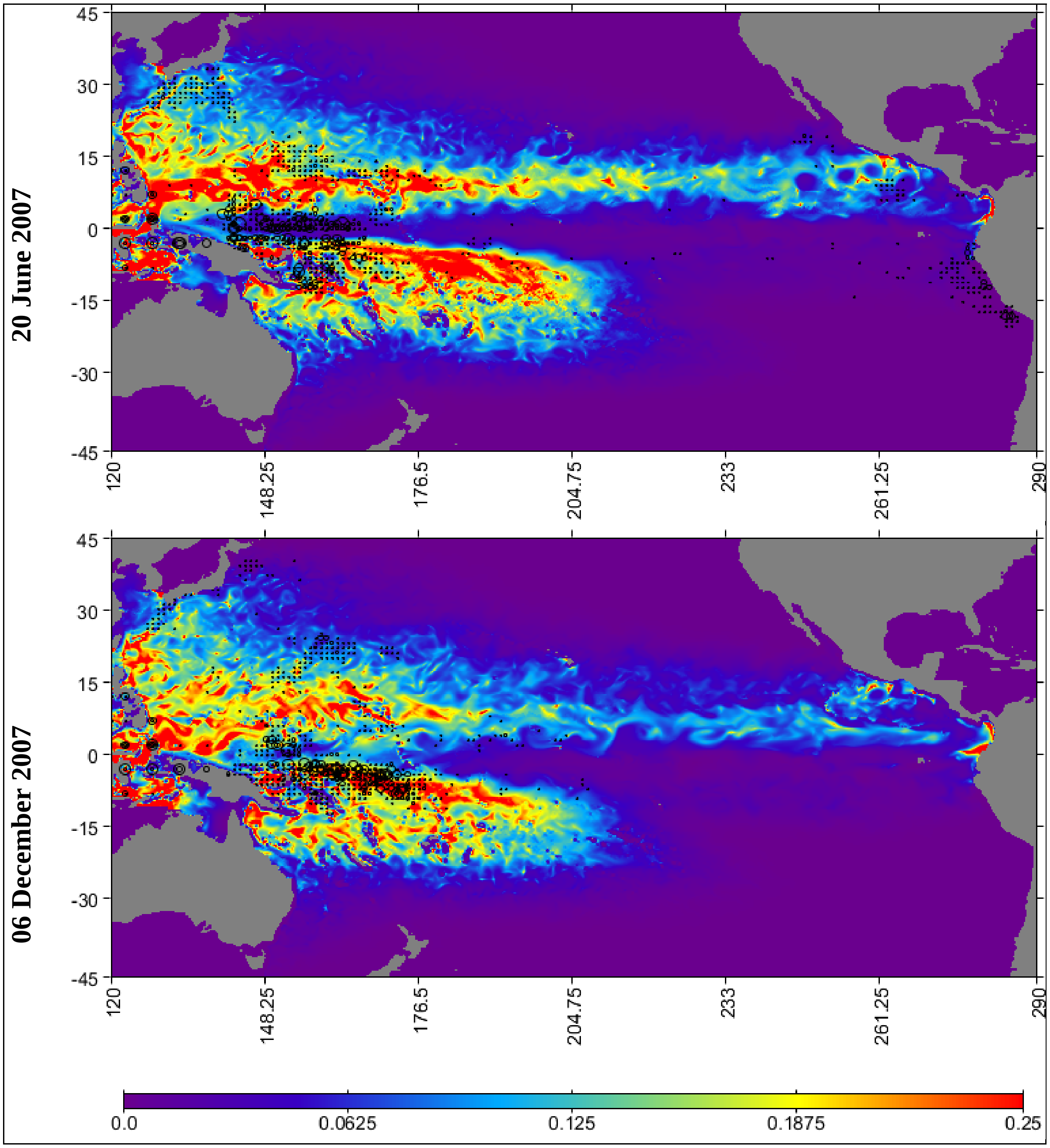

Figure 3.7. Predicted density of skipjack (sum of all cohorts) and total observed monthly catch (proportional to circles) for the weeks centered on 20 June and 6 December 2007, using the SEAPODYM-GLORYS.0.25° configuration calibrated with SODA.1° optimization experiments

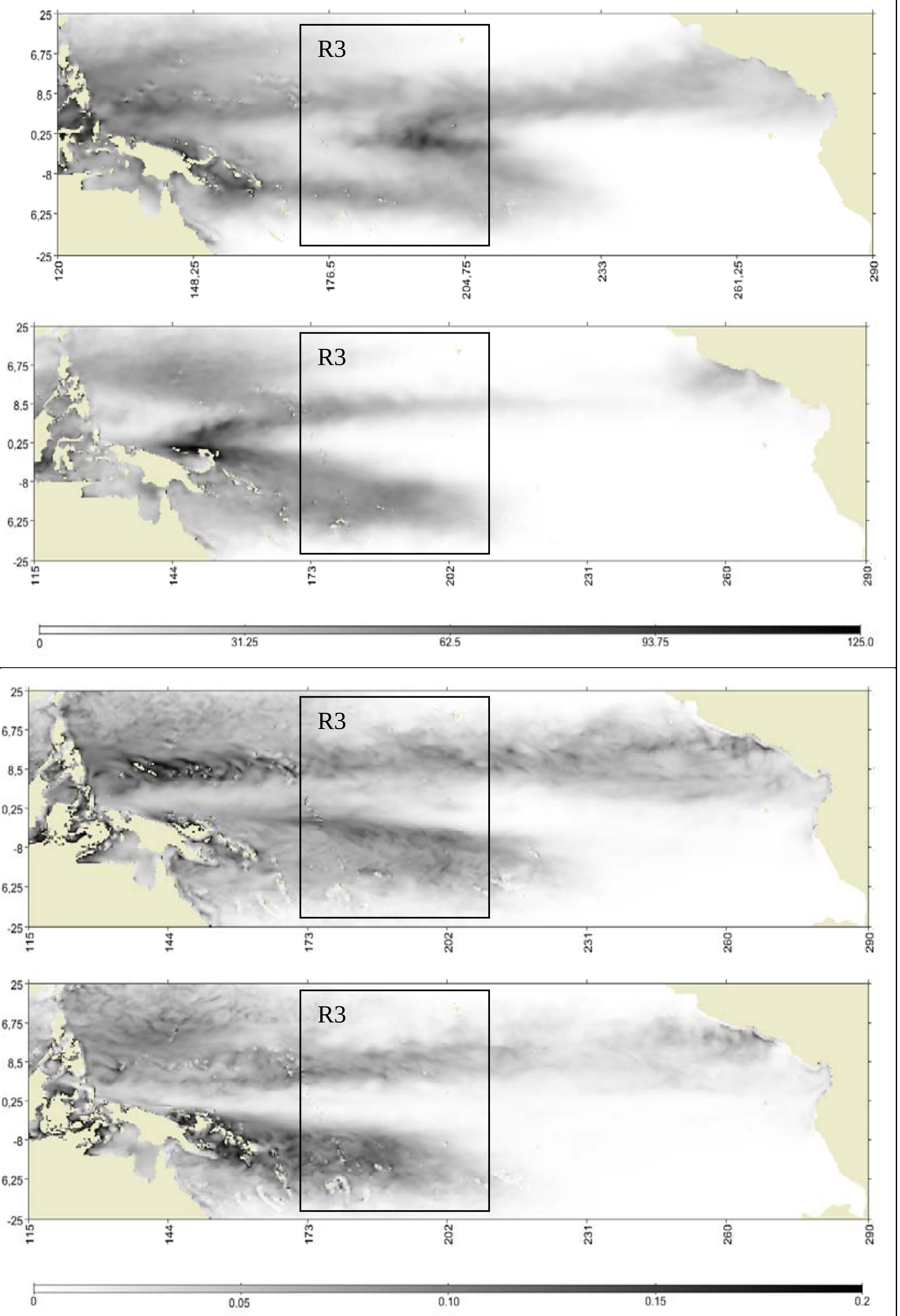

El Niño event:
average larvae
density

Oct 2009
-
Feb 2010

La Niña event:
average larvae
density

Oct 2010
-
Feb 2011

Post El Niño:
average
biomass of
young fish

Mar 2010
-
Apr 2010

Post la Niña:
average
biomass of
young fish

Mar 2011
-
Apr 2011

Figure 3.8. Impact of ENSO on Pacific skipjack (SEAPODYM-GLORYS &Mercator-Ocean). Predicted distribution of larval recruits (density in number per km^2) during last El Niño and La Niña events and following recruitment in the young cohorts. The region R3 defined for MULTIFAN-CL assessment is superimposed to highlight the change in this region due to ENSO.

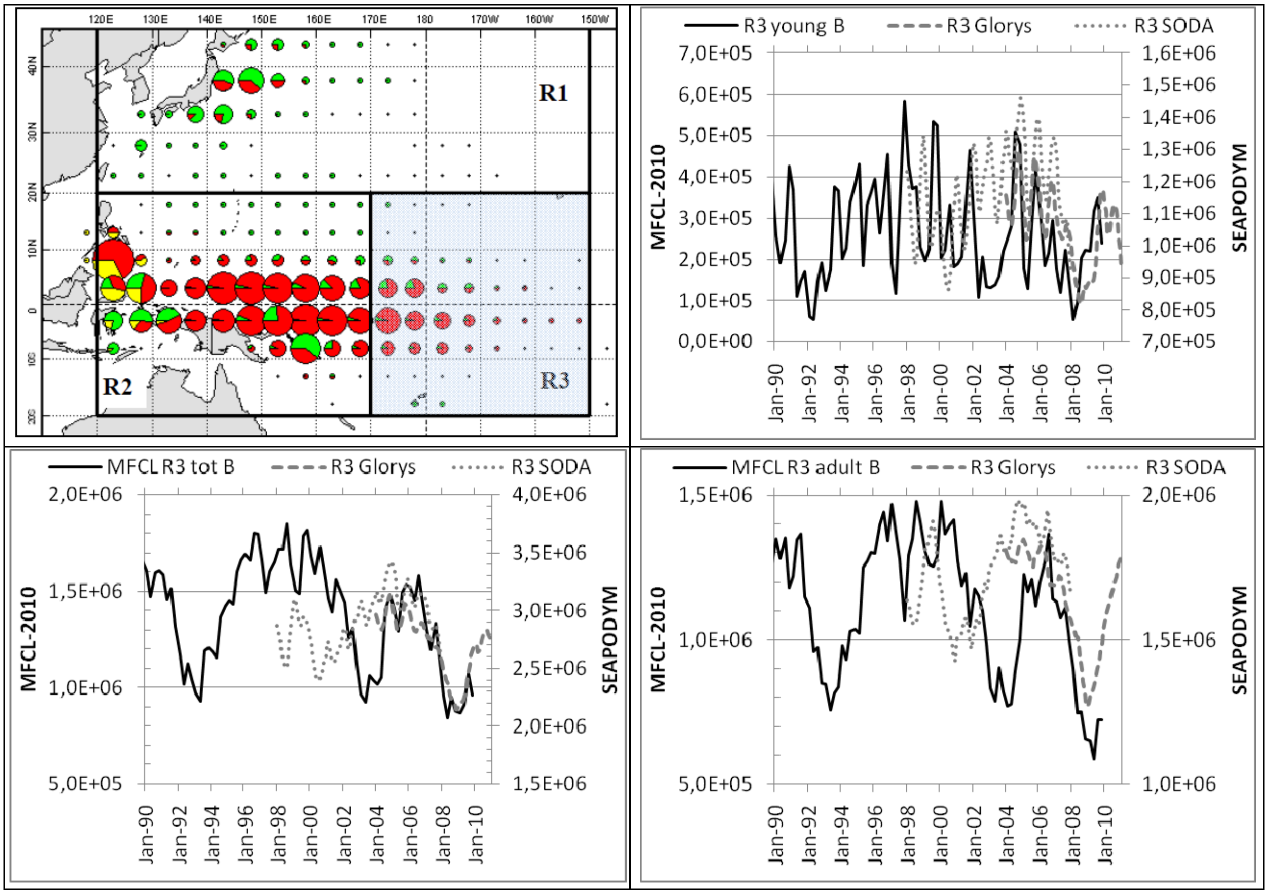

Figure 3.9. Map of skipjack catch (by gear) showing the region R3 defined for MULTIFAN-CL application, and for which estimates of young, adult and total biomass are extracted for comparison between SEAPODYM (dotted lines: SODA 1° and GLORYS-PSY3) and Multifan-CL (continuous line).

4.2.2 Regional analysis for the north-western Pacific

A detailed analysis for the north-western Pacific area was conducted to investigate the decrease of skipjack catch rate in the domestic Japanese fishery in 2008-09. This decrease was mainly observed in the middle-sized pole-and-line fishery and the coastal troll fishery that recorded its lowest catch at least since 2005 (Uosaki et al 2010). The study area coincides with the region R1 of the Multifan-CL application (Hoyle et al. 2010).

4.2.2.1 Oceanography

The region R1 is characterized by a highly dynamic circulation with the warm Kuroshio Current flowing along the south-eastern coast off Japan and encountering the cold water of the Oyashio Current to create a marked front extending far to the east. This Kuroshio extension (KE) shows low frequency variability with regular switches between elongated and contracted modes. In an elongated mode, the KE has a fairly stable energetic meandering jet while in the contracted mode, it has a weaker, variable and convoluted jet (Qiu and Chen 2005; Pierini and Dijkstra 2009). These different modes can be detected using altimetry data or by computing the kinetic energy from currents. Using altimetry data (AVISO CNES/CLS DUACS products) and the kinetic energy computed from surface currents of the GLORYS reanalysis, it appears that the Kuroshio extension has switched from the previous elongated mode of 2000-2005 to a new contracted mode in 2006 with a particularly well marked decrease of kinetic energy in 2009 in the main skipjack offshore fishing ground north of 35°N, between longitudes 140-160°E. In 2010, the KE was apparently switching again to a new elongated phase (Fig. 3.10). These phases were associated to changes in horizontal and vertical temperature structures (3.11) and also a decrease in primary production in the region between 15 and 30 % when comparing the periods 2002-05 (elongated) and 2008-09 (contracted). This decrease propagated in the groups at mid-trophic level (tuna forage) but in different proportions due to temperature and currents impact on their dynamics.

4.2.2.1 Variability in Japanese domestic skipjack fisheries

In addition to its tropical purse seine fleet, Japan has two pole-and-line fleets that catch skipjack: the domestic off-shore fleet and the tropical fleet. The offshore fleet is consisting of medium-size boats fishing seasonally in the sub-tropical and temperate home waters of Japan, mainly between May to November. The tropical fleet includes large boats fishing year-round in the tropical region except during the albacore fishing season between June to September, when the fleet moves to the temperate water far east off Japan. A domestic purse seine fleet also started to develop in the1980s and since contributed to increasing catch of skipjack, to reach about ~50% of the total domestic catch in the last few years. There are also miscellaneous fisheries (troll, set net and gillnet) catching skipjack and other tunas and tuna like species along the coasts of Japan. A gradual reduction in numbers of vessels has occurred in all pole-and-line fleets over the past decades leading in parallel to the decrease of catches by the Japanese distant-water and offshore fleet. In the 2000-2008 period, the skipjack catch oscillated between 112,000 and 183,000 t. In 2009, the catch dropped to a low record of 80,607 t (Uosaki et al 2010). This decline was mainly observed in the middle-sized pole-and-line fishery and the coastal troll fishery that recorded its lowest catch at least since 2005 (Uosaki et al 2010). Part of the overall catch decrease however, was due to a reduction of fishing effort for these fleets in 2007-2009 that was 23% below the average level of effort for the 2000-2005 period. The size structure of catch also changed since 2008 with an increasing ratio of small to large fish.

SEAPODYM and MULTIFAN-CL skipjack estimates are relatively close in their maximum level of biomass for region 1 (Fig. 3.12) but MULTIFAN-CL predicted higher range of variability of total biomass (~300,000-1,200,000 t) than SEAPODYM (~950,000-1,300,000). Both SEAPODYM model configurations with SODA 1°x month and GLORYS-PSY3 1/4°x week reproduced the changes observed in Japanese domestic fisheries for catch, CPUE and catch size (Fig. 3.13, and 3.14). These simulations also predicted a decrease in abundance of large skipjack in 2008-2009 in the KE and the subtropical North Pacific, while there is no predicted weak recruitment event in the young age classes (Fig. 3.12 and 3.15). Though the available MULTIFAN-CL assessment stopped in 2009, a low adult biomass was also predicted for the last year (Fig. 3.12).

A simulation was carried out to investigate the link between the tropical purse seine fishery and the Japanese domestic fishery, by removing the fishing effort of all tropical purse seine fisheries during the period of simulation. The result (Fig. 3.16) showed a large increase of biomass in the equatorial region that is the core habitat of the population where the maximum catch occurs, but no direct effect on the subtropical region. Of course, this result is to a certain extent linked to the total stock biomass estimate that needs to be confirmed with further optimization experiments using still more realistic forcing, higher resolution and better fishing data. At this stage of the analysis, the preliminary explanation for the recent decrease of adult biomass in region 1 would be a less favorable habitat in the KE and sub-tropical northern region for adult fish, leading to southward movements searching for better feeding habitat. This may have concentrated more large fish in the tropical region and contributed to exceptional catch rates by the tropical purse seine fishery in recent years (Fig 3.16). To confirm this hypothesis, additional simulations should be run with scenarios allowing to estimate the contribution of region 1 to the catch by tropical fisheries (e.g., simply setting spawning habitat to zero in this region).

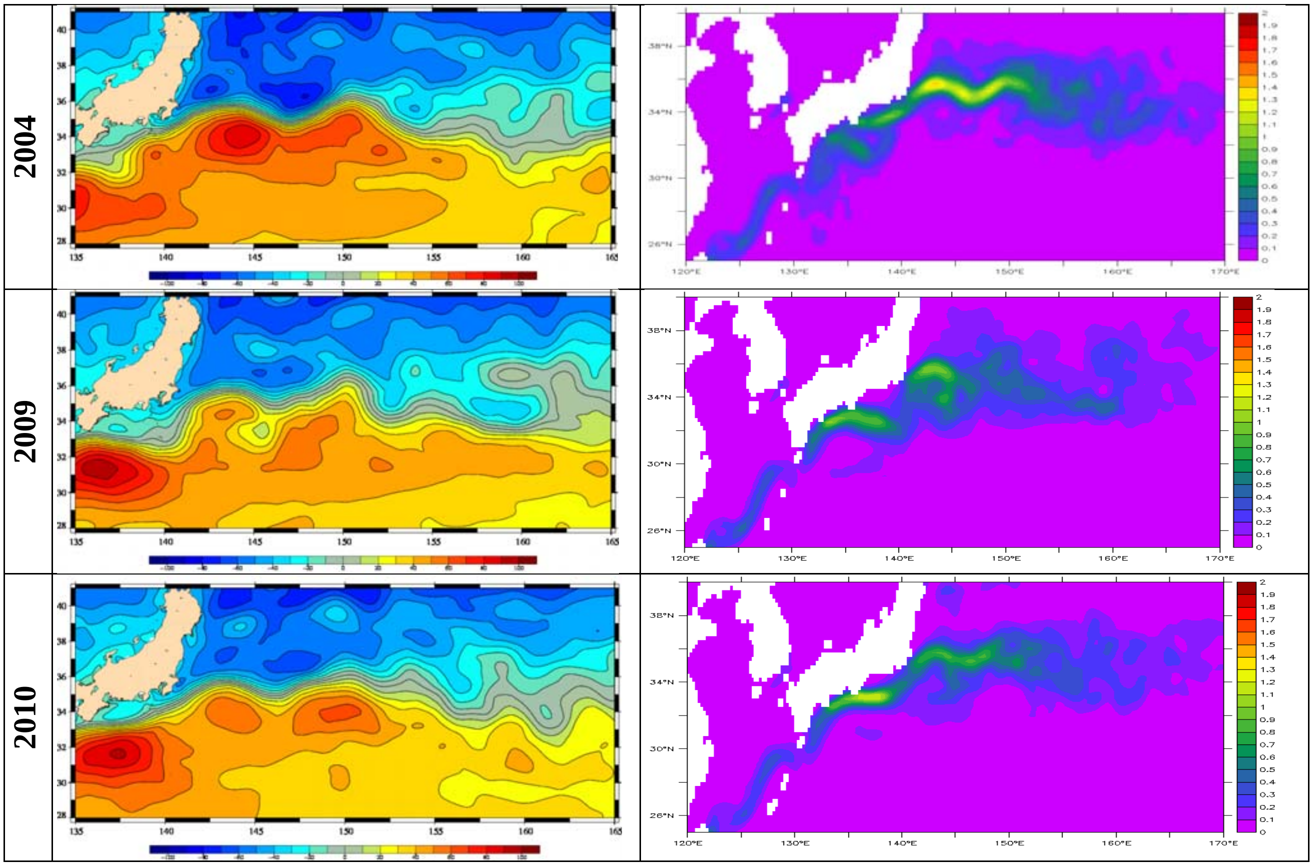

Figure 3.10. Yearly averaged Sea Surface Height fields (left) and kinetic energy in the surface layer (GLORYS reanalysis) in the Kuroshio extension showing a transition in 2006 between previous elongated mode (2000-2005) and a contracted mode in 2006-2009.

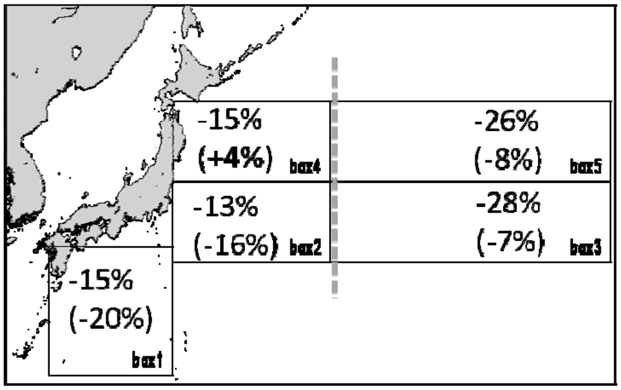

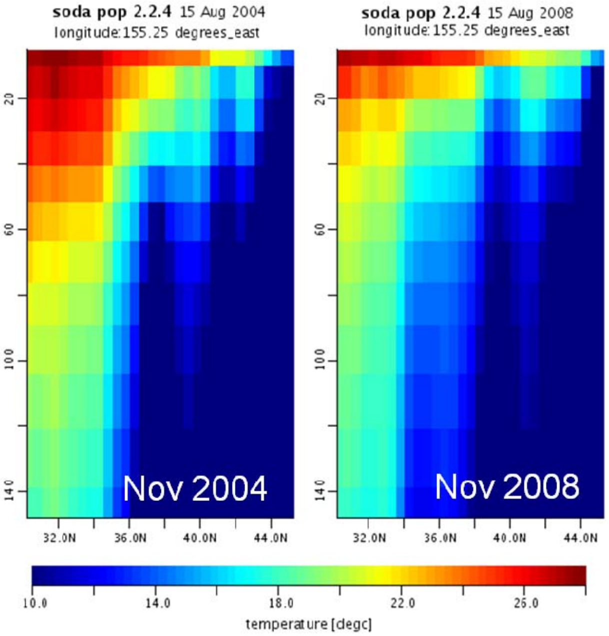

Figure 3.11. Change in mean primary production and surface daytime forage (between brackets) in geographical boxes along the Kuroshio extension, between 2002-05 and 2008-09. Vertical temperature structure from SODA reanalysis along a transect at 155.5° (grey dotted line) during an elongated (Nov 2004) and contracted (Nov 2008) phase.

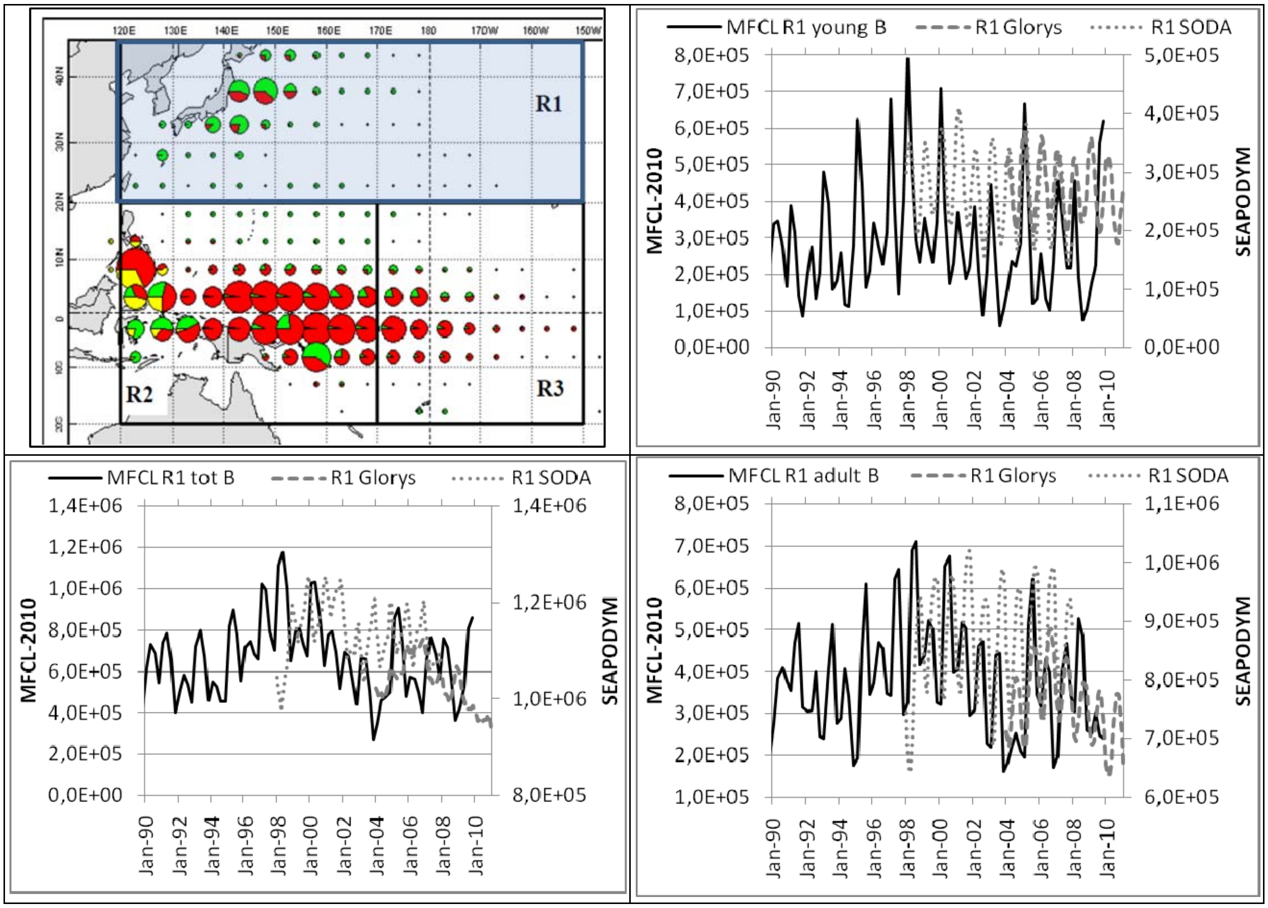

Figure 3.12. Map of skipjack catch (by gear) showing the study area coinciding with the region 1 of the MULTIFAN-CL application, and comparison for this region of SEAPODYM (dotted lines: SODA 1° and GLORYS-PSY3) and Multifan-CL (continuous line) estimates for young, adult and total biomass.

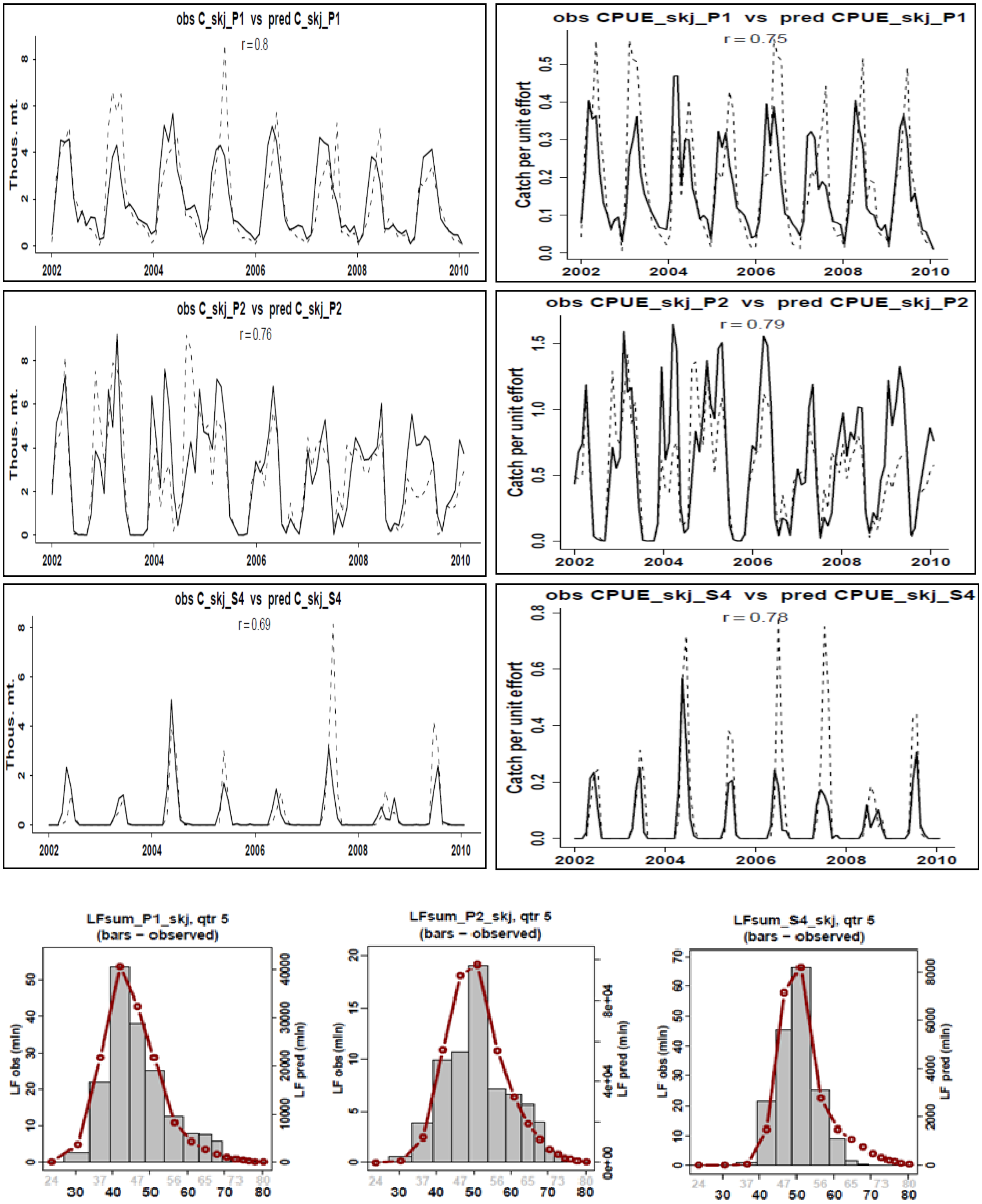

Figure 3.13. Observed and predicted weekly catch and CPUE, and size structure for small-medium (P1) and large (P2) pole and line, and purse seine (S4) Japanese domestic fisheries.

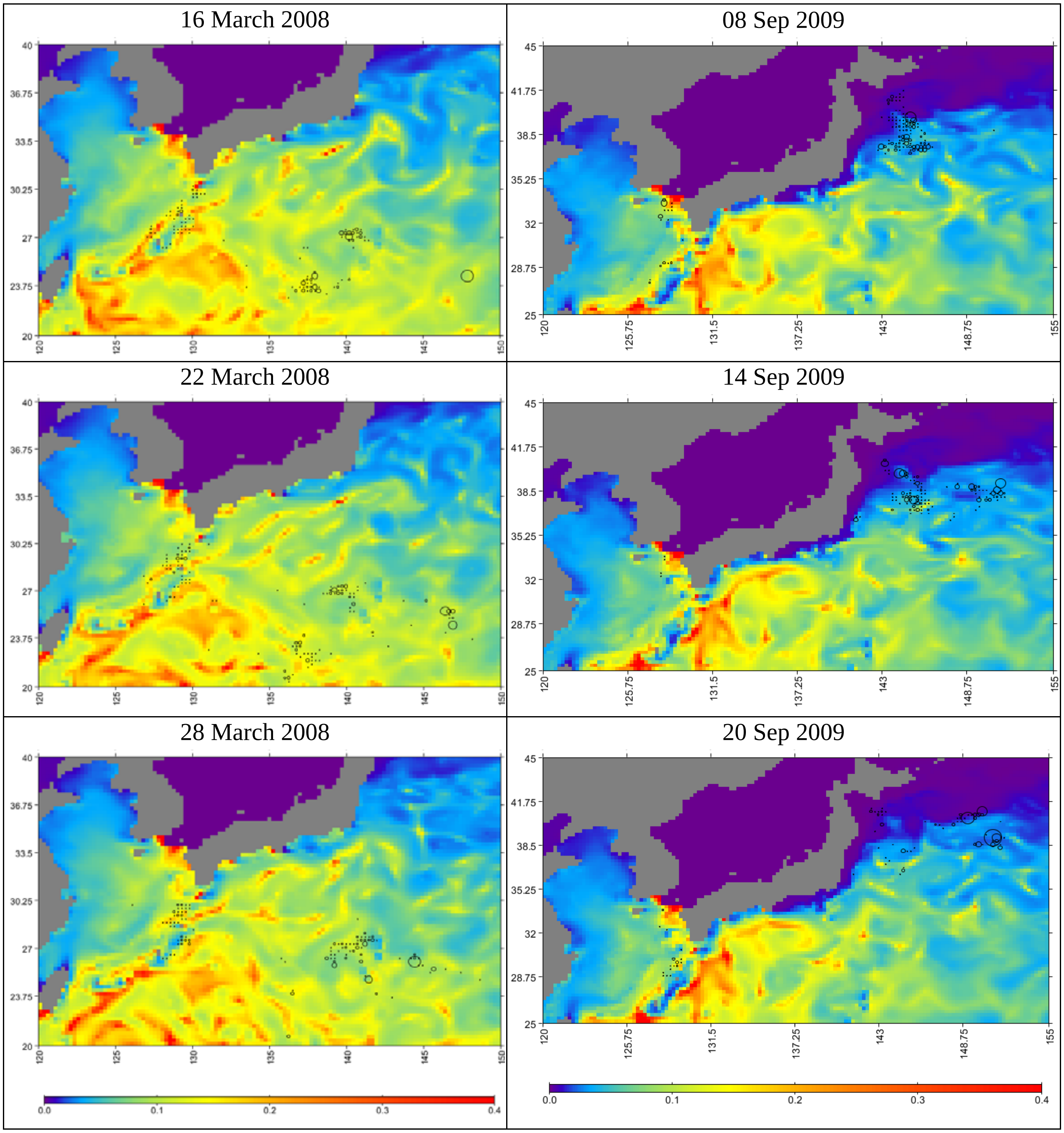

Figure 3.14. Two sequences of three 6-day periods with predicted density of skipjack (sum of all cohorts) and Japanese pole-and-line observed catch (proportional to circles)

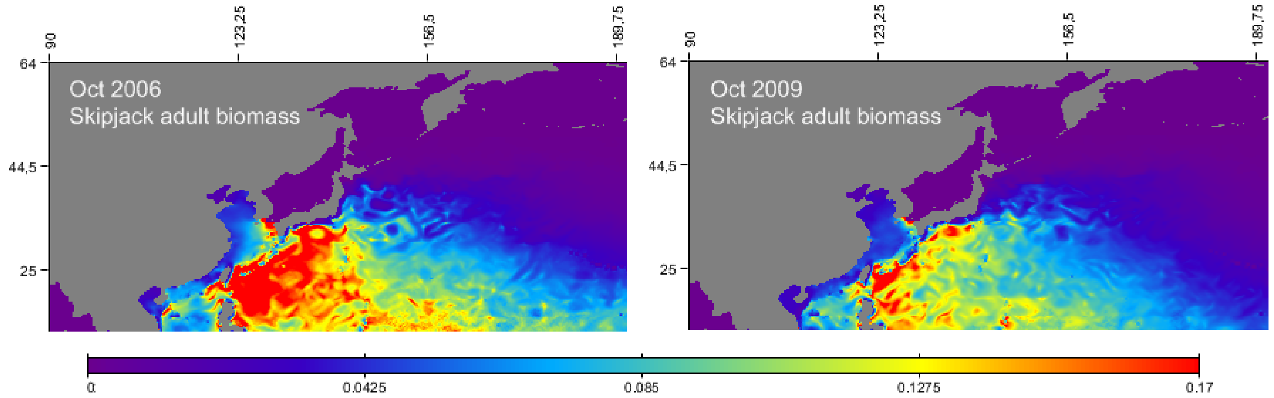

Figure 3.15. Comparison of spatial distribution (bottom) of adult density (g/m^2) in October 2006 and 2009.

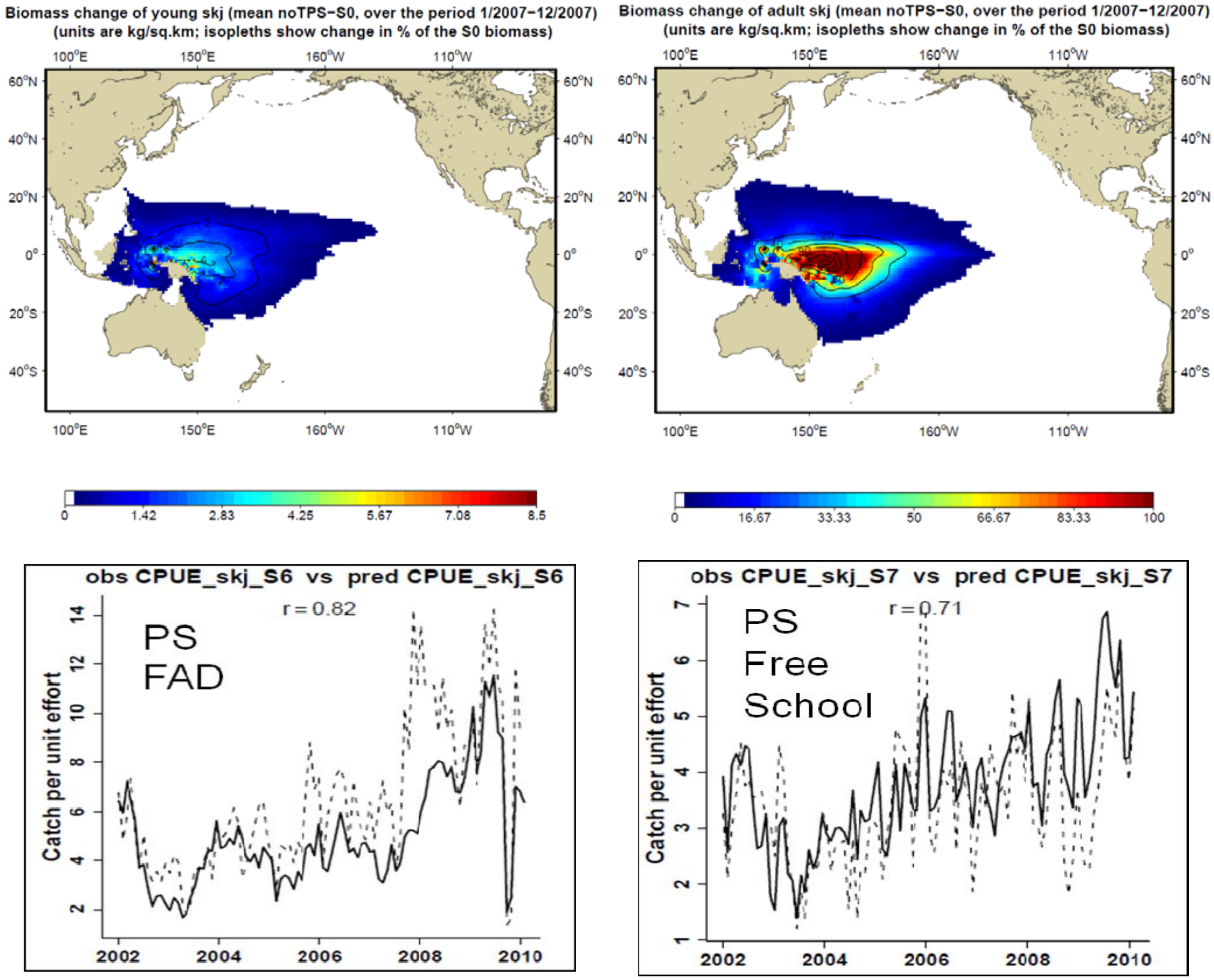
Biomass change of young skj (mean noTPS−S0, over the period 1/2007−12/2007) (units are kg/sq.km; isopleths show change in % of the S0 biomass)

Biomass change of adult skj (mean noTPS−S0, over the period 1/2007−12/2007) (units are kg/sq.km; isopleths show change in % of the S0 biomass)

obs CPUE_skj_S6 vs pred CPUE_skj_S6

obs CPUE_skj_S7 vs pred CPUE_skj_S7

Figure 3.16. Top: change for the year 2007 in biomass of young (left) and adult (right) skipjack in a scenario with no tropical purse seine fishing. Bottom: Observed (dotted line) and predicted (continuous line) CPUE for the tropical FAD and Free School purse-seine fisheries.

4.2.3 EEZ analysis of skipjack (Papua New Guinea)

Using the model configuration and optimal parameterization achieved for the reference fit above, it becomes possible to investigate in detail the dynamics of skipjack and its fisheries at the level of Pacific Countries' EEZ. Model outputs for the EEZ of Papua New Guinea are provided as an example.

4.2.3.1 Oceanography

Tropical waters flowing westward in the South Equatorial Current (SEC) enter the Solomon Sea between PNG and the Solomon Islands turning through the south-east under the constraint of the bathymetry. Closer to the coast of PNG, the circulation is dominated by the New Guinea Coastal Current (NGCC) and its associated under-current (NGCU). Off the southern coast of PNG, the North Queensland Current (NQC) flowing northward along the Australia coast turns east and connects to the Gulf of Papua and then the Solomon Sea. During the southeast monsoon (May to September), the NGCC current flows northwestward along the coast, generally reaching speeds close to or above 0.5 m/s. During the northwest monsoon (November to March), it weakens and usually reverses direction to flow southeastward at similar speeds (Kuroda, 2000). However this reversal does not always happen. In particular, Ueki et al. (2003) observed that the NGCC did not reverse at all during the 1997-1998 El Niño event. ENSO is clearly the dominant interannual signal in the region.

The current structure and the complex bathymetry in the Solomon Sea induce important meso-scale activity modulated by intra-seasonal to interannual (ENSO) variability. In particular, transition phases between El Niño and La Niña phases showed intense mesoscale activity with a well-marked cyclonic signature at the mouth of the Solomon strait. Such structures associated with strong eddy mixing should contribute to significant water mass transformations (Melet et al. 2010).

Water exits the Solomon Sea to the Bismark Sea in the northwest through three passages: Vitiaz Strait with the NGCC, St. George's Channel and Solomon Strait. Circulation in the Bismarck Sea is constrained by the topography and the fluxes from these three passages, and the reverse of the NGCC. Undercurrent branches of these three currents finally join the under equatorial current and likely play an important role by enriching the equatorial waters with iron (coming from the runoff and the Sepik river) that is a limiting factor for primary production in the central Pacific. The Solomon and Bismark Seas likely benefit also of the coastal runoff to support higher local primary productivity.

4.2.3.1 Variability of Skipjack biomass and fisheries in PNG

First, the estimates of the model are compared at a regional scale level with MULTIFAN-CL estimate (Hoyle et al. 2010), for the western equatorial region R2 (Fig. 3.17). This is the core region for skipjack fisheries. Biomass estimates from SEAPODYM are two times higher than with MULTIFAN-CL. Abrupt increases due to strong El Nino events of 1997-98, 2004-05 and 2009-10 are noticeable in MULTIFAN-CL series of young fish, but not all the low peaks expected due to La Nina events (1998-99; 2000-01; 2007-08;2010-11), while they occur in SEAPODYM series. The adult biomass estimated from MULTIFAN-CL showed a drastic decline between 2007 and 2009, which is not the case for the SEAPODYM estimate based on GLORYS-PSY3 configuration. From the three regions, it is the one with the largest discrepancies between estimates from MULTIFAN-CL and SEAPODYM, and particularly the GLORYS-PSY3 configuration for the most recent period after 2008. While SEAPODYM results suggest an increase in adult biomass in this region, MULTIFAN-CL predicted a large decrease in adult biomass, very similar to the one predicted in region 3 (Fig 3.9). A possible reason of this difference between models is that MULTIFAN-CL cannot take into account the dominant inter-annual variability (ENSO) in the biomass exchanges between regions 2 and 3.

Total biomass and recruitment estimates were extracted for the EEZ area and are shown on figure 3.18. The total biomass was estimated to have fluctuated between four and six hundred thousand metric tonnes since 2008. The recruitment showed a weak seasonal signal peaking between May and July. Considering the age of 3 months for the recruited cohort, the seasonal peak of spawning would thus occur during the transition period between southeast and northwest monsoon from March to May. The most favourable areas with highest density of larvae are predicted to currently occur north of the Solomon and Bismarck Seas (Fig. 3.20), though during El Niño phases, it seems that larvae concentrate closer to the coasts (Fig. 3.8). The model predicts that Solomon and Bismarck Seas support a high density of both young and adult skipjack most of the time, with a more patchy distribution in the Solomon Sea influenced by the meso-scale activity in this area (Fig. 3.20).These two regions are effectively key areas of the purse seine fisheries, and though high resolution fishing data were not available after 2008, i.e., for the most reliable period of simulation with this configuration, there is already a very good match between observed and predicted catch of the different fleets operating in the PNG’s EEZ (Fig. 3.21 and 3.22).

The model can be used to investigate fishing strategy and fishing management options at the EEZ scale. It becomes also possible to envisage near real time update of this simulation. The interest of such products for the monitoring of fisheries need to be discussed and evaluated.

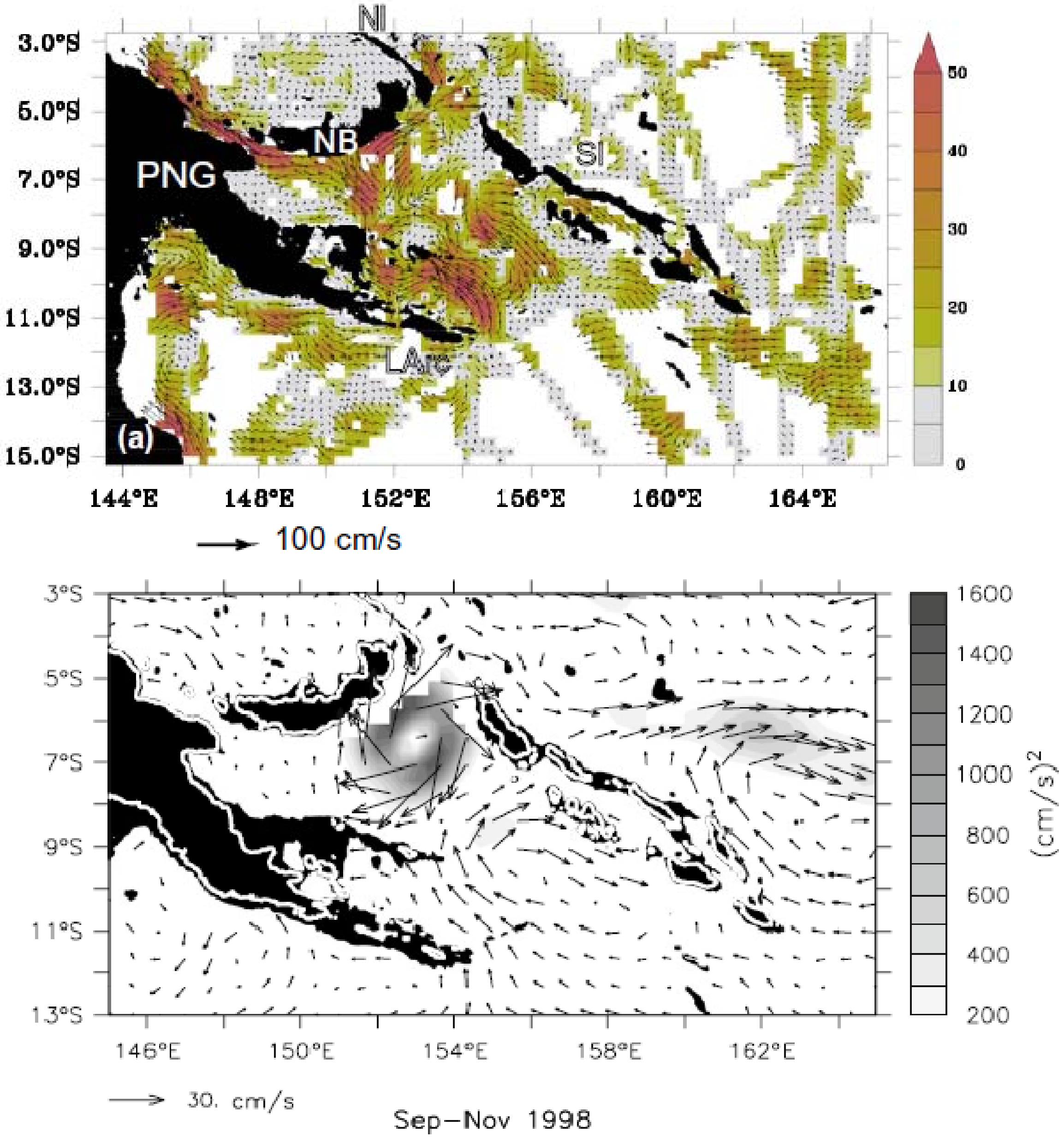

Figure 3.17. Circulation around Papua New Guinea. **Top** (from Cravatte et al. 2011): mean surface currents (20-100 m) in cm/s (grid points with no data are blanked). **Bottom** (from Melet et al., 2010): Plot of the Eddy Kinetic Energy (cm^2/s^2) for the Sep-Nov 1998 period (background color) and surface anomalies of the geostrophic current for the same periods. PNG: Papua New Guinea; NB: New Britain; NI: New Ireland; SI: Solomon Islands; LArc: Louisiane Archipelago.

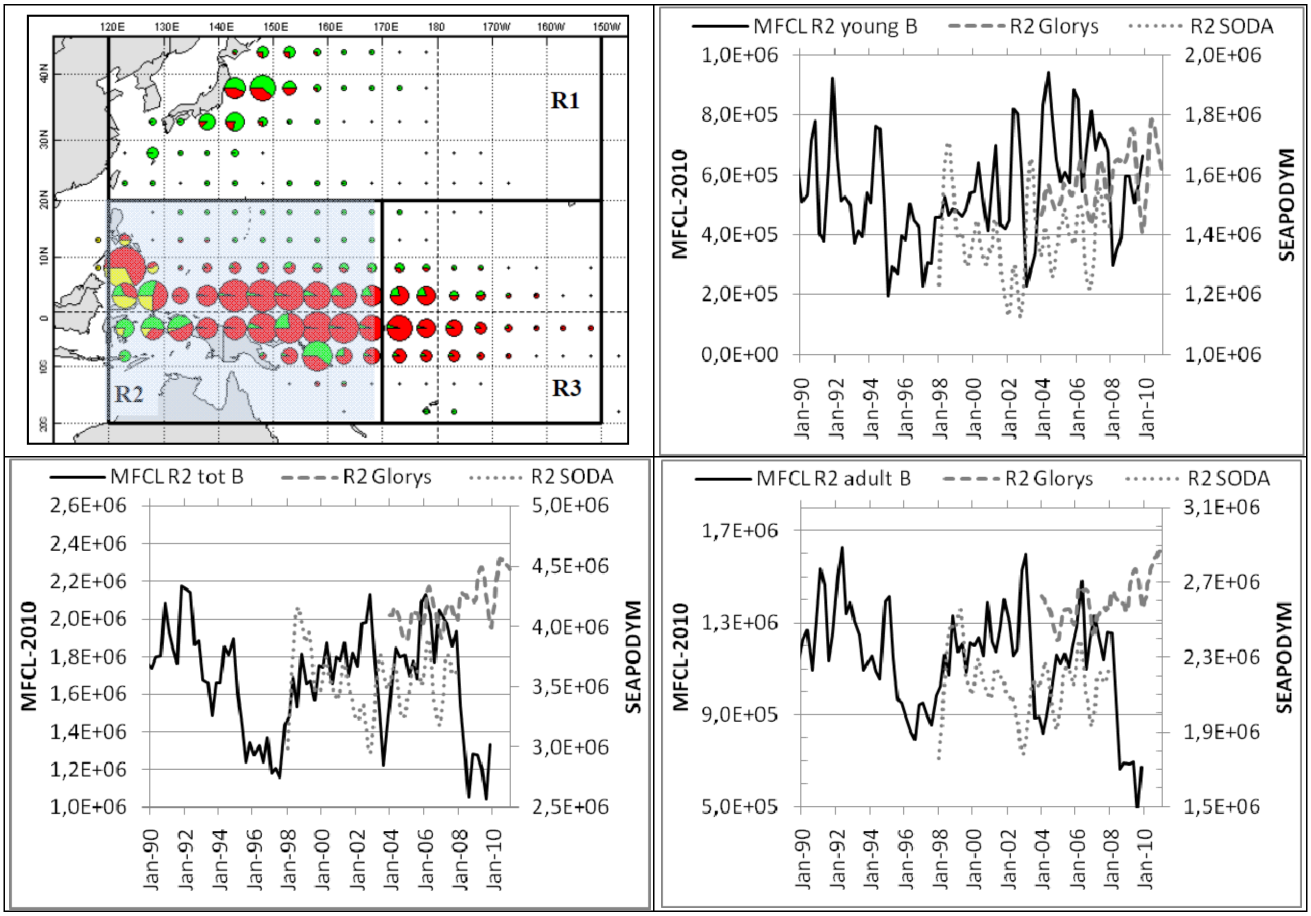

Figure 3.18. Comparison of time series estimates from SEAPODYM (dotted lines: SODA and GLORYS-PSY3) and MULTIFAN-CL (continuous line) for total, young and adult biomass of skipjack in the region 2 (R2).

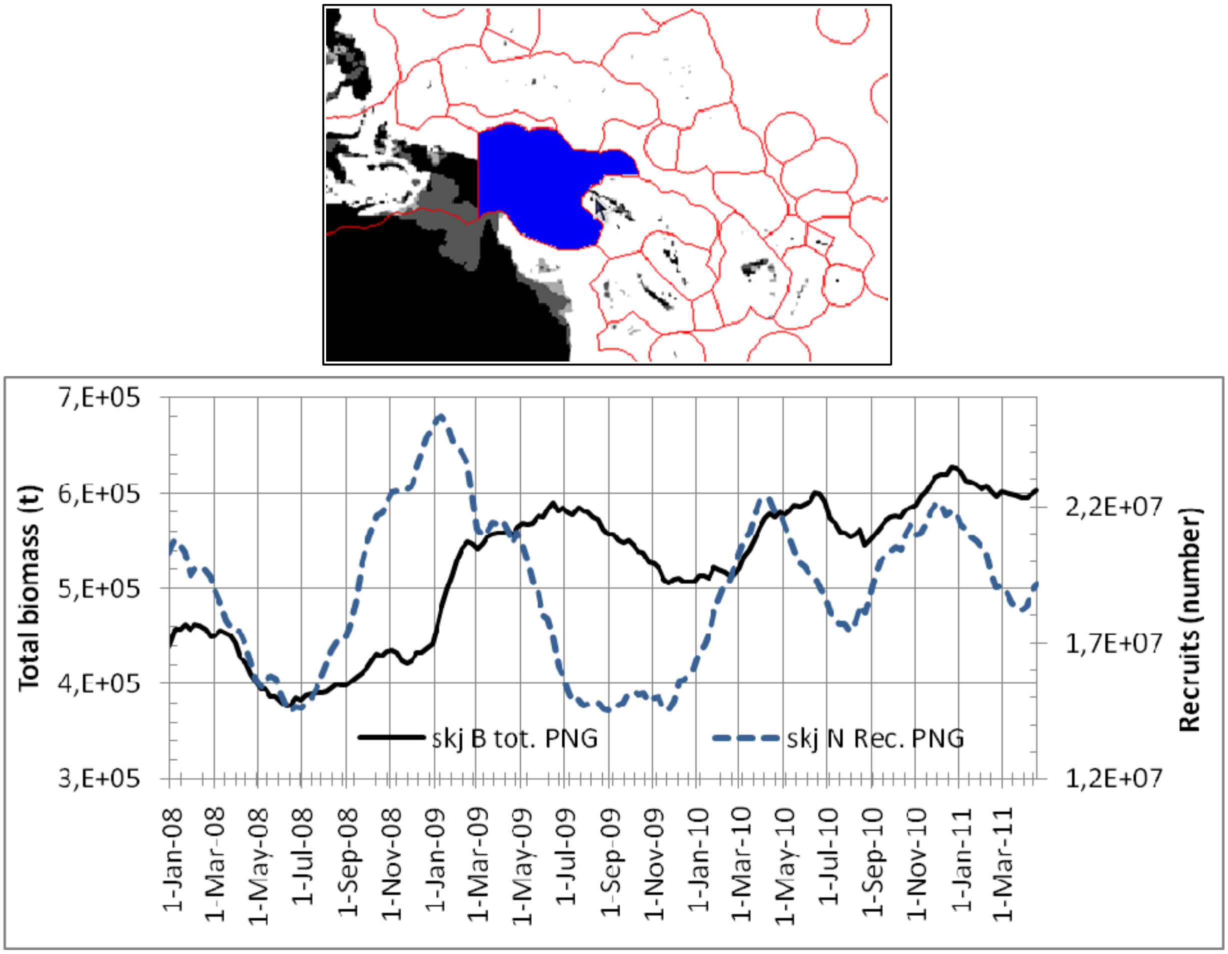

Figure 3.19. Time series of recruitment (dotted line; in number of fish) and total biomass (black line; in metric tonnes) of skipjack predicted for the EEZ of Papua New Guinea (blue area) based on the SEAPODYM –GLORYS-PSY3 ¼°x week configuration.

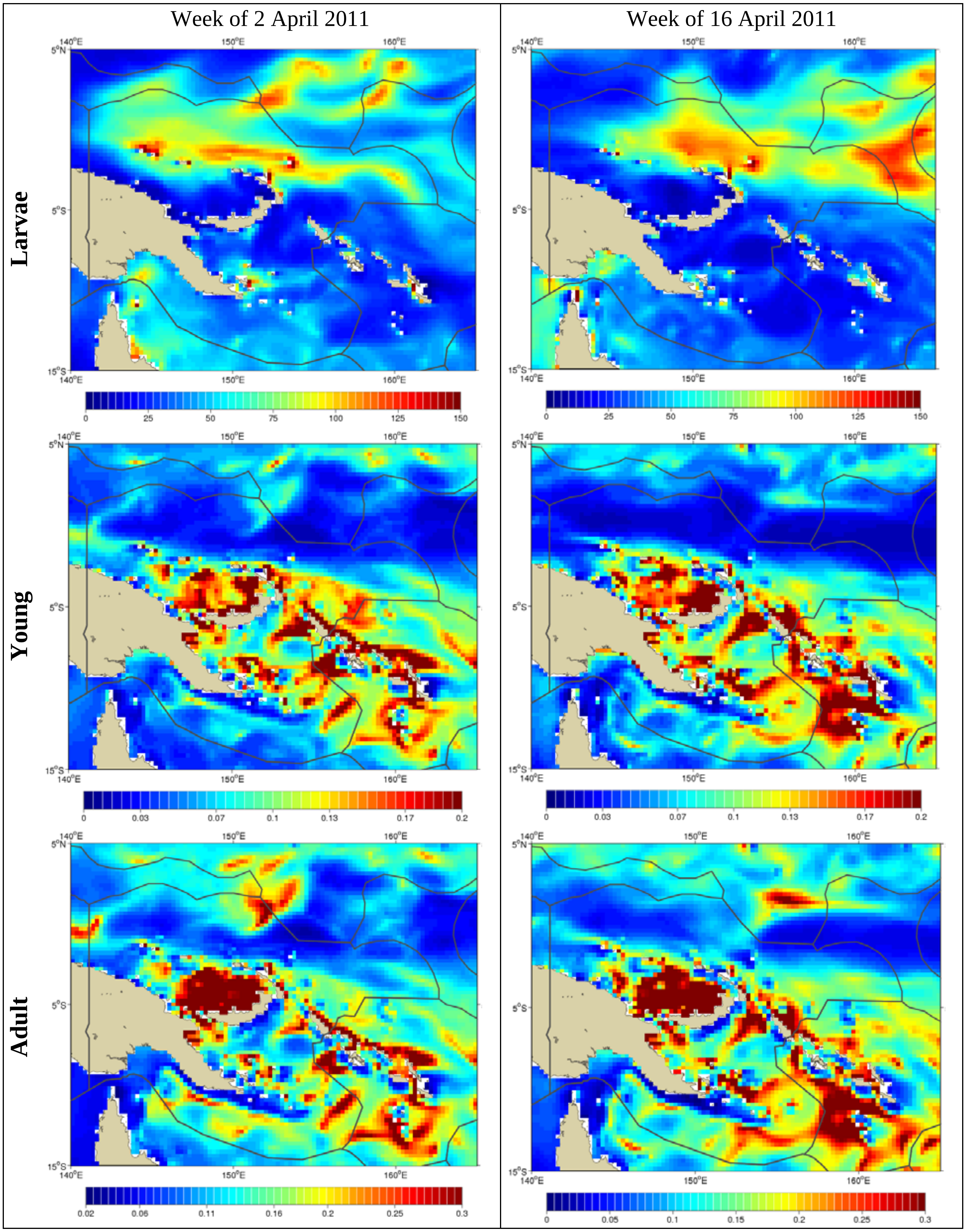

Figure 3.20: Model prediction of skipjack larvae, young fish (sum of cohorts between age 3 and 9 months) and adult (sum of cohorts between age 10 and 48+ months) density for the last available month in the weeks centered on 2 April 2011 and 16 April 2011.

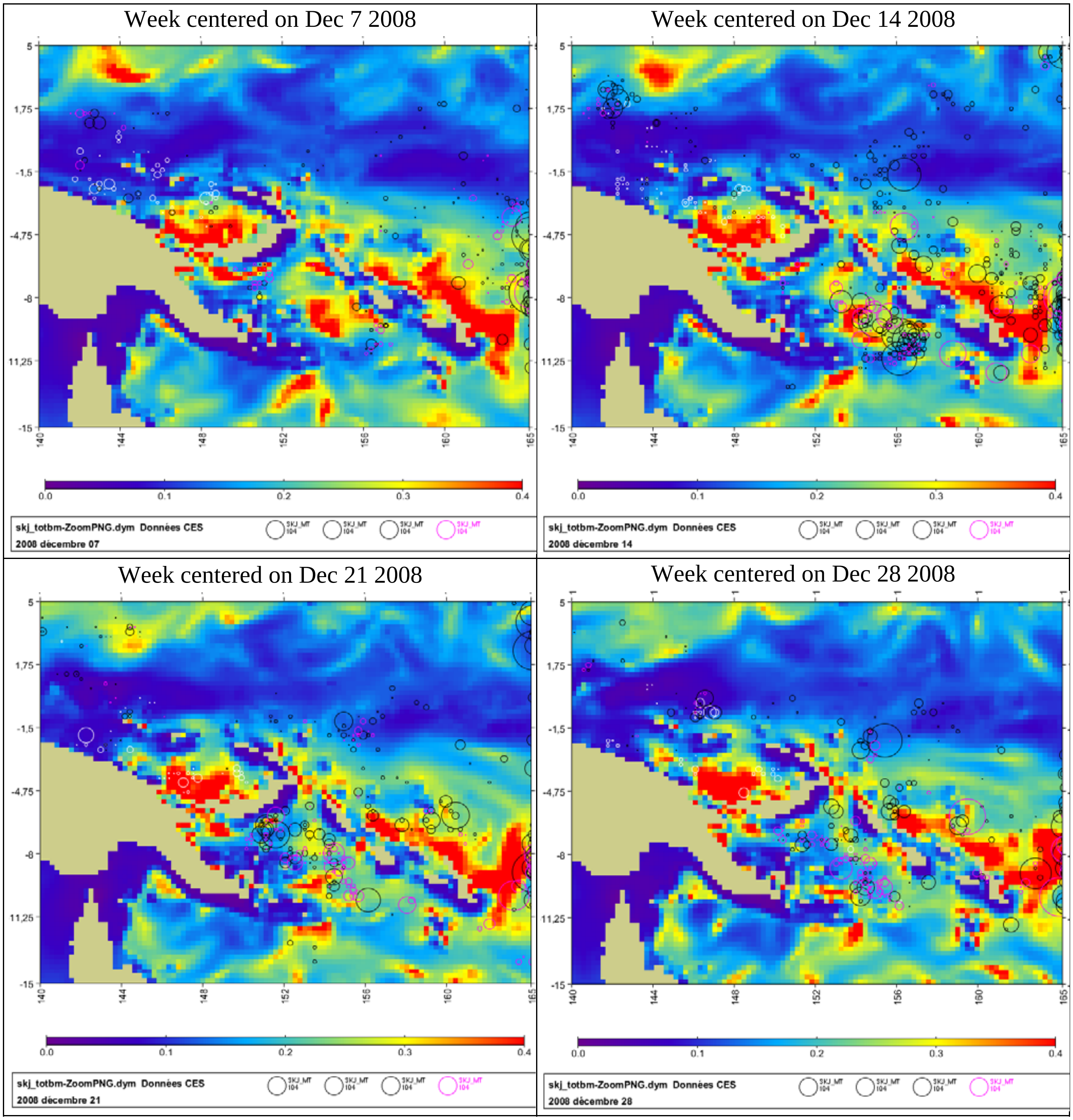

Week centered on Dec 7 2008

Week centered on Dec 14 2008

Week centered on Dec 21 2008

Week centered on Dec 28 2008

Figure 3.21: Model prediction of skipjack stock (sum of all young and adult cohorts) density for the last 4 weeks of Dec 2008 for which ¼° x week fishing data were available, with CPUE of purse seine fisheries characterized by the fishing strategy, i.e. anchored (white circles), free school (purple circles) and associated (log, object and FAD; black circles) sets.

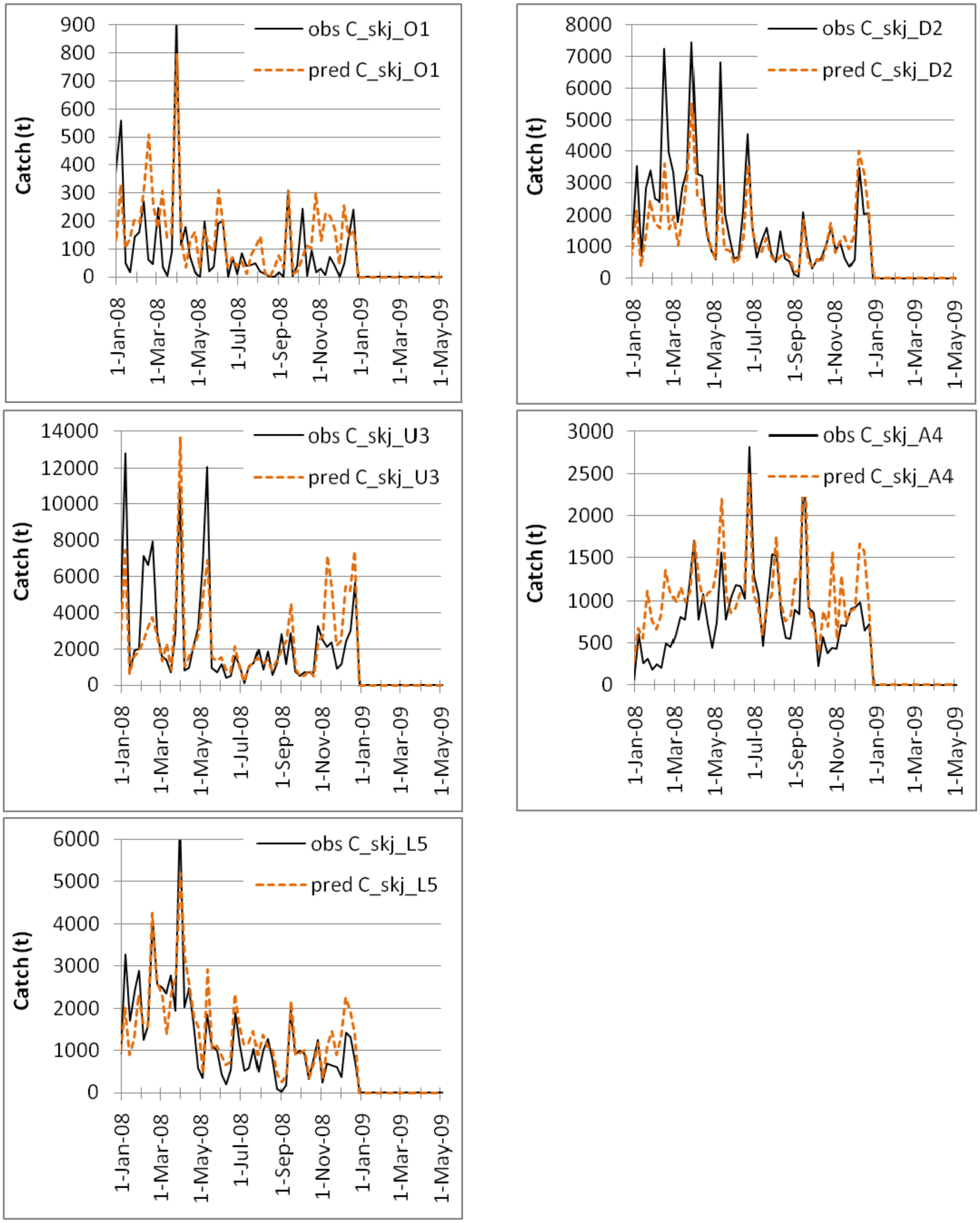

Figure3.22: Predicted catch of skipjack by purse seine fisheries in PNG EEZ. O1: sets associated to floating object; D2: drifting FADs; U3: unassociated (free school); A4: anchored FAD; L5: logs.

4.2.4 ENSO-related forecast

The present results confirm those obtained in previous works showing a strong influence of ENSO events on the dynamics of Pacific skipjack. There is enhancement of spawning and larvae survival conditions during and just after El Niño periods all over the equatorial Pacific. Conversely during la Niña events, only the western central Pacific is favorable. The result is a higher recruitment in the following cohorts that is propagated until in the oldest (4+ years) adult cohorts, with a high correlation between SOI and recruitment shifted by eight months (Senina et al 2008). The propagation of higher recruitment due to the major El Niño events in 1997-98, 2004-04 and the most recent one in 2009-10 is clearly visible in the estimated biomass time series. However, since 1999, La Niña events have been more frequent and intense than El Niño events, with marked events between 1998-2001, 2007-08 and recently in 2010-11, leading to an overall decreasing trend of average skipjack biomass for the last decade (Fig. 3.9).

Given the strong relationship between ENSO and skipjack recruitment, a simple index of skipjack biomass based on recruitment proportional to the Southern Oscillation Index (SOI) has been proposed (Lehodey 2000) to forecast the trend of the stock with several months in advance. This simple index shows a relatively good match (Fig. 3.9) with the last estimate of relative biomass with Multifan-CL (Hoyle et al 2010).

Since ENSO-neutral conditions have developed in the 2nd quarter of 2011 and are expected to continue until the end of the year, this forecast is based on a neutral ENSO situation (SOI = 0). ***In this case, skipjack biomass would reach a low peak at the end of 2011. Unless an El Niño event develops in 2012, the skipjack biomass forecasted for 2012-13 should remain in the low range of long term productivity.***

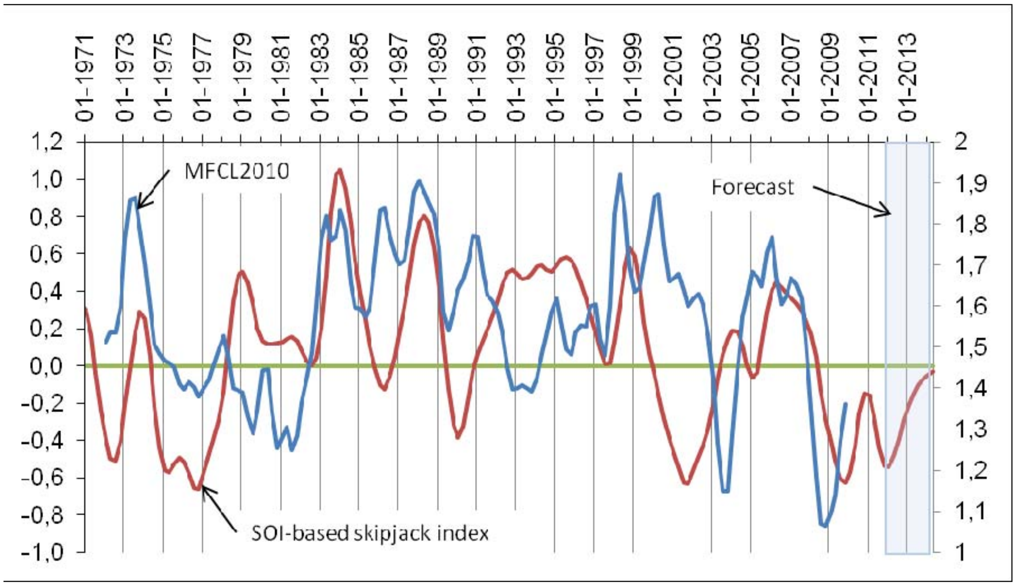

Figure 3.23. Pacific skipjack biomass index (red line) assuming a recruitment of skipjack linked to Southern Oscillation Index (SOI) with positive effect due to El Niño events (Lehodey, 2000). Last available estimate from stock assessment model Multifan-CL (Hoyle et al., 2010) is superimposed (blue line). Forecast is based on a neutral ENSO situation.

5 Climate Change impact on tuna stocks

Results from preliminary simulations carried out with SEAPODYM to investigate the impact of climate change on Pacific tuna stocks have been published in Lehodey et al. (2010) and updated in a chapter of the SPC Climate Change Risk Assessment Report (SPC, *in press*) together with a detailed review of the links between the main expected changes in environmental variables and the physiology and biology of tunas.

Environmental forcing inputs for SEAPODYM are predicted from a biogeochemical model (PISCES) coupled to a climate model (IPSL-CM4). The scenario used was the SRES A2 IPCC scenario for the 21th century, i.e., atmospheric CO_2 concentrations reaching 850 ppm in the year 2100, and historical data between 1860 and 2000.

Important sources of uncertainty and gaps in knowledge have been highlighted that limit the confidence in these preliminary results:

1- Global climate models simulating changes in the Earth's climate by coupling the atmosphere, ocean, land surface and ice regions, and the exchanges and interactions between them still run to a coarse spatial resolution resulting in some biases. While these biases are not critical to analyse projected trends of climate, they have larger consequences for assessing the effects on ecosystems and the biology of key species. For example, an error in projecting water temperature of 1 or 2 °C could significantly misrepresent the location of suitable spawning habitat for a tuna species.

2- A crucial gap in knowledge is the uncertainty about projected dissolved O_2 concentrations in the ocean associated with the carbon-to-nitrogen (C/N) ratio of organic matter. Using a fixed C/N ratio, the IPSL-CM4 simulations projected increased concentrations of O_2 in the equatorial thermocline due to reduced biological production within the water masses flowing to the equator. However, it is possible that under higher CO_2 levels conditions, the C/N ratio increases and that the respiration of this excess organic carbon decrease O_2 in tropical sub-surface waters, therefore reinforcing the existing low levels of $O_{2,}$ and suboxic areas in the eastern Pacific.

3- The calibration of the SEAPODYM model used for projection was done using fisheries catch data from 1985 to 2000 and compared against results from the simulation forced by the climate model during the historical period. Biases in the environmental forcing (cf above) and the mismatch between actual and predicted ENSO timing during the historical period make the model parameter optimization much more difficult to achieve and increase the uncertainty on parameter estimates.

The new climate simulations produced for the next IPCC assessment report (AR5) should provide enhanced forcing, especially with increased resolution in atmospheric models. Nevertheless, before using these new climate model outputs, a second series of optimization experiment and forecast with SEAPODYM is currently conducted to investigate the sensitivity of results to oxygen concentration, after a correction of the bias in the ocean temperature fields.

5.1 Method

5.1.1 Correction of temperature

Too coarse resolution in the atmospheric component of the climate model system can create a latitudinal shift in the atmospheric circulation that is propagated to the ocean dynamics. The figure 4.1 shows an example of the temperature bias that can result from this lack of resolution. While there is a good fit between model prediction and climatological data (Levitus) in the tropical region, a difference that can reach 5°C is observed in the subtropical and temperate region.

To correct this bias, the temperature anomaly of the IPSL simulation has been extracted using a climatological average from the model for the historical period (1900-2000). Then a weighting function based on latitude has been used to correct the anomaly (Figure 4.1), with the objective of keeping unchanged the original prediction in the tropical region but correcting the temperature in higher latitude according to the climatology from observation (Eq. 4.1).

$$T_c = \left[\left(f(lat) \cdot T_{cl-obs}\right) + \left(\left(1 - f(lat)\right) \cdot T_{cl-mod}\right)\right] + T_{anom} \qquad (4.1)$$

where
T_c: Corrected temperature (IPSL corrected)
T_{cl-obs}: Temperature climatology from observation (Levitus)
T_{cl-mod}: Temperature climatology from biased model (average IPSL 1900-2000)
T_{anom}: Temperature anomaly (difference between IPSL temperature and T_{cl-mod})

and

$$f(lat) = a/\left[(1-a) \cdot e^{(-b|lat+5|)} + a\right] \qquad (4.2)$$

with a = 5e-12 and b = 0.95

5.1.2 Dissolved oxygen concentration

The sensitivity of the model projection to dissolved oxygen concentration is investigated with a simulation using a climatology of historical observations (Levitus) instead of the prognostic value predicted from the biogeochemical model. Therefore, the effect of projected increase in oxygen from the IPSL simulation is compared to a scenario with "no change" from historical values (Fig. 4.2).

5.2 Skipjack optimization based on IPSL - corrected historical forcing

The correction of temperature bias in IPSL-CM4 climate outputs and the upgrade of the skipjack fishing dataset resulted in a major improvement in prediction of catch and CPUE of all fisheries (see detail in appendix 2), a reasonable overall spatial correlation (Fig. 4.2) and more coherent parameterization than in previous experiment (Table 1) even if all parameters cannot be estimated together. But this is also the case in other experiments. In general, there is not enough realism in the forcing and a lack of critical data for some life stage (e.g., larvae) or mechanisms (e.g., movement) to achieve optimization of all parameters. Nevertheless, temperature and oxygen parameters for habitat are more realistic than in previous IPSL forcing experiments and it was possible to optimize α that is a key parameter to define the spawning habitat.

The total Pacific skipjack biomass estimate fluctuates in a range of 10.5- 12.5 million tonnes, close to the range estimated in SODA optimization experiment (9-11 million tonnes). The spatial dynamics and overall density distribution of larvae, young and adult fish (Fig. 4.5) are also very similar to the results of SODA experiment, with obviously more diffuse patterns due to lower resolution, lack of mesoscale activity and also parameterization of temperature spawning habitat that had to be fixed to a relatively large value. Nevertheless, the fit to fishing data and the optimization close to the most realistic SODA experiment indicate a major improvement in comparison of previous IPSL-CM4 simulations.

Table 4.1: Estimates of habitats and movement parameters of previous simulations and the new one with IPSL after correction of temperature bias (IPSL-c). Note that the fishing data set also has been upgraded in the last experiments.

Parameters estimated by the model		Unit	NCEP	SODA-1°	IPSL	IPSL-c
	Habitats					
T_s	Optimum of the spawning temperature function	°C	29.8	28.68	29.48	30*
σ_s	Std. Err. of the spawning temperature function	°C	2.05	0.75*	3.5*	3*
α	Larvae food-predator trade-off coefficient	-	2]	1.03	0.001*	0.498
T_a	Optimum of the adult temperature function at maximum age	°C	23.4	20.64	25*	20.1
σ_a	Std. Err. of the adult temperature function at maximum age	°C	3.5]	4.5]	1.1	4.09]
$\hat{O}$	Oxygen value at Ψ_O =0.5	ml · l^{-1}	1.5	2.47	5.46	2.07
γ	Curvature coefficient of the oxygen function	-	0.001*	0.001*	0.001*	0.001*
	Movements					
V_M	Maximum sustainable speed	B.L.·s^{-1}	1.13	[1	0.949	0.723
C	coefficient of diffusion habitat dependence	-	0.3	6]**	0.267	4.99]**

*Fixed; [val = value close to mimimum boundary value; val] = value close to maximum boundary value

** The maximum value of the function has been changed

5.3 Projection under IPCC A2 scenario (without fishing effort)

With this new parameterization and corrected forcing, the projection under the A2 scenario of skipjack dynamics showed different tendency in the changes of spatial densities of fish (Fig 4.6). Favourable grounds for spawning and larvae survival extend to the central Pacific as in the first simulation but also reach the eastern Pacific and the subtropical latitudes in both hemispheres. By the end of the 21st Century these regions become the main spawning grounds while the western equatorial Pacific is becoming much less favourable. Young and adult fish distribute toward central and eastern Pacific but also with a much clear extension to the higher latitudes. The conditions in the northwest Pacific support an enhanced biomass extending far in the east following the Kuroshio extension.

At the basin-scale and without considering fishing effect, the total biomass is increasing then stabilizes and starts to decrease after 2060. This trend is due to the change in the WCPO (west of 150°W), since in the EPO, as in the first simulation experiment, the total biomass of skipjack is projected to increase (by a factor two).

Results are identical with the simulation using the O_2 climatology.

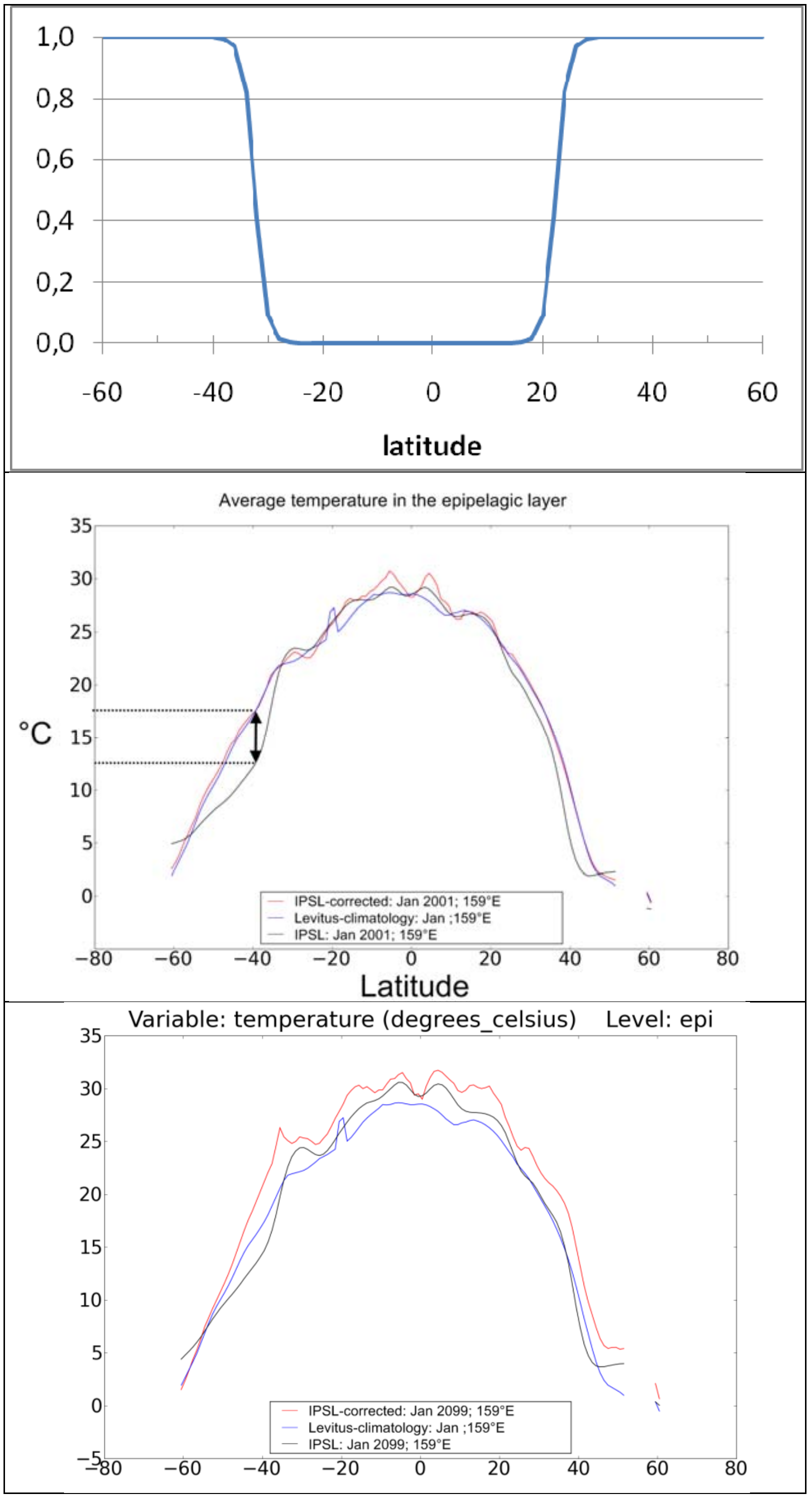

Figure 4.1. Correction of temperature fields. Function based on latitude used to correct the bias (top) and latitudinal temperature transects along 159°E in January, for the Levitus climatology (blue) and the original (black) and corrected (red) IPSL-CM4 temperature outputs, averaged in the epipelagic layer defined for SEAPODYM in January 2001 (center) and 2099 (bottom).

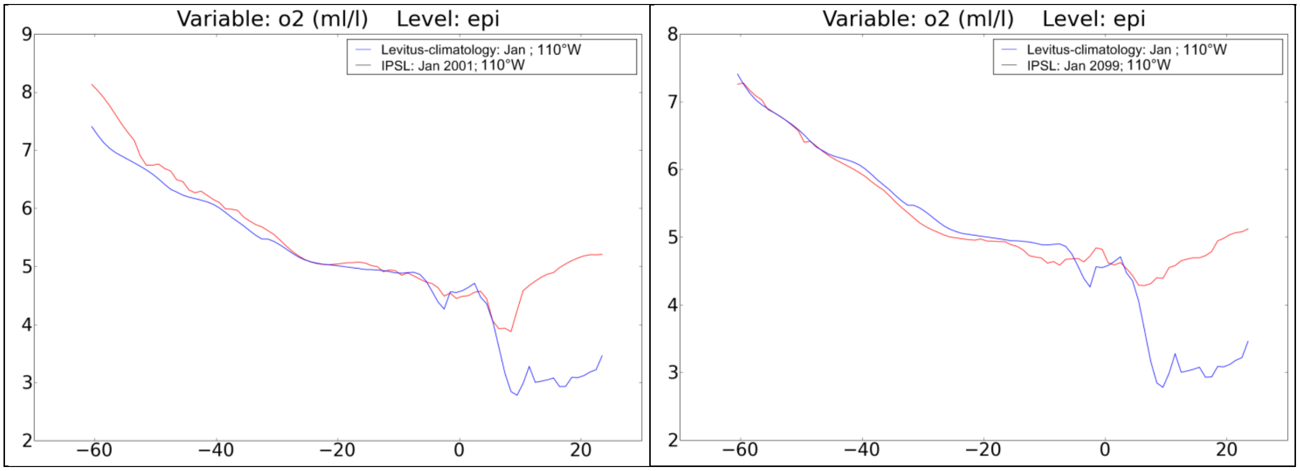

Figure 4.2. Latitudinal transects of dissolved oxygen concentration along 110°W in January, for the Levitus climatology (blue) and the IPSL-CM4 prediction (red), averaged in the epipelagic layer defined for SEAPODYM in January 2001 (left) and 2099 (right).

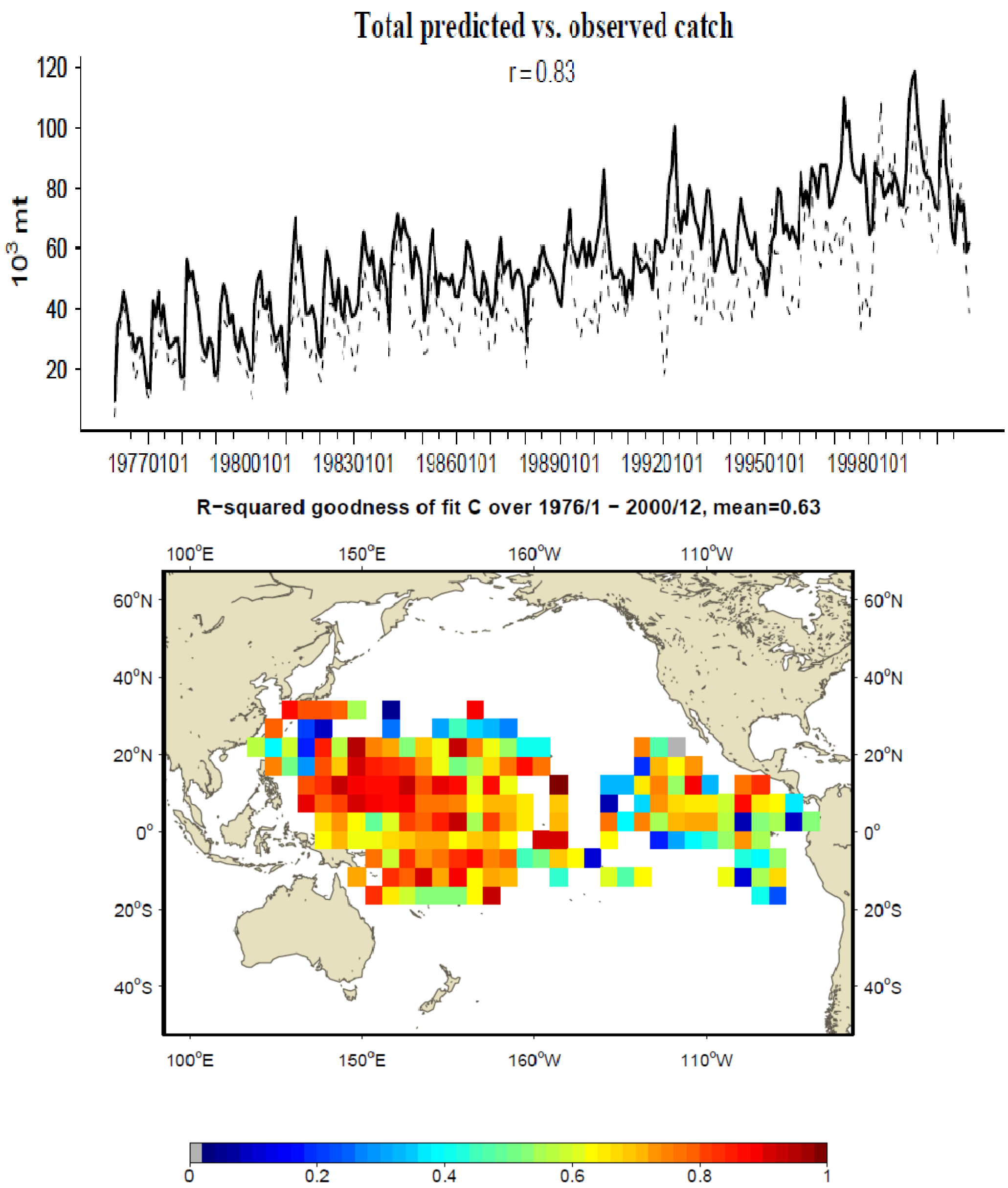

Figure 4.3. Time series of predicted (continuous line) and observed (dotted line) catch (sum of all fisheries) for the historical period used in the optimization experiment with environmental forcing from IPSL-CM4 model after correction of temperature.

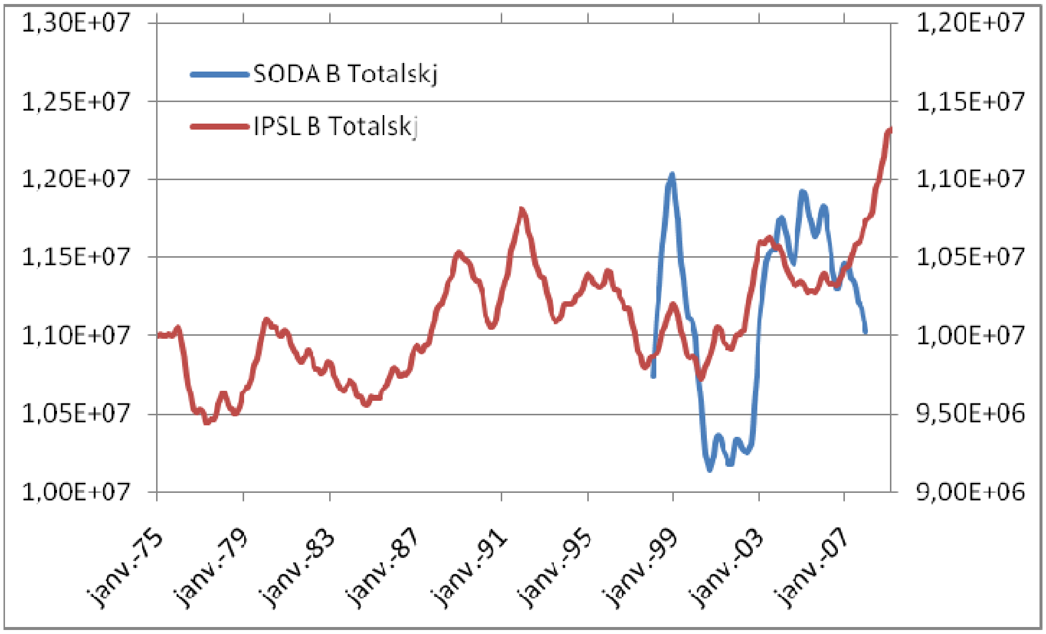

Figure 4.4. Predicted total Pacific skipjack biomass with IPSL-corrected forcing compared to biomass estimated with SODA experiment.

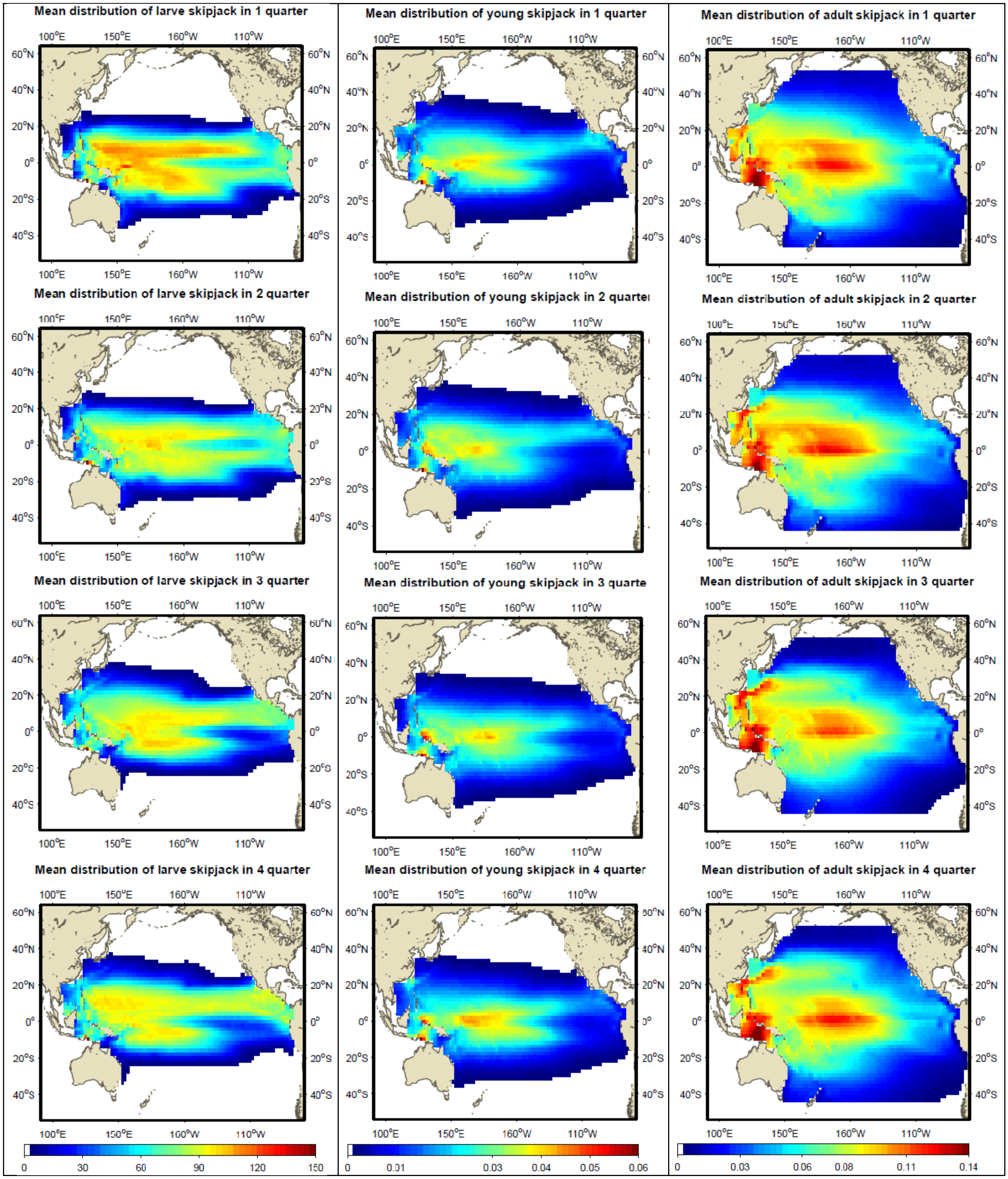

Figure 4.5 Average quarterly distributions of larvae, young and adult cohorts predicted for the decade 1990-1999 with the optimization experiment using the forcing of IPSL-CM4 climate model after correction of temperature.

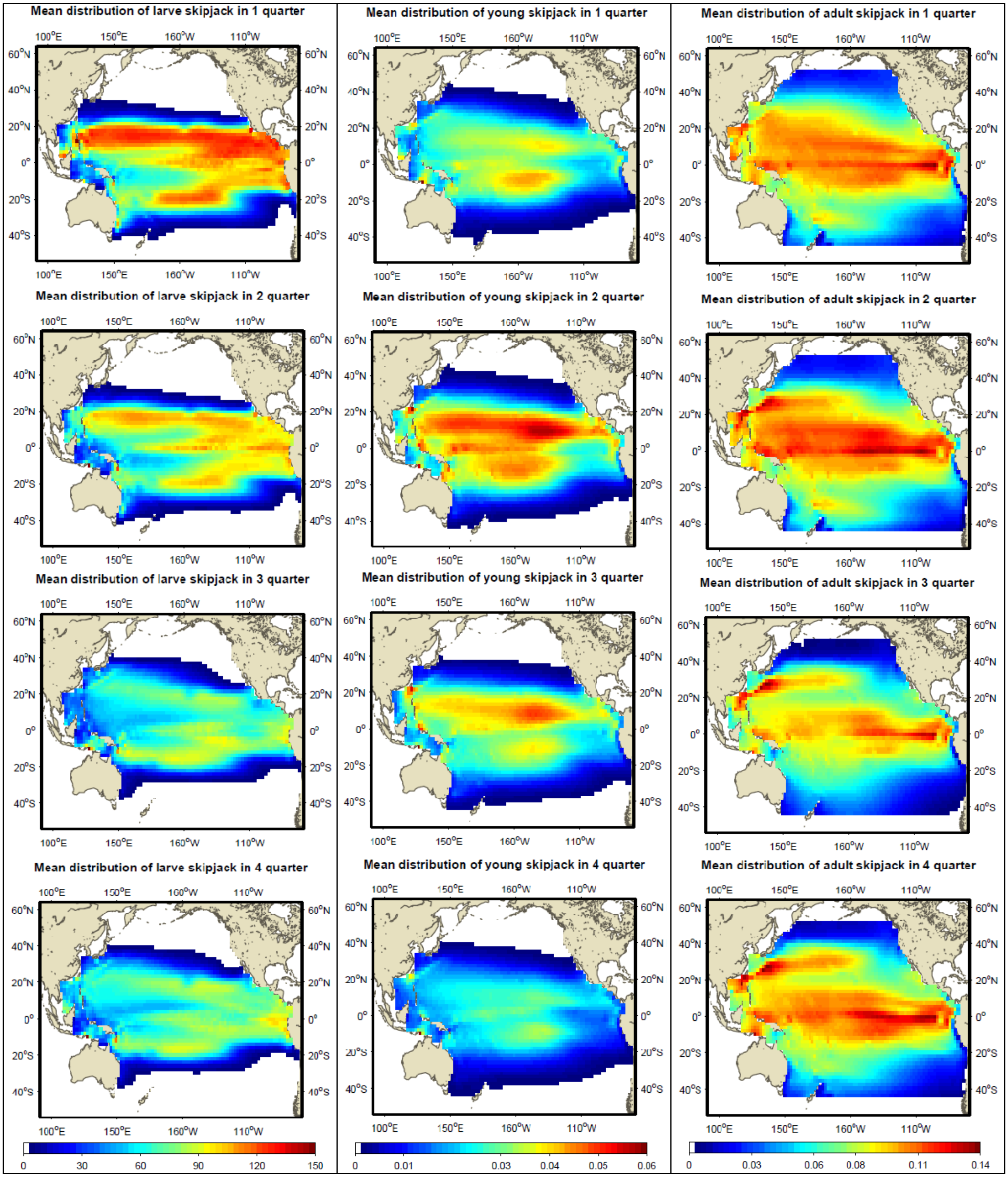
Mean distribution of larve skipjack in 1 quarter

Mean distribution of young skipjack in 1 quarter

Mean distribution of adult skipjack in 1 quarter

Mean distribution of larve skipjack in 2 quarter

Mean distribution of young skipjack in 2 quarter

Mean distribution of adult skipjack in 2 quarter

Mean distribution of larve skipjack in 3 quarter

Mean distribution of young skipjack in 3 quarter

Mean distribution of adult skipjack in 3 quarter

Mean distribution of larve skipjack in 4 quarter

Mean distribution of young skipjack in 4 quarter

Mean distribution of adult skipjack in 4 quarter

Figure 4.5 Average quarterly distributions of larvae, young and adult cohorts predicted for the decade 2090-2099 with the optimization experiment using the forcing of IPSL-CM4 climate model under the IPCC A2 scenario and after correction of temperature fields.

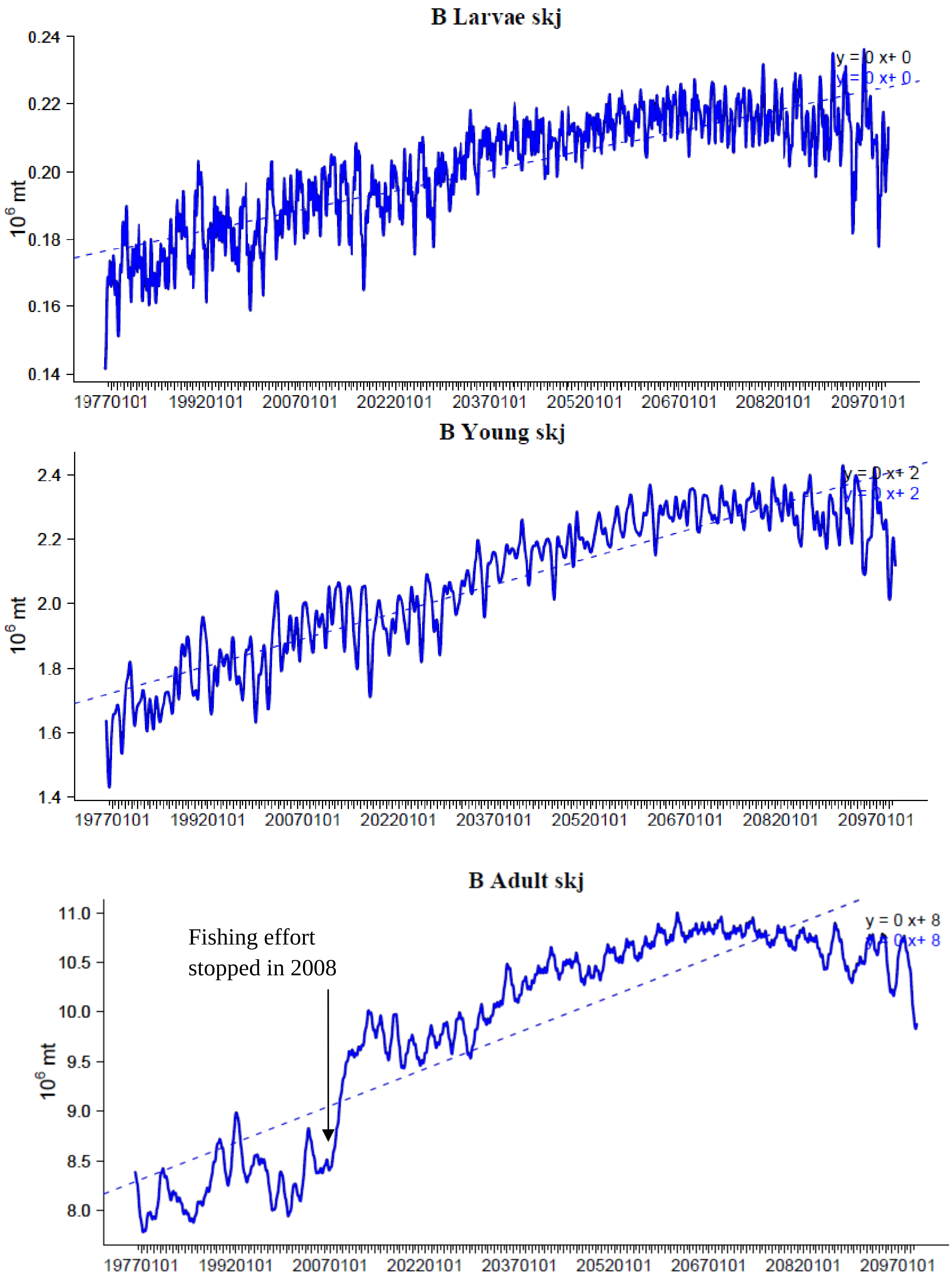

Figure 4.6 Projection under climate change scenario A2 of the biomass for larvae, young, and adult skipjack. Both simulations with oxygen climatology or IPSL outputs are confounded.

6 Conclusion

The use of higher resolution with more realistic oceanic environment, increased resolution of fishing data and robustify-normal likelihood allowed major improvements in the optimization of parameters for skipjack tuna. Nevertheless, it is still difficult to estimate all parameters together and additional information (e.g., tagging data, larvae density …) need to be included in the optimization approach to help in this task. These new simulation experiments gave a better fit to fishing data and a lower biomass estimate. It would be critical to investigate if such a tendency remains while continuing to run optimization experiments with increased resolution, e.g., 0.5° x 2 weeks, and corresponding resolution of fishing data sets (at least partially).

The scaling of this new parameterization to a pre-operational model at resolution 0.25°x week opens the way to fine scale analysis and eventually, near real time monitoring of the stock. This should help also by providing simulation outputs at spatial and temporal scales close to those of observation at sea.

After correction of a temperature bias in the climate model outputs, a new projection of skipjack dynamics under future climate change (IPCC A2 scenario) was achieved with parameter estimates close to the values obtained using more realistic reanalyses of the historical fishing period. Substantial changes appeared with a more clear extension of habitat towards higher latitude, especially in the north hemisphere and stabilization of skipjack total biomass in the WCPO until 2060s (without considering fishing). The result is insensitive to a “no change” scenario of oxygen, but the hypothesis of a decrease of dissolved oxygen concentration due to a C/N ratio increase under higher CO_2 levels conditions still needs to be tested. Other key mechanisms are also research priorities like the competition between species, and the estimation of the energy transfer efficiency between lower and mid-trophic (micronekton) levels, to help define more realistically, the carrying capacity of the pelagic ecosystem in the tropical Pacific Ocean for tuna.

7 Acknowledgments

The authors wish to thank Peter Williams of SPC and Michael Hinton of the Inter-American Tropical Tuna Commission for supplying critical fishing data from the WCPO and the EPO respectively. The authors also thank the Groupe Mission Mercator Coriolis and the GLORYS members (Mercator-Ocean, INSU-CNRS and the team “DRAKKAR”) for providing the GLORYS1V1 reanalysis and the PSY3 Mercator-Ocean model outputs. Climatological ocean data were provided by the NOAA/OAR/ESRL PSD, Boulder, Colorado, USA, from their Web site at http://www.esrl.noaa.gov/psd/. Primary production VGPM for 1998-2009 was downloaded from the Oregon State University web site at http://www.science.oregonstate.edu/ocean.productivity/index.php.

8 References

Behrenfeld, M.J, and Falkowski, P.G. (1997) A consumer's guide to phytoplankton primary productivity models. *Limnology and Oceanography*, **42**: 1479-1491

Hoyle S, Kleiber P, Davies N, Harley S and Hampton J (2010). Stock Assessment of Skipjack Tuna in the Western and Central Pacific Ocean. Rev.1. WCPFC-SC6-2010/SA-WP-10, Western and Central Pacific Fisheries Commission Scientific Committee Sixth Regular Session, 10-19 August 2010 Nuku'alofa, Kingdom of Tonga.

Lehodey P., Senina I., (2009). A user manual for SEAPODYM version 2.0: application with data assimilation. Fifth regular session of the Scientific Committee of the Western and Central Pacific Fisheries Commission, 10–21 August 2009, Port Vila, Vanuatu, WCPFC-SC5-2009/ EB-IP-13, 82 pp. http://www.wcpfc.int/meetings/2009/5th-regular-session-scientific-committee

Lehodey P., Senina I., Calmettes B., Abecassis M., Jurado Molina J., Briand K., Hampton J., Polovina J., Williams P., Nicol S. (2010). Project 62: SEAPODYM applications in WCPO – Progress Report. 6th regular session of the Scientific Steering Committee, 10-19 August 2010, Nukualofa, Tonga. WCPFC-SC6-2010/EB- IP 02.

Lehodey, P. 2000. Impacts of the El Niño Southern Oscillation on tuna populations and fisheries in the tropical Pacific Ocean. 13th Standing Committee on Tuna and Billfish, Noumea, 5-12 July 2000, Secretariat of the Pacific Community, Noumea, *Working Paper* RG-1: 32 pp.

Sibert J., Senina I., Lehodey P. (2011). Prospects for effective conservation of bigeye tuna stocks in the Western Central Pacific Ocean. 7th Regular Session of the Scientific Committee of the Western Central Pacific Fisheries commission, Ponhpei, Micronesia, 9-17 Aug 2011. SC7-MI-WP-05: 26 pp.

Uosaki, K., Kiyofuji,H., Hashimoto, Y., Okamoto, S., Ogura M. (2010). Recent status of Japanese skipjack fishery in the vicinity of Japan. WCPFC-SC6-2010/SA- WP-07

List of references for SEAPODYM

Scientific literature:

Lehodey, P., Hampton, J., Brill, R.W., Nicol, S., Senina, I., Calmettes, B., Pörtner, H.O., Bopp, L., Ilyina,T., Johann D. Bell, and J. Sibert (*in press*). Vulnerability of oceanic fisheries in the tropical Pacific to climate change. *In* Bell J., Johnson JE, Hobday AJ (Ed.), Vulnerability of Tropical Pacific Fisheries and Aquaculture to Climate Change. Secretariat of the Pacific Community. Noumea New Caledonia.

Lehodey P., Senina I., Sibert J., Bopp L, Calmettes B., Hampton J., Murtugudde R. (2010). Preliminary forecasts of population trends for Pacific bigeye tuna under the A2 IPCC scenario. *Progress in Oceanography*. 86: 302–315

Lehodey P., Murtugudde R., Senina I. (2010). Bridging the gap from ocean models to population dynamics of large marine predators: a model of mid-trophic functional groups. *Progress in Oceanography*, **84**: 69–84

Senina I., Sibert J., & Lehodey P. (2008). Parameter estimation for basin-scale ecosystem-linked population models of large pelagic predators: application to skipjack tuna. *Progress in Oceanography*, **78**: 319-335.

Lehodey P., Senina I., & Murtugudde R. (2008). A Spatial Ecosystem And Populations Dynamics Model (SEAPODYM) - Modelling of tuna and tuna-like populations. *Progress in Oceanography*, **78**: 304-318.

Lehodey P., Chai F., & Hampton J. (2003). Modelling climate-related variability of tuna populations from a coupled ocean-biogeochemical-populations dynamics model. *Fisheries Oceanography,* **12**(4): 483-494

Lehodey P., (2001). The pelagic ecosystem of the tropical Pacific Ocean: dynamic spatial modelling and biological consequences of ENSO. *Progress in Oceanography,* 49: 439-468.

Bertignac M., Lehodey P., Hampton J., (1998). A spatial population dynamics simulation model of tropical tunas using a habitat index based on environmental parameters. *Fisheries Oceanography*, 7: 326-334.

Lehodey P., André J-M., Bertignac M., Hampton J., Stoens A., C. Menkès, L., Memery, Grima N., (1998). Predicting skipjack tuna forage distributions in the Equatorial Pacific using a coupled dynamical bio-geochemical model. *Fisheries Oceanography*, 7: 317-325.

SCTB and WCPFC documents:

Lehodey P., Senina I., Calmettes B., Abecassis M., Jurado Molina J., Briand K., Hampton J., Polovina J., Williams P., Nicol S. (2010). Project 62: SEAPODYM applications in WCPO – Progress Report. 6th regular session of the Scientific Steering Committee, 10-19 August 2010, Nukualofa, Tonga. WCPFC-SC6-2010/EB- IP 02.

Lehodey P., Senina I., (2009). A user manual for SEAPODYM version 2.0: application with data assimilation. Fifth regular session of the Scientific Committee of the Western and Central Pacific Fisheries Commission, 10–21 August 2009, Port Vila, Vanuatu, WCPFC-SC5-2009/ EB-IP-13, 82 pp.

Lehodey P., Senina I., (2009). An update of recent developments and applications of the SEAPODYM model. Fifth regular session of the Scientific Committee of the Western and Central Pacific Fisheries Commission, 10–21 August 2009, Port Vila, Vanuatu, WCPFC-SC5-2009/EB-WP-10, 44 pp.

Lehodey P., Senina I., Sibert J., Hampton J. (2008). SEAPODYM.v2: A Spatial Ecosystem And Population Dynamics Model with parameter optimization providing a new tool for tuna management. Fourth regular session of the Scientific Committee of the Western and Central Pacific Fisheries Commission, 11–22 August 2008, Port Moresby, Papua New Guinea. WCPFC-SC4-2008/EB-WP-10: 15 pp.

Senina I.N., Sibert J.R., Lehodey P., (2005). SEAPODYM on a mixed-resolution spatial scale. First meeting of the Scientific Committee of the Western and Central Pacific Fisheries Commission WCPFC-SC1, Noumea, New Caledonia, 8-19 August 2005. ME-WP-2

Lehodey P., (2005a). Reference manual for the Spatial Ecosystem And Populations Dynamics Model SEAPODYM. First meeting of the Scientific Committee of the Western and Central Pacific Fisheries Commission WCPFC-SC1, Noumea, New Caledonia, 8-19 August 2005. ME IP–1: 54 pp.

Lehodey P., (2005b). Application of SEAPODYM to the Pacific Pelagic Ecosystem. Recent results and perspectives First meeting of the Scientific Committee of the Western and Central Pacific Fisheries Commission WCPFC-SC1, Noumea, New Caledonia, 8-19 August 2005. EB WP–8: 29 pp.

Lehodey P., (2005c). First application of SEAPODYM to Pacific bigeye tuna. First meeting of the Scientific Committee of the Western and Central Pacific Fisheries Commission WCPFC-SC1, Noumea, New Caledonia, 8-19 August 2005. ME-WP-1:

Lehodey P., (2004a). A Spatial Ecosystem And Populations Dynamics Model (SEAPODYM) for tuna and associated oceanic top-predator species: Part I – Lower and intermediate trophic components. 17th meeting of the Standing Committee on Tuna and Billfish, Majuro, Republic of Marshall Islands, 9-18 Aug. 2004, Oceanic Fisheries Programme, Secretariat of the Pacific Community, Noumea, New Caledonia, *Working Paper*: ECO-1: 26 pp.

Lehodey P., (2004b) A Spatial Ecosystem And Populations Dynamics Model (SEAPODYM) for tuna and associated oceanic top-predator species: Part II – Tuna populations and fisheries. 17th meeting of the Standing Committee on Tuna and Billfish, Majuro, Republic of Marshall Islands, 9-18 Aug. 2004, Oceanic Fisheries Programme, Secretariat of the Pacific Community, Noumea, New Caledonia, *Working Paper*: ECO-2: 36 pp.

Lehodey P., (2003) SEPODYM application to skipjack tuna (*Katsuwonus pelamis*) in the Pacific Ocean: impact of ENSO on recruitment and population. 16th meeting of the Standing Committee on Tuna and Billfish, Mooloolaba, Queensland, Australia, 9-16 July 2003, Oceanic Fisheries Programme, Secretariat of the Pacific Community, Noumea, New Caledonia, *Working Paper*: SKJ-5

Lehodey P., (2003) First application of SEPODYM to yellowfin tuna population and fisheries in the Pacific Ocean. 16th meeting of the Standing Committee on Tuna and Billfish, Mooloolaba, Queensland, Australia, 9-16 July 2003, Oceanic Fisheries Programme, Secretariat of the Oceanic Fisheries Programme, Secretariat of the Pacific Community, Noumea, New Caledonia, *Working Paper*: YFT-4

Lehodey P., (2003) SEPODYM application to albacore (*Thunnus alalunga*) in the Pacific Ocean. 16th meeting of the Standing Committee on Tuna and Billfish, Mooloolaba, Queensland, Australia, 9-16 July 2003, Oceanic Fisheries Programme, Secretariat of the Pacific Community, Noumea, New Caledonia, *Working Paper*: ALB-9

Lehodey P., (2002) SEPODYM development and application to skipjack population and fisheries. 15th meeting of the Standing Committee on Tuna and Billfish, Honolulu, Hawaii, USA, 22-27 July 2002, Oceanic Fisheries Programme, Secretariat of the Pacific Community, Noumea, New Caledonia, *Working Paper*: SKJ-5

Lehodey, P. 2001. Sepodym skipjack analysis. 14th Standing Committee on Tuna and Billfish, Noumea, 9-16 August 2000, Secretariat of the Pacific Community, Noumea, *Working Paper* **SKJ-2**: 24 pp.

Lehodey, P. 2000. Impacts of the El Niño Southern Oscillation on tuna populations and fisheries in the tropical Pacific Ocean. 13th Standing Committee on Tuna and Billfish, Noumea, 5-12 July 2000, Secretariat of the Pacific Community, Noumea, *Working Paper* **RG-1**: 32 pp.

Lehodey, P. 2000. Update on the Spatial Environmental Population Dynamics Model: SEPODYM. 13th Standing Committee on Tuna and Billfish, Noumea, 5-12 July 2000, Secretariat of the Pacific Community, Noumea, *Working Paper* **RG-2**: 6 pp.

9 Appendix 1: Skipjack tuna optimization with SODA-1°x month

9.1 Catch and CPUE

Comparison between observed (dotted lines) and predicted (continuous lines) total catch (left) and catch rate (right) by fishery (cf. table 3.1), with the residuals.

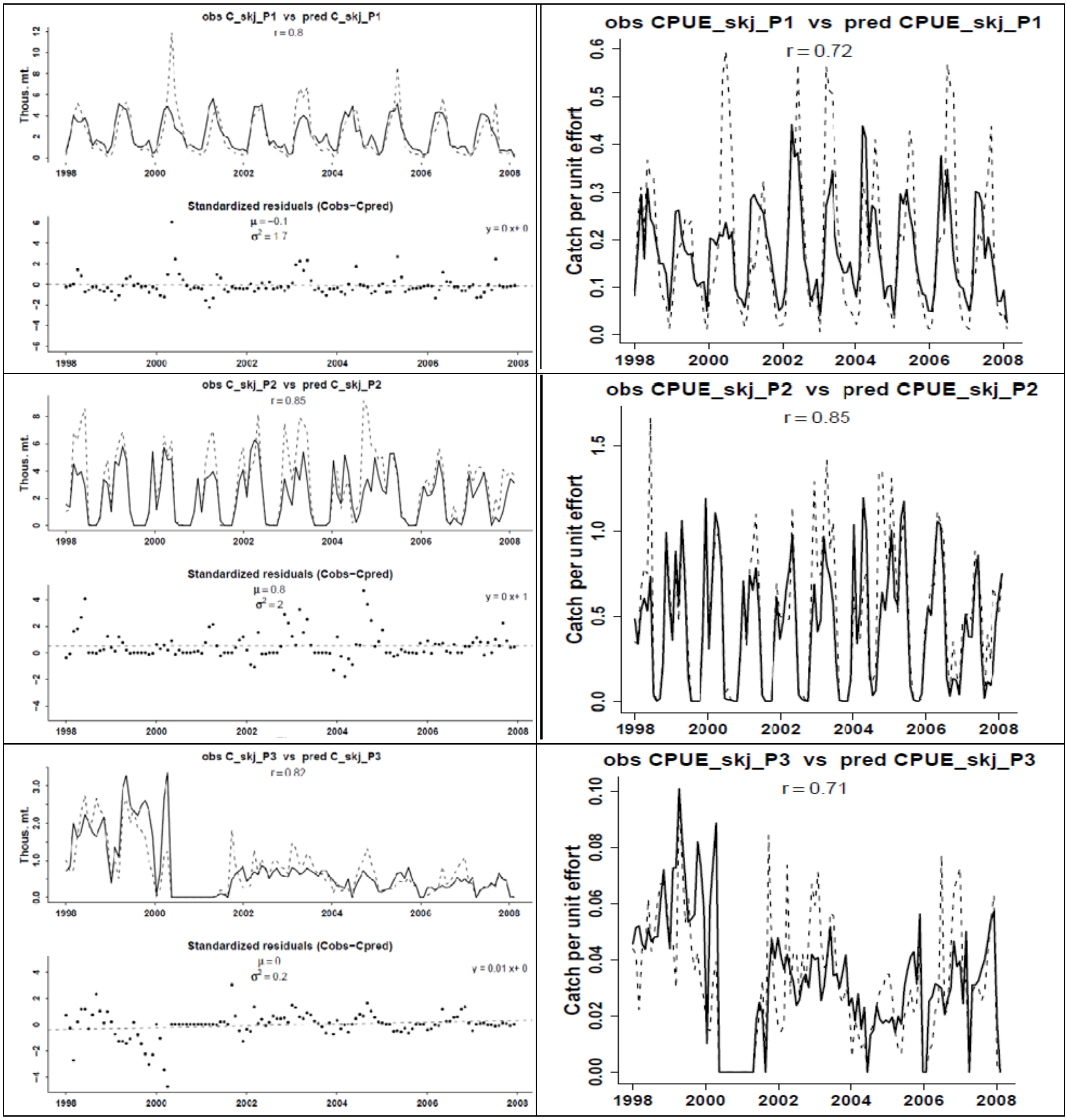

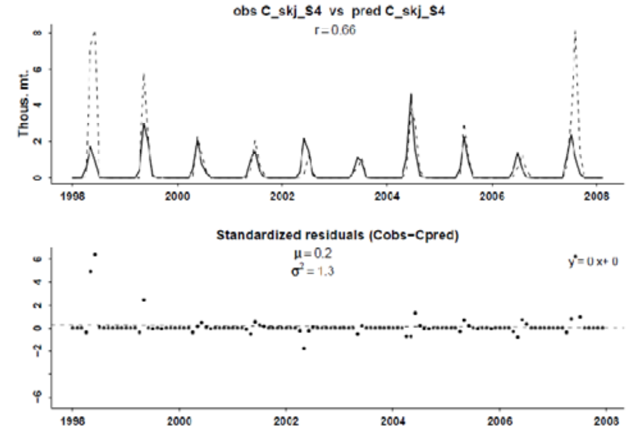
obs C_skj_S4 vs pred C_skj_S4
r = 0.66
Thous. mt.
Standardized residuals (Cobs−Cpred)
μ = 0.2
σ² = 1.3
y = 0 x + 0
1998
2000
2002
2004
2006
2008

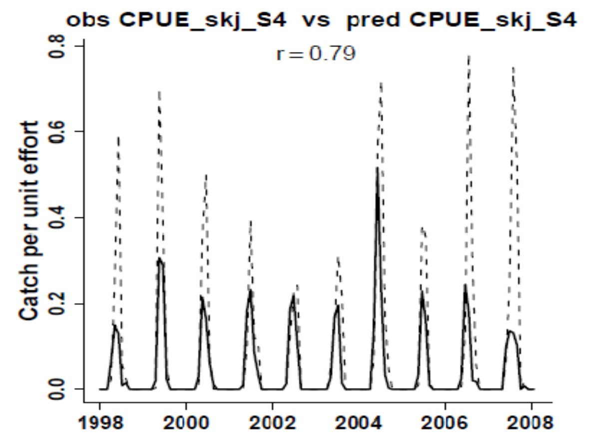
obs CPUE_skj_S4 vs pred CPUE_skj_S4
r = 0.79
Catch per unit effort
0.0
0.2
0.4
0.6
0.8
1998
2000
2002
2004
2006
2008

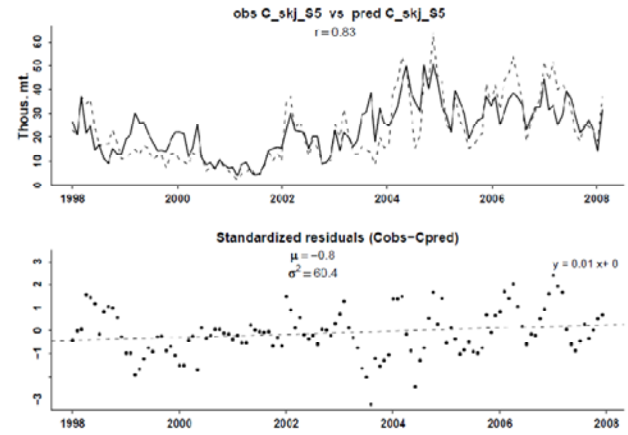
obs C_skj_S5 vs pred C_skj_S5
r = 0.83
Thous. mt.
Standardized residuals (Cobs−Cpred)
μ = −0.8
σ² = 60.4
y = 0.01 x + 0
1998
2000
2002
2004
2006
2008

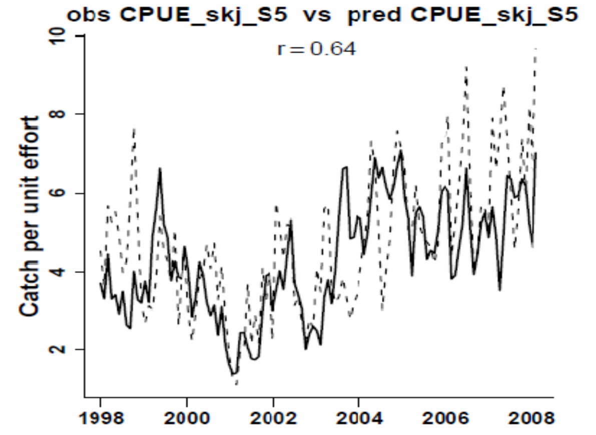
obs CPUE_skj_S5 vs pred CPUE_skj_S5
r = 0.64
Catch per unit effort
2
4
6
8
10
1998
2000
2002
2004
2006
2008

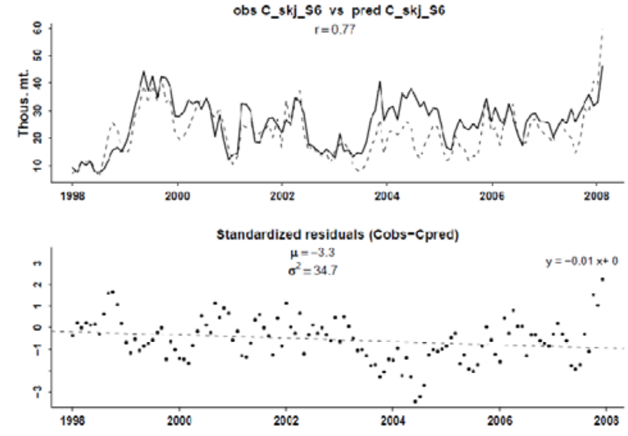
obs C_skj_S6 vs pred C_skj_S6
r = 0.77
Thous. mt.
Standardized residuals (Cobs−Cpred)
μ = −3.3
σ² = 34.7
y = −0.01 x + 0
1998
2000
2002
2004
2006
2008

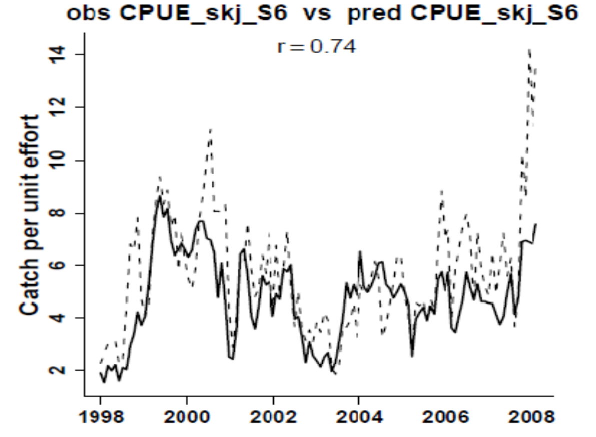
obs CPUE_skj_S6 vs pred CPUE_skj_S6
r = 0.74
Catch per unit effort
2
4
6
8
10
12
14
1998
2000
2002
2004
2006
2008

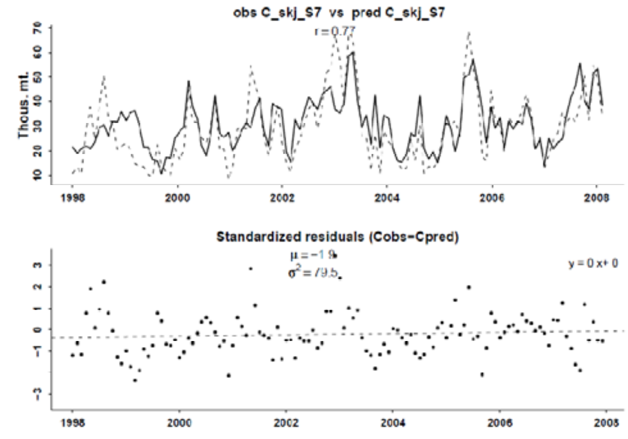
obs C_skj_S7 vs pred C_skj_S7
r = 0.77
Thous. mt.
Standardized residuals (Cobs−Cpred)
μ = −1.9
σ² = 79.5
y = 0 x + 0
1998
2000
2002
2004
2006
2008

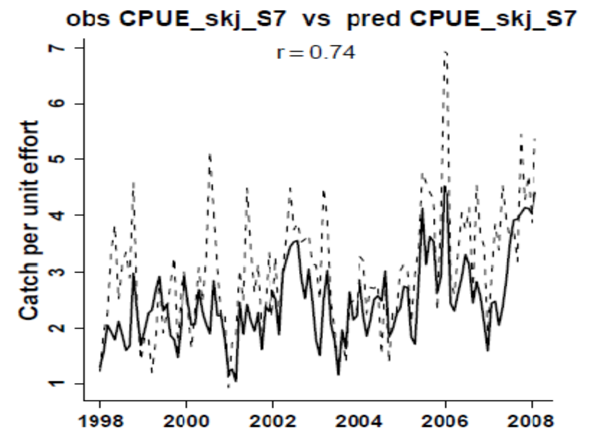
obs CPUE_skj_S7 vs pred CPUE_skj_S7
r = 0.74
Catch per unit effort
1
2
3
4
5
6
7
1998
2000
2002
2004
2006
2008

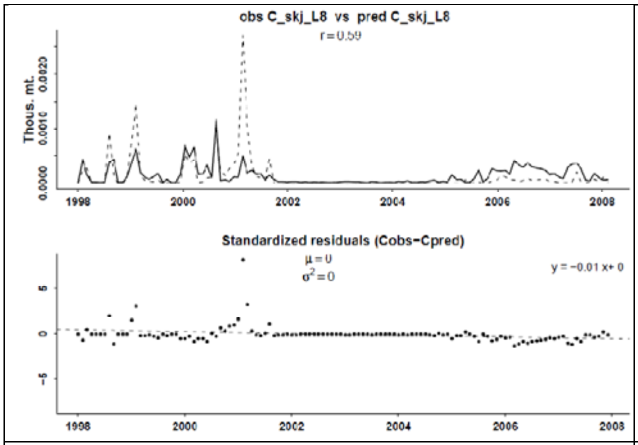
obs C_skj_L8 vs pred C_skj_L8
r = 0.59
Thous. mt.
0.0000
0.0010
0.0020
1998
2000
2002
2004
2006
2008
Standardized residuals (Cobs−Cpred)
μ = 0
σ² = 0
y = −0.01 x+ 0
5
0
-5

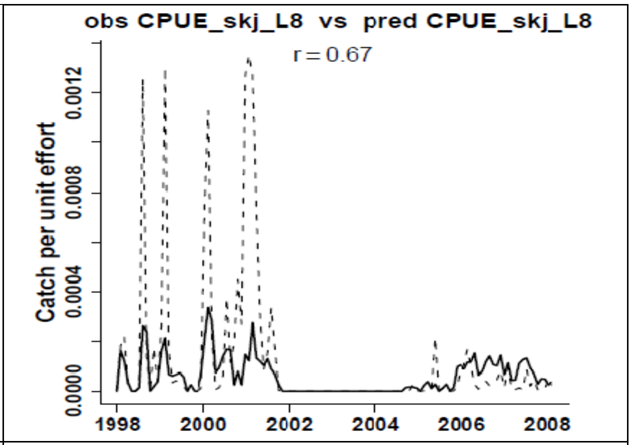
obs CPUE_skj_L8 vs pred CPUE_skj_L8
r = 0.67
Catch per unit effort
0.0000
0.0004
0.0008
0.0012
1998
2000
2002
2004
2006
2008

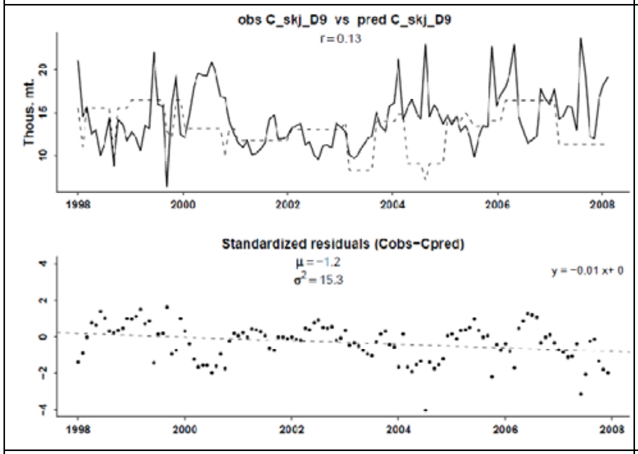
obs C_skj_D9 vs pred C_skj_D9
r = 0.13
Thous. mt.
10
15
20
1998
2000
2002
2004
2006
2008
Standardized residuals (Cobs−Cpred)
μ = −1.2
σ² = 15.3
y = −0.01 x+ 0
4
2
0
-2
-4

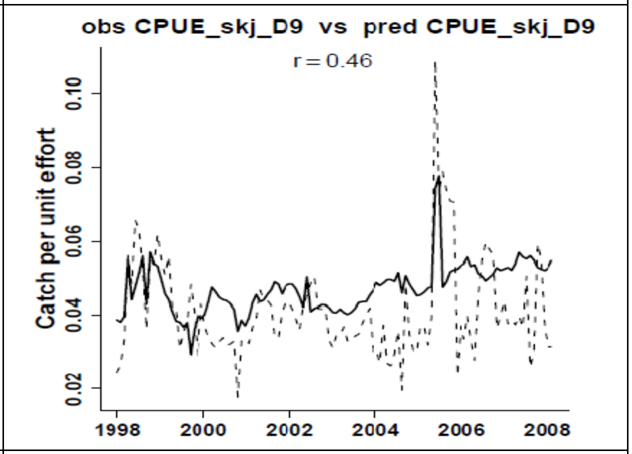
obs CPUE_skj_D9 vs pred CPUE_skj_D9
r = 0.46
Catch per unit effort
0.02
0.04
0.06
0.08
0.10
1998
2000
2002
2004
2006
2008

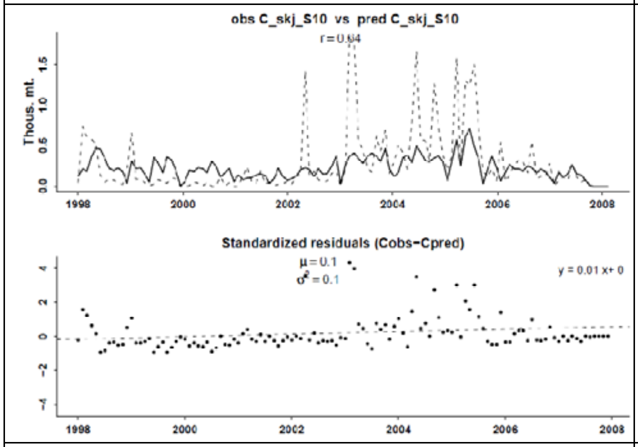
obs C_skj_S10 vs pred C_skj_S10
r = 0.84
Thous. mt.
0.0
0.5
1.0
1.5
1998
2000
2002
2004
2006
2008
Standardized residuals (Cobs−Cpred)
μ = 0.1
σ² = 0.1
y = 0.01 x+ 0
4
2
0
-2
-4

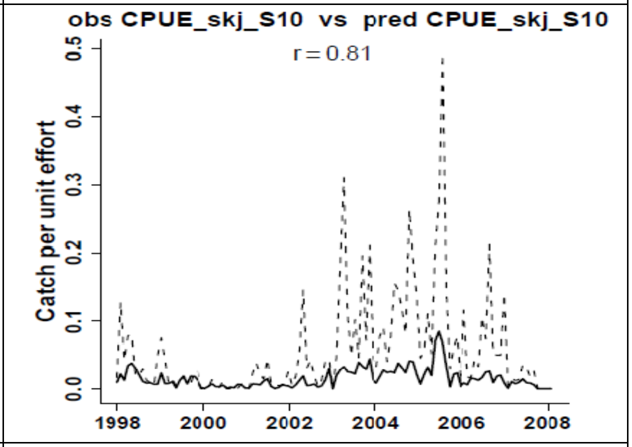
obs CPUE_skj_S10 vs pred CPUE_skj_S10
r = 0.81
Catch per unit effort
0.0
0.1
0.2
0.3
0.4
0.5
1998
2000
2002
2004
2006
2008

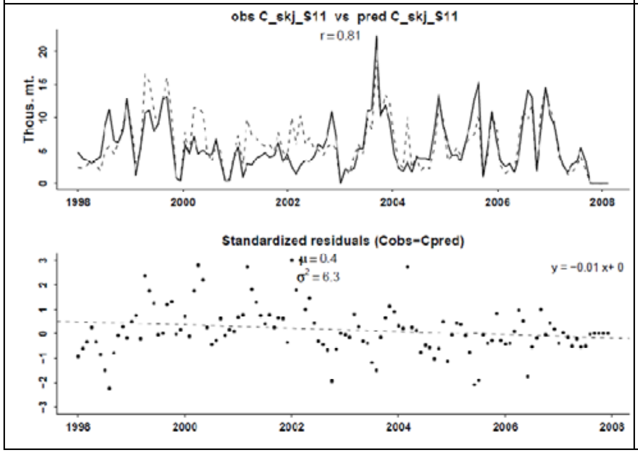
obs C_skj_S11 vs pred C_skj_S11
r = 0.81
Thous. mt.
0
5
10
15
20
1998
2000
2002
2004
2006
2008
Standardized residuals (Cobs−Cpred)
μ = 0.4
σ² = 6.3
y = −0.01 x+ 0
3
2
1
0
-1
-2
-3

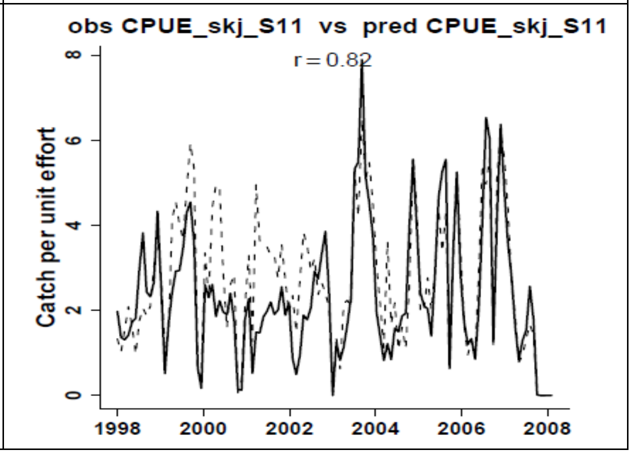
obs CPUE_skj_S11 vs pred CPUE_skj_S11
r = 0.82
Catch per unit effort
0
2
4
6
8
1998
2000
2002
2004
2006
2008

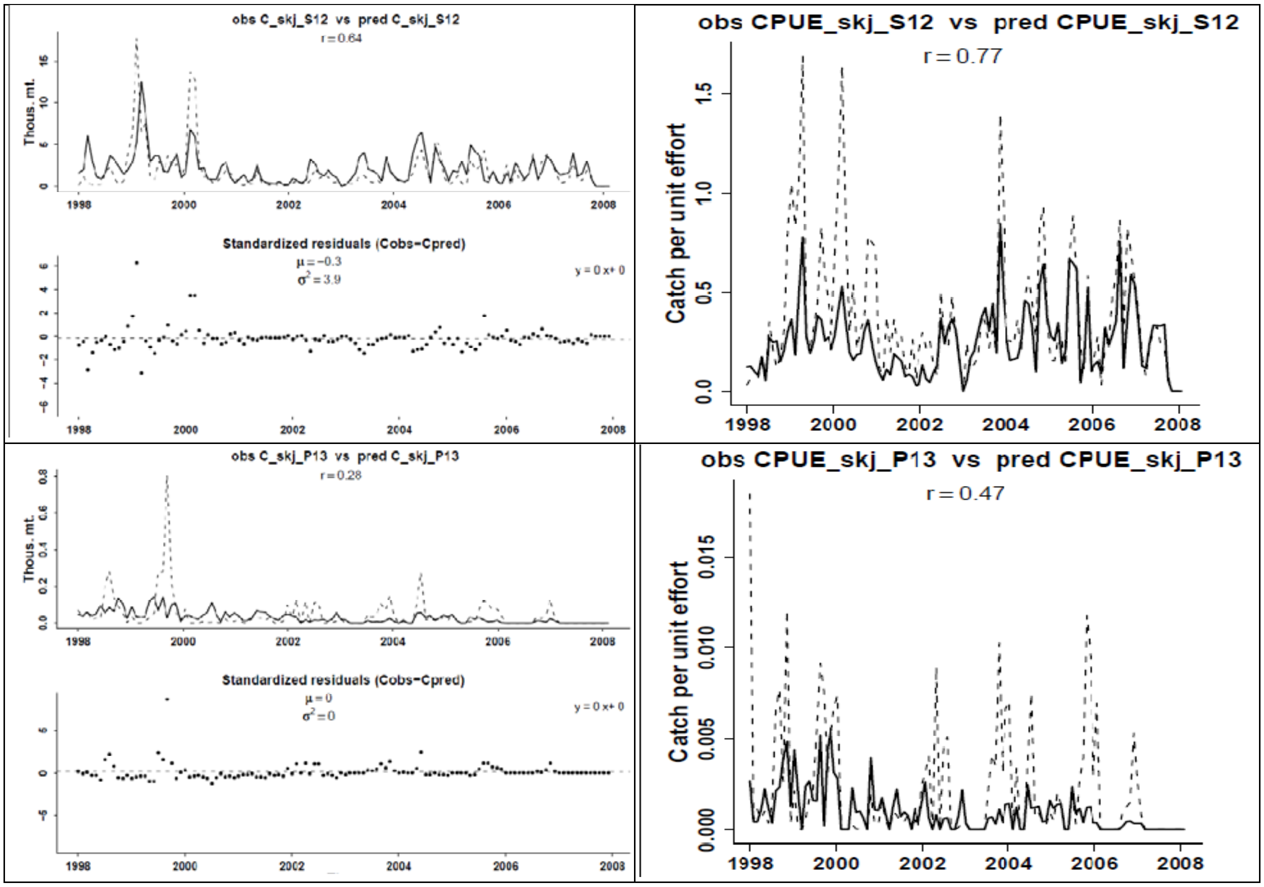
obs C_skj_S12 vs pred C_skj_S12
r = 0.64
Thous. mt.
0
5
10
15
1998
2000
2002
2004
2006
2008
Standardized residuals (Cobs−Cpred)
μ = −0.3
σ² = 3.9
y = 0 x+ 0
−6
−4
−2
0
2
4
6
1998
2000
2002
2004
2006
2008
obs CPUE_skj_S12 vs pred CPUE_skj_S12
r = 0.77
Catch per unit effort
0.0
0.5
1.0
1.5
1998
2000
2002
2004
2006
2008
obs C_skj_P13 vs pred C_skj_P13
r = 0.28
Thous. mt.
0.0
0.2
0.4
0.6
0.8
1998
2000
2002
2004
2006
2008
Standardized residuals (Cobs−Cpred)
μ = 0
σ² = 0
y = 0 x+ 0
−5
0
5
1998
2000
2002
2004
2006
2008
obs CPUE_skj_P13 vs pred CPUE_skj_P13
r = 0.47
Catch per unit effort
0.000
0.005
0.010
0.015
1998
2000
2002
2004
2006
2008

9.2 Size frequency distribution by fishery (all data aggregated in time and space)

Histogram: observed
Line with circles: predicted

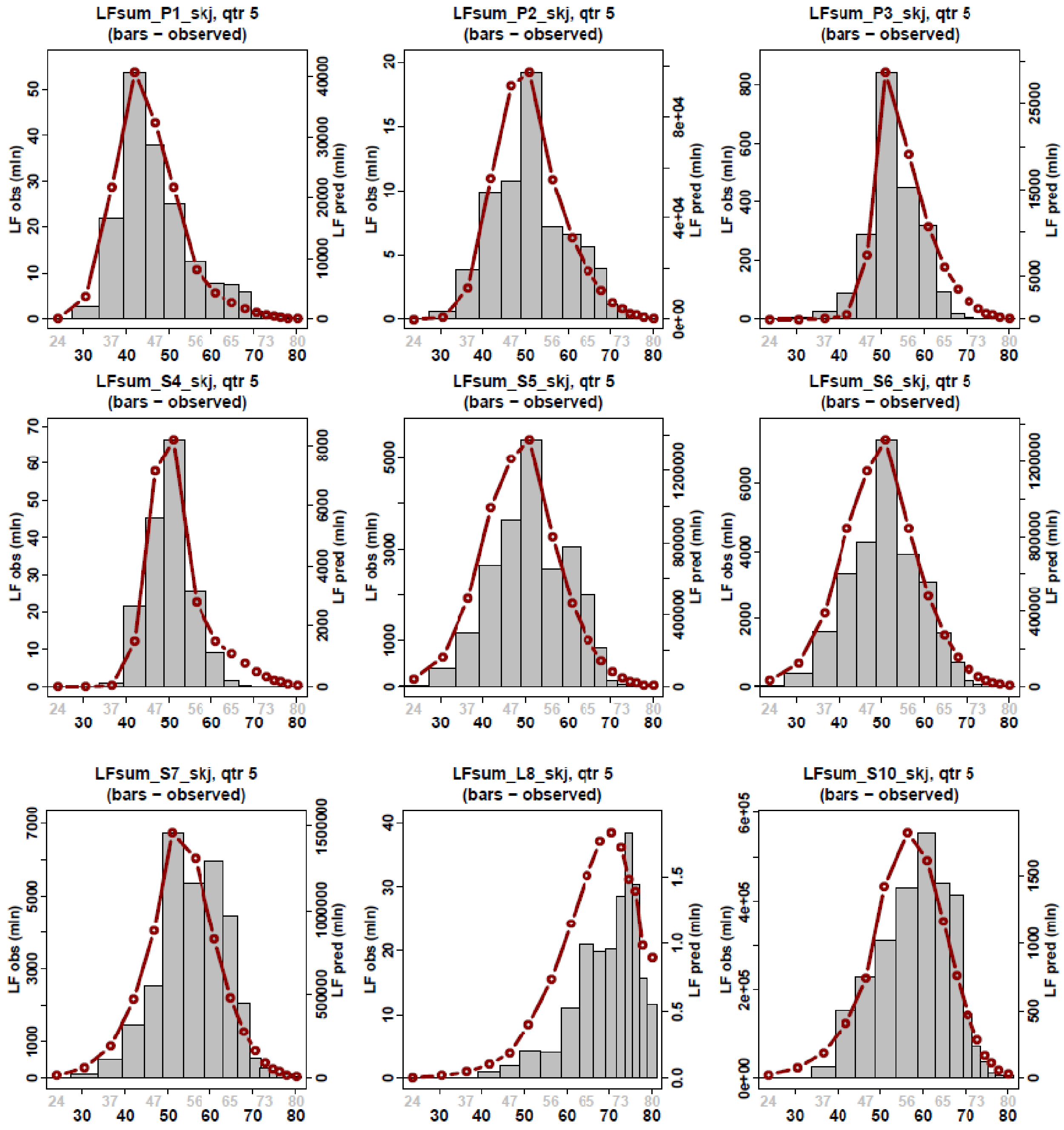

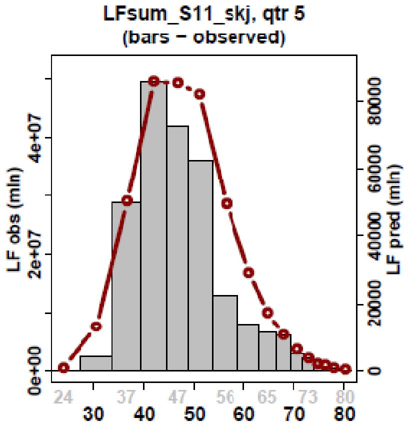
LFsum_S11_skj, qtr 5
(bars – observed)
LF obs (mln)
0e+00
2e+07
4e+07
LF pred (mln)
0
20000
40000
60000
80000
24
37
47
56
65
73
80
30
40
50
60
70
80

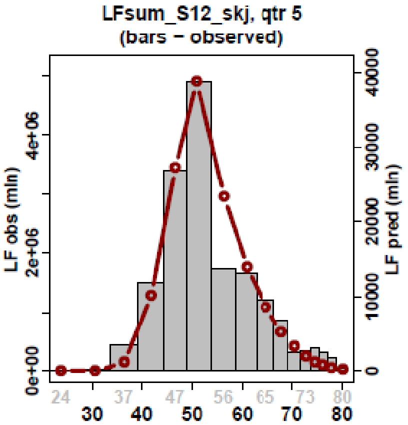
LFsum_S12_skj, qtr 5
(bars – observed)
LF obs (mln)
0e+00
2e+06
4e+06
LF pred (mln)
0
10000
20000
30000
40000
24
37
47
56
65
73
80
30
40
50
60
70
80

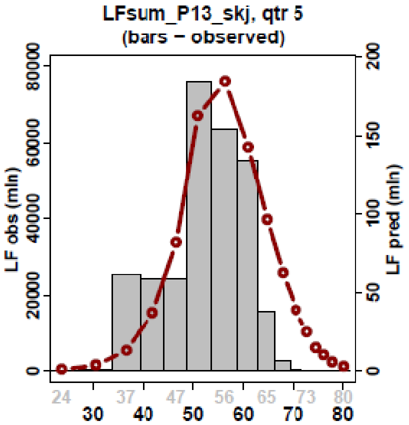
LFsum_P13_skj, qtr 5
(bars – observed)
LF obs (mln)
0
20000
40000
60000
80000
LF pred (mln)
0
50
100
150
200
24
37
47
56
65
73
80
30
40
50
60
70
80

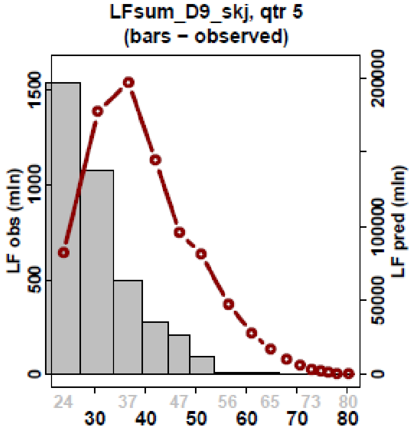
LFsum_D9_skj, qtr 5
(bars – observed)
LF obs (mln)
0
500
1000
1500
LF pred (mln)
0
50000
100000
200000
24
37
47
56
65
73
80
30
40
50
60
70
80

9.3 Size frequency distribution by fishery and time (quarter)

Black line and grey bars: observed average size of catch in the fishery with size range between first and last quantile
Red line with circles and Line with circles: predicted

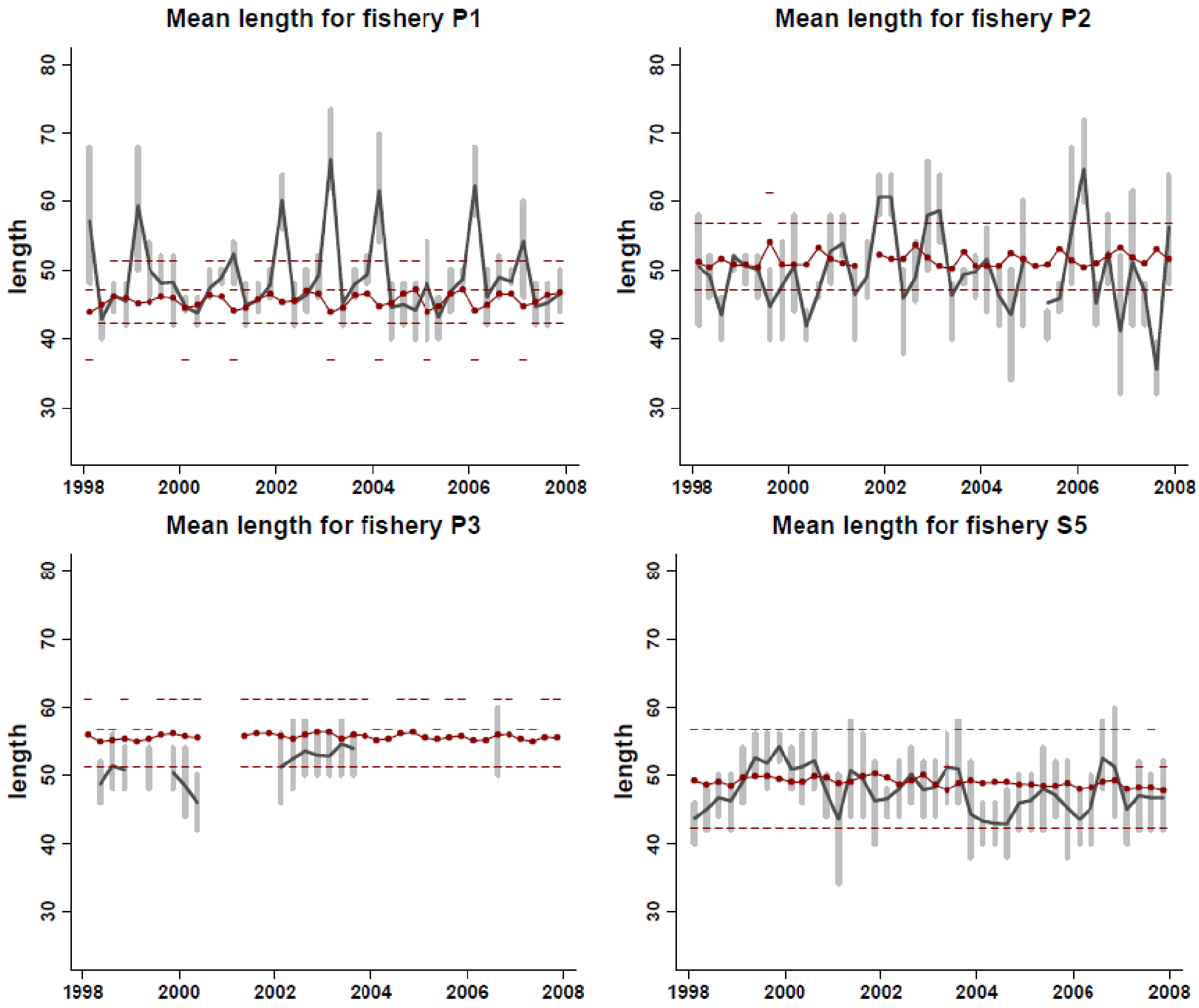

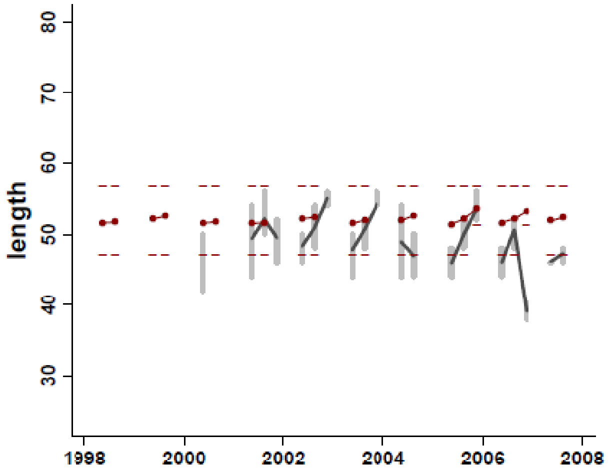

Mean length for fishery S4

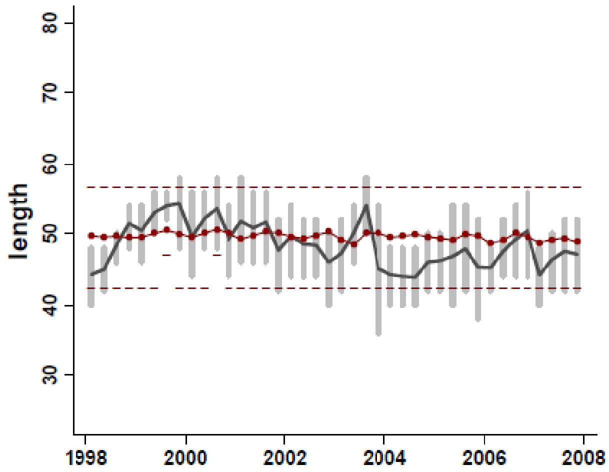

Mean length for fishery S6

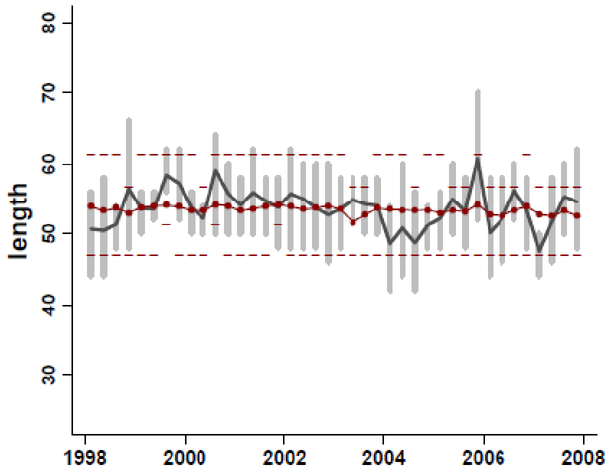

Mean length for fishery S7

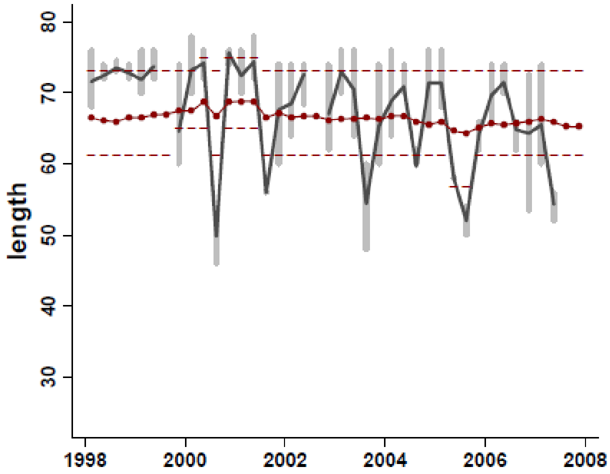

Mean length for fishery L8

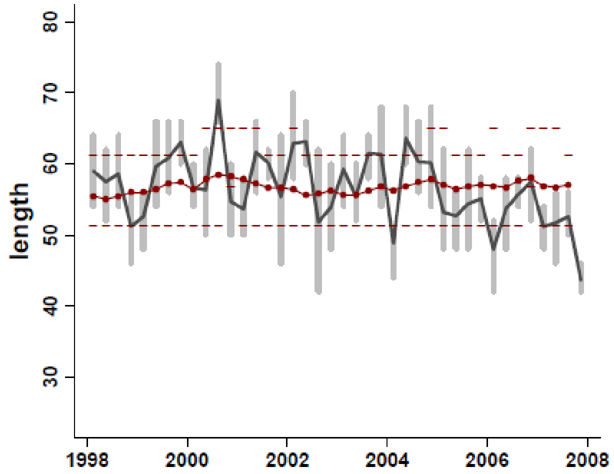

Mean length for fishery S10

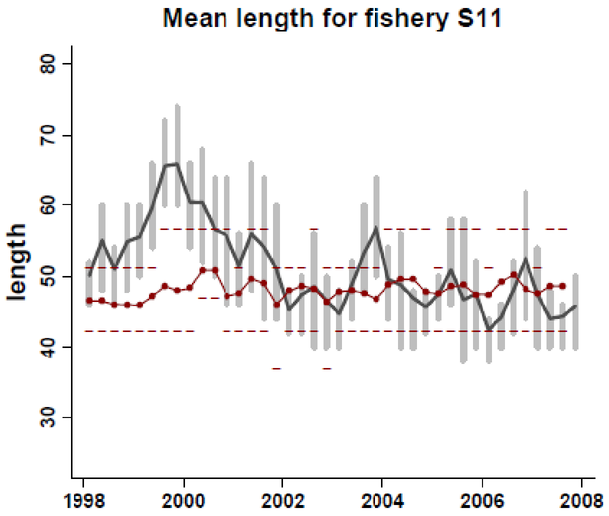
Mean length for fishery S11

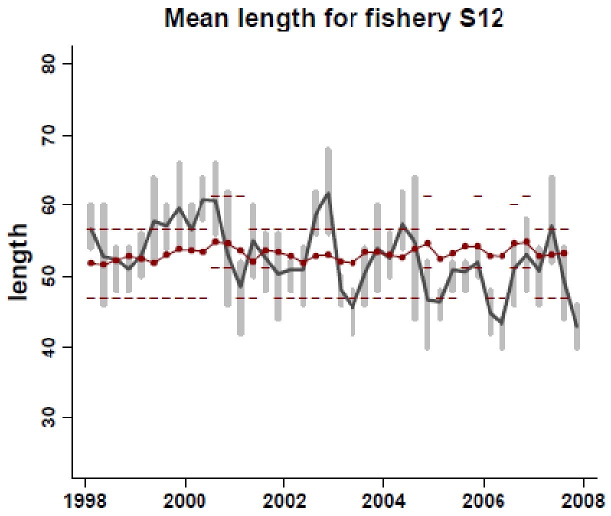
Mean length for fishery S12

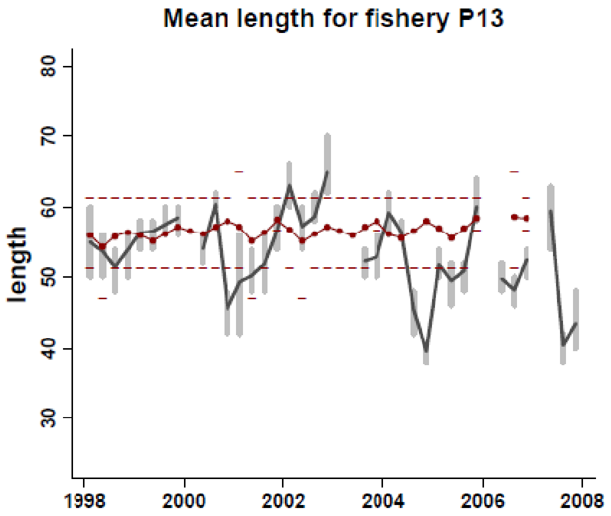
Mean length for fishery P13

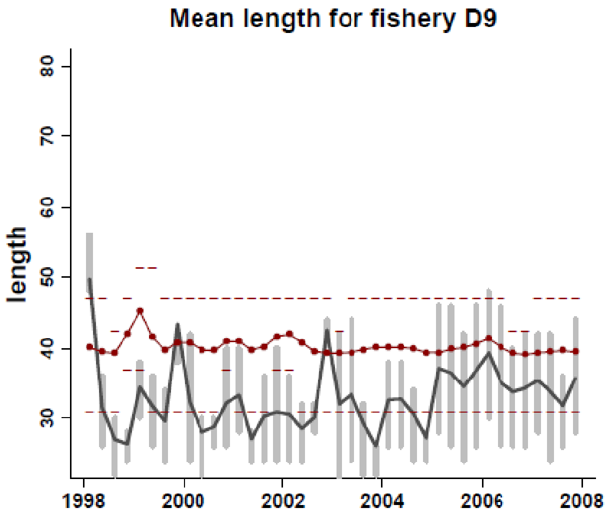
Mean length for fishery D9

10 Appendix 2: Skipjack optimization with IPSL- CM4 - corrected

10.1 CPUE

Observed (dotted lines) and predicted (continuous lines) CPUE by fishery (cf. table 3.1)

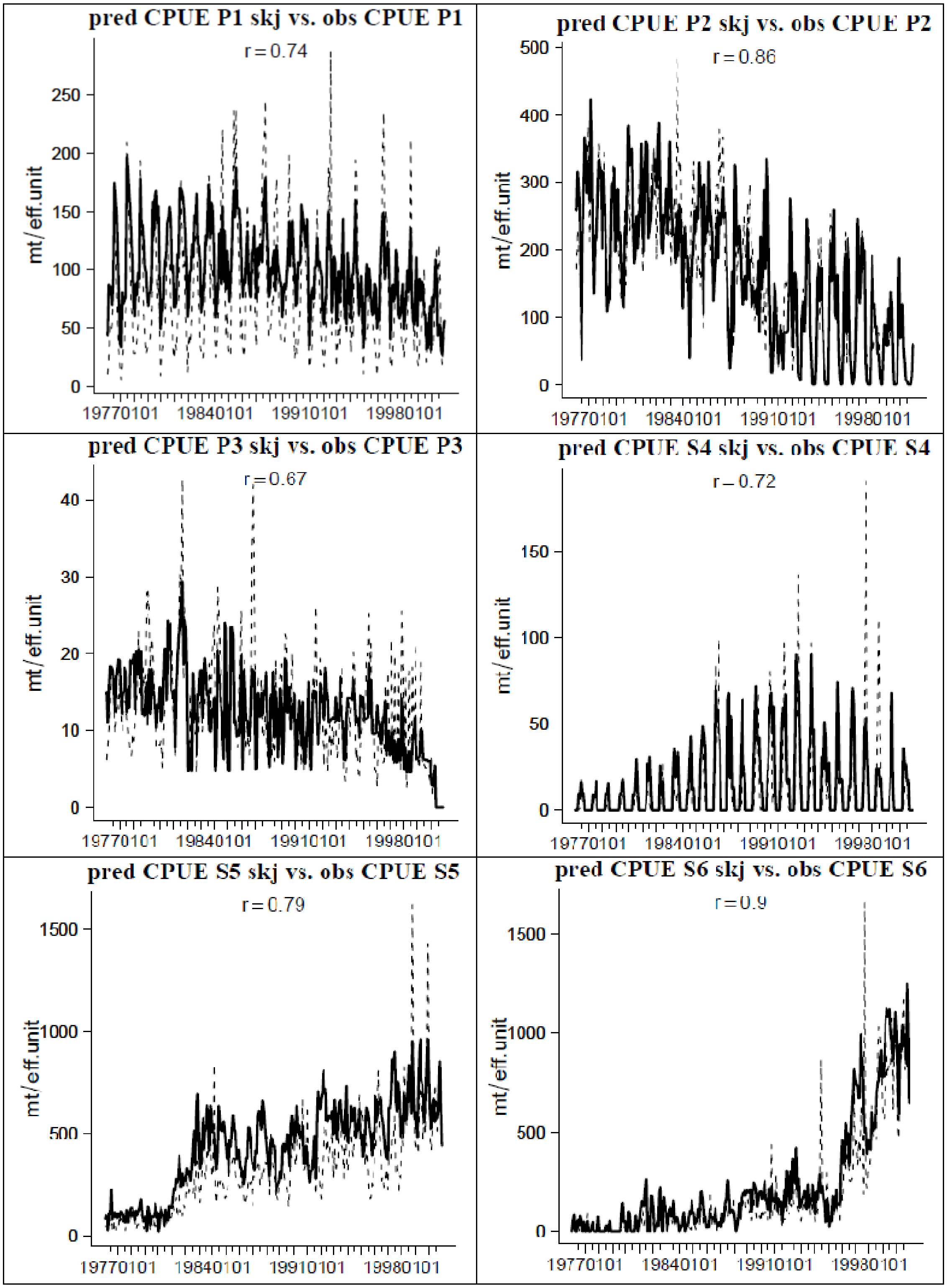

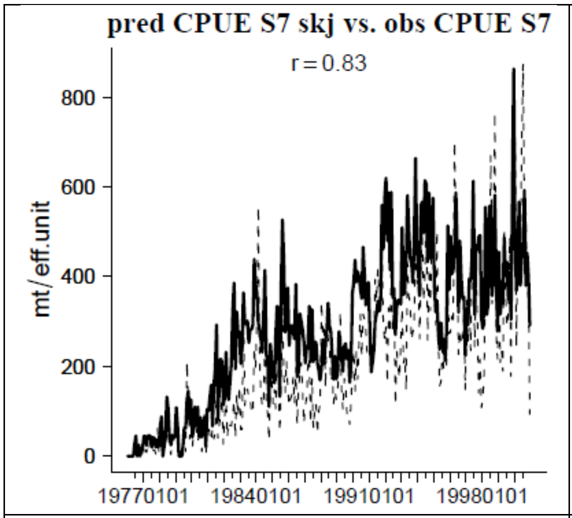
pred CPUE S7 skj vs. obs CPUE S7
r = 0.83
mt/eff.unit
0
200
400
600
800
19770101
19840101
19910101
19980101

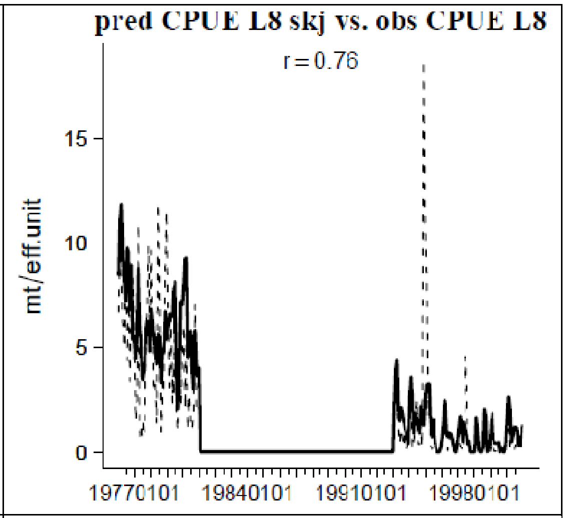
pred CPUE L8 skj vs. obs CPUE L8
r = 0.76
mt/eff.unit
0
5
10
15
19770101
19840101
19910101
19980101

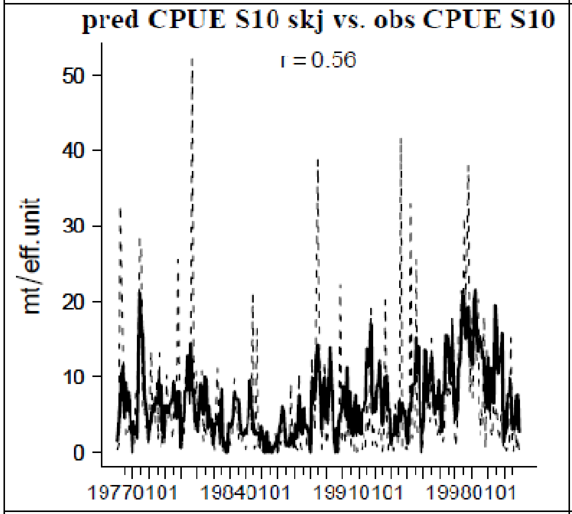
pred CPUE S10 skj vs. obs CPUE S10
r = 0.56
mt/eff.unit
0
10
20
30
40
50
19770101
19840101
19910101
19980101

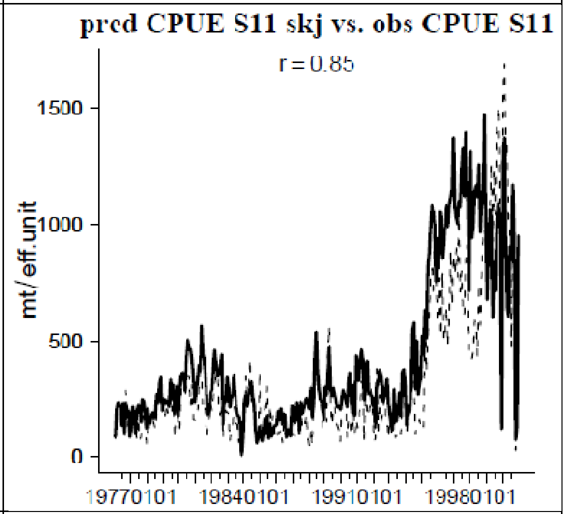
pred CPUE S11 skj vs. obs CPUE S11
r = 0.85
mt/eff.unit
0
500
1000
1500
19770101
19840101
19910101
19980101

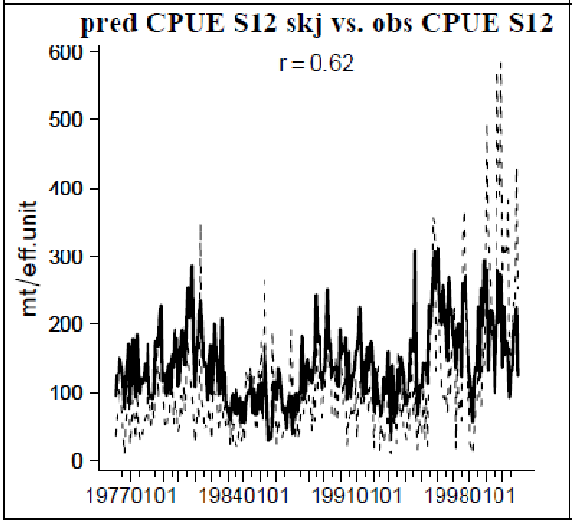
pred CPUE S12 skj vs. obs CPUE S12
r = 0.62
mt/eff.unit
0
100
200
300
400
500
600
19770101
19840101
19910101
19980101

10.1 Size frequency distribution by fishery (all data aggregated in time and space)

Histogram: observed
Line with circles: predicted

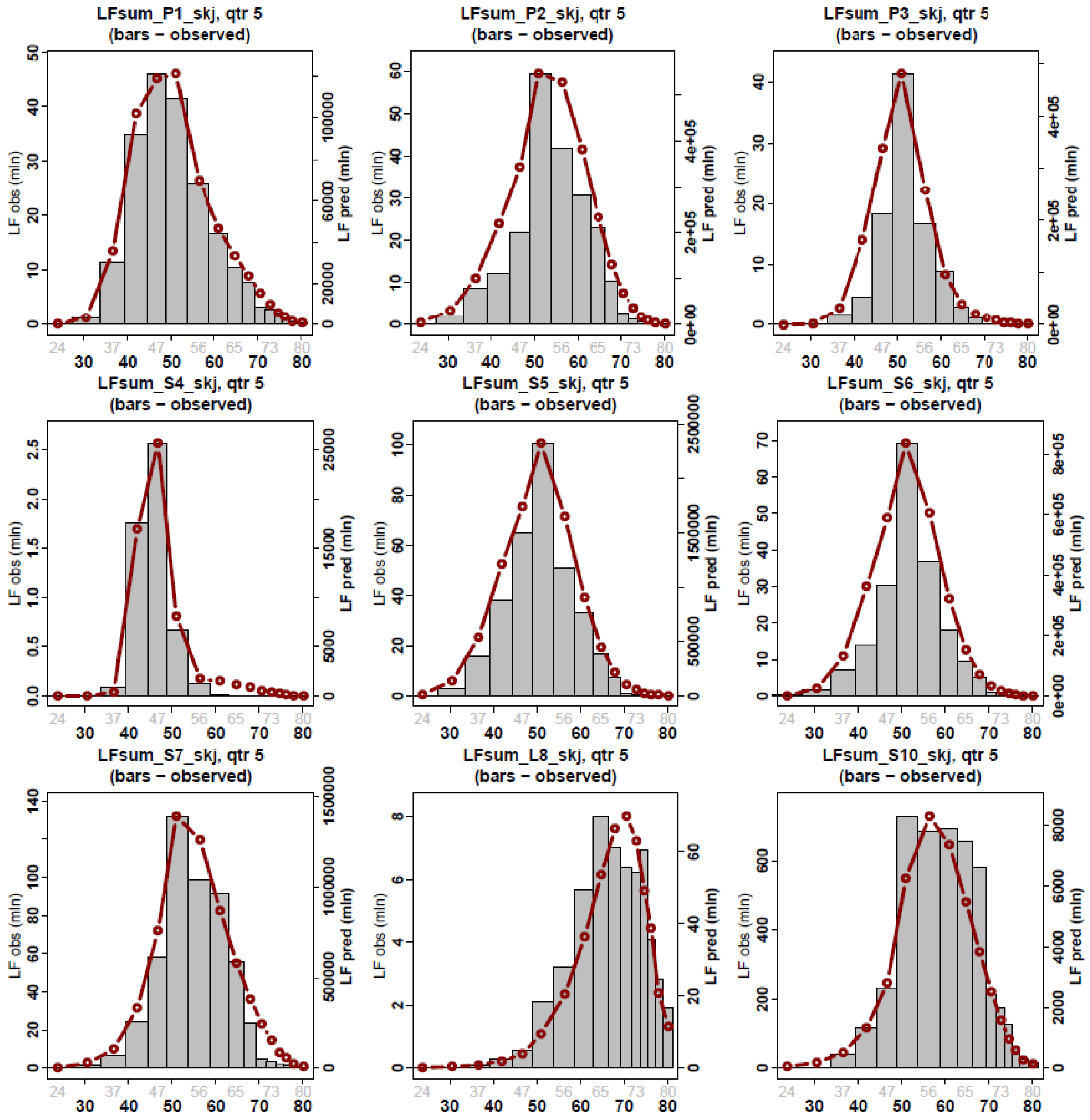

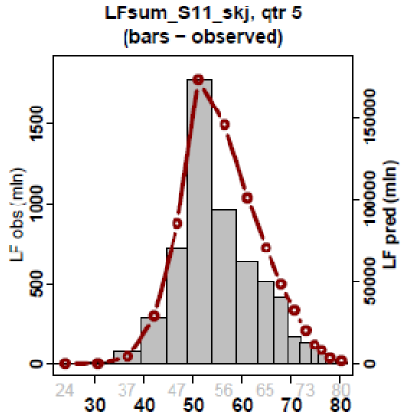
LFsum_S11_skj, qtr 5
(bars – observed)
LF obs (mln)
LF pred (mln)
0
500
1000
1500
0
50000
100000
150000
24
37
47
56
65
73
80
30
40
50
60
70
80

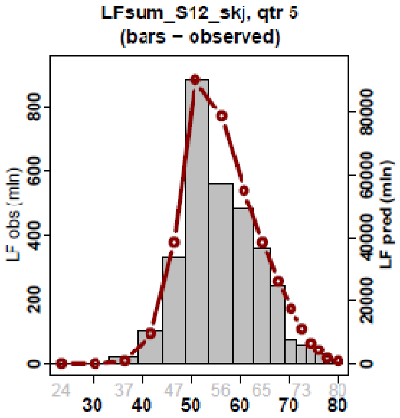
LFsum_S12_skj, qtr 5
(bars – observed)
LF obs (mln)
LF pred (mln)
0
200
400
600
800
0
20000
40000
60000
80000
24
37
47
56
65
73
80
30
40
50
60
70
80